The Impact of Fault Current Contribution from Converter Based Power Plants on Power System Stability

Jesse Majuri

School of Electrical Engineering

Thesis submitted for examination for the degree of Master of Science in Technology.

Espoo 21.11.2016

Thesis supervisor:

Prof. Matti Lehtonen

Thesis advisor:

M.Sc. (Tech.) Antti Kuusela

Aalto University
School of Electrical
Engineering

AALTO UNIVERSITY
SCHOOL OF ELECTRICAL ENGINEERING

ABSTRACT OF THE
MASTER'S THESIS

Author: Jesse Majuri

Title: The Impact of Fault Current Contribution from Converter Based Power Plants on Power System Stability

Date: 21.11.2016 Language: English Number of pages: 10+114

Department of Electrical Engineering and Automation

Professorship: Electrical Power and Energy Engineering

Supervisor: Prof. Matti Lehtonen

Advisor: M.Sc. (Tech.) Antti Kuusela

A power system must be able to maintain an operating equilibrium in the state of the network even after potential critical disturbances. The impact of disturbances on the system is determined by the responses of components connected to it. The responses providing additional stability to the system are crucial especially during the faults. Converter based power plants also produce their own portion of these responses. Therefore, for a secure and reliable operation of the power system, determining requirements for their responses is also important.

The aim of this thesis was to determine fault current contribution requirements for converter based power plants in Finland. The subjects of this study were variable speed wind power plants. The determination was conducted by studying the impact of fault current contribution on power system stability. In addition to this study, three parameters influencing the contribution were analysed. The plants were modelled as a part of the Nordic power system. They were located geographically in the western coast area of Finland.

The research illustrated that the fault current contribution of the plants can enhance the power system stability. This enhancement was the most substantial when they prioritized reactive fault current contribution. In contrast, some stability study results from plants prioritizing active fault current illustrated that the enhancement was poorer in comparison with results from plants without any fault current injection. With the consistent results, a requirement of prioritizing reactive fault current contribution was able to be determined.

Additional results from studying two other parameters influencing the contribution illustrated that in comparison with each other, they had a different impact on the power system stability. Studying their interact with each other was not within the scope of this thesis, but would be useful for determining the remainder of requirements for the fault current contribution of the plants.

Keywords: Converter based power plant, fault current contribution, power system stability, reactive fault current gain, active power recovery time

AALTO-YLIOPISTO
SÄHKÖTEKNIIKAN KORKEAKOULU

DIPLOMITYÖN
TIIVISTELMÄ

Tekijä: Jesse Majuri

Työn nimi: Konvertterikytkettyjen voimalaitosten vikavirran syötön vaikutus voimajärjestelmän stabiiliuteen

Päivämäärä: 21.11.2016 Kieli: Englanti Sivumäärä: 10+114

Sähkötekniikan ja Automaation laitos

Professuuri: Sähköenergiatekniikka

Työn valvoja: Prof. Matti Lehtonen

Työn ohjaaja: DI Antti Kuusela

Voimajärjestelmän on kyettävä ylläpitämään verkon toiminnan tasapainotilaa jopa mahdollisten kriittisten vikojen jälkeen. Vikojen vaikutus verkkoon määräytyy järjestelmään liittyneiden komponenttien vasteista. Verkon stabiiliutta tukevat vasteet ovat tärkeitä eritoten vikojen aikana. Konvertterikytketyt voimalaitokset tuottavat myös oman osansa näistä vasteista. Täten, turvallisen ja luotettavan voimajärjestelmän toiminnan ylläpitämiseksi vaatimuksien määrittäminen myös niiden vasteille on tärkeää.

Tämän diplomityön tavoitteena oli määrittää vikavirran syötön vaatimukset konvertterikytketyille voimalaitoksille Suomessa. Työn painopiste oli muuttuvanopeuksisissa tuulivoimalaitoksissa. Määrittelyn menettelytapa oli tutkia vikavirran syötön vaikutusta voimajärjestelmän stabiiliuteen. Vikavirran syötön tutkimuksen lisäksi työssä analysoitiin kolmea syöttöön vaikuttavaa parametria. Laitokset oli mallinnettu osaksi pohjoismaista voimajärjestelmää. Ne sijaitsivat maantieteellisesti Suomen länsirannikolla.

Tutkimus osoitti, että voimajärjestelmän stabiiliutta voidaan parantaa konvertterikytkettyjen voimalaitosten vikavirran syötöllä. Tämä parannus oli kaikista suurin silloin, kun voimalaitokset priorisoivat loisvikavirran syöttöä. Toisaalta, pätövikavirran syötön priorisoinnilla stabiiliuden parannus oli joissain tutkimuksissa jopa heikompi verrattaessa tilanteisiin, joissa voimalaitokset eivät syöttäneet vikavirtaa ollenkaan. Yhdenmukaisten tulosten johdosta vaatimus loisvikavirran syötön priorisoimisesta voitiin määrittää.

Tutkimustulokset kahden muun syöttöön vaikuttavan parametrin osalta osoittivat, että verrattaessa toisiinsa näillä oli erilainen vaikutus voimajärjestelmän stabiiliuteen. Parametrien keskinäisen vuorovaikutuksen tutkiminen ei kuulunut tämän diplomityön aihepiiriin, mutta olisi tarpeellinen määrittelemään muut vaatimukset laitosten vikavirran syötölle.

Avainsanat: Konvertterikytketty voimalaitos, vikavirran syöttö, voimajärjestelmän stabiilius, loisvikavirran vahvistus, pätötehon palautumisnopeus

Preface

This thesis was prepared for the transmission system operator Fingrid Oyj. The supervisor of this thesis was professor Matti Lehtonen from the Department of Electrical Engineering and Automation in Aalto University. The advisor of this thesis was M.Sc. (Tech.) Antti Kuusela from Fingrid Oyj.

I would like to express appreciation for Matti Lehtonen for the scientific comments related to my thesis.

In addition, I would like to thank my advisor Antti Kuusela for competent ideas and supportive comments. I would also like to express my gratitude to the steering group for all important comments. In particular, I would like to thank Ilkka Luukkonen for all the help with the models and cases.

Finally, I would like to express my deepest gratitude to my family for all the support during my studies. This also includes you, Katariina.

Etelä-Haaga, 21.11.2016

Jesse Majuri

Contents

Nomenclature

Symbols

A_1	Kinetic energy gained during the acceleration period of a generator
A_2	Kinetic energy injected during the deceleration period of a generator
A_r	Swept area of a wind turbine rotor blade
C_p	Coefficient of efficiency of a wind turbine
E_G	Stator field voltage of a generator
E_M	Stator field voltage of a motor
i_d^*	Actual d-axis current in the rotor- and grid-side converter control
i_dI	Reference d-axis current in the grid-side converter control
i_dR	Reference d-axis current in the rotor-side converter control
i_q^*	Actual q-axis current in the rotor- and grid-side converter control
i_qI	Reference q-axis current in the grid-side converter control
i_qR	Reference q-axis current in the rotor-side converter control
I_n	Maximum continuous current a wind power plant is designed to deliver
I_Q	Reactive current delivered or absorbed by electricity-generating unit
ΔI_B	Change in delivered or absorbed reactive current from prior a disturbance to during a disturbance by a renewable-based generating facility
P^*	Actual active power in the rotor-side converter control
P_e	Electrical power output of a generator
P_G	Reference active power in the rotor-side converter control
P_m	Mechanical power output of a generator
P_mdI	D-axis active power modulation index in the grid-side converter control
P_mqI	Q-axis active power modulation index in the grid-side converter control
P_wt	Power output of a wind turbine
Q^*	Actual reactive power in the rotor-side converter control
Q_G	Reference reactive power in the rotor-side converter control
Q_T	Reference reactive power in the grid-side converter control
R_t	Radius of a wind turbine rotor blade
T_D	Damping torque coefficient
T_S	Synchronization torque coefficient
ΔT_e	Change in electrical torque of a synchronous machine
U_c	Normal operating voltage of a wind power plant
U_n	Nominal voltage of a wind power plant
U_PGC	Voltage measured on the terminal of a wind turbine
ΔU	Change in voltage during a voltage dip

V_{ac}^{*}	Actual alternative current voltage of a wind turbine generator
V_{acG}	Reference alternative current voltage of a wind turbine generator
V_{dc}	Reference direct current voltage of the DC-link of a wind turbine generator
V_{dc}^{*}	Actual direct current voltage of the DC-link of a wind turbine generator
V_{dR}	D-axis voltage modulation index in the rotor-side converter control
V_{qR}	Q-axis voltage modulation index in the rotor-side converter control
v_{wind}	Velocity of wind
X''	Subtransient reactance
X_{G}	Reactance of a generator
X_{L}	Reactance of a transmission line
X_{M}	Reactance of a motor
X_{T}	Transient reactance; a summation of generator, transmission line, and motor reactance
β	Blade pitch angle
δ	Rotor angle
$\Delta\delta$	Rotor angle deviation
λ	Tip-speed ratio
ρ_{air}	Density of air
ω_{act}	Actual speed of a wind turbine rotor
ω_{ref}	Reference speed of a wind turbine rotor
ω_{t}	Rotational speed of a wind turbine rotor
$\Delta\omega$	Rotor speed deviation

Abbreviations

AC	Alternative current
ACER	Agency for the Cooperation of Energy Regulators
ATP	Alternative Transient Program
AVR	Automatic voltage regulator
DC	Direct current
DSO	Distribution system operator
DFIG	Double fed induction generator
EMTP	Electromagnetic transient program
ENTSO-E	European Network of Transmission System Operators for Electricity
EPRI	Electric Power Research Institute
FC	Full converter
HVAC	High voltage alternative current
HVDC	High voltage direct current
NC RfG	Network Code of Requirements for Generators
PCC	Point of common coupling
PI	Proportional-integral
PMSG	Permanent magnet synchronous generator
PSCAD	Power System Computer-Aided Design
PSS/E	Power System Simulator for Engineering
PV	Photovoltaic
STATCOM	Static synchronous compensator
SVC	Static var compensator
TSO	Transmission system operator
TSP	Transient stability program
VSC	Voltage-source converter

1 Introduction

Power system must be able to maintain an operating equilibrium in the state of the network even after potential disturbances. The impact of these disturbances on the system is determined by the responses of components connected to the network. These responses are crucial especially during the fault circumstances. If they are insufficient in supporting the power system to recover a new stable state, the system loses its stability. In the worst case scenario, this can hypothetically lead to collapse of the entire power system.

Converter based power plants are partly or completely connected to the network through a frequency converter. The complete decoupling of the power plant from the frequency of the power system causes the operation principles of the plant to differ from conventional power plants. The interaction between the converter based power plants and the system depends on the various control systems used by the converters. The characteristics and functionality of conventional synchronous machine power plants are well taken into account in the planning of the power system and in the network connection requirements of these plants. However, the requirements for converter based power plants are not as comprehensive as they are for the conventional plants. The increasing number of these plants in the power system has an augmenting impact on the stability of the system. The more the capacity of these plants is in proportion to the overall production capacity, the more different are the responses for finding a new stable state after altered conditions of the system. This raises the need for the determination of more extensive requirements for the responses of the plants.

Network connection requirements for converter based power plants have been implemented in the grid codes of transmission system operators [1–8]. The requirements determine the operation principles of the plants during normal and under fault conditions of the system. However, some of the grid codes do not specify the operation under fault conditions. A comprehensive study with sufficiently modelled power system is required if such specifications are yet to be determined.

Studying power system stability is mandatory in long-term power system planning. The stability studies can determine the robustness and stability of the system when the equilibrium state is interfered. They are commonly reviewed with electromechanical transient studies. These transient studies have focused on the operation of the system and its components in the state of change. The simulation scenario used in this sort of study includes the dynamic models of the power system components.

The aim of this study is to determine fault current contribution requirements for converter based power plants in Finland. This is conducted by studying the impact of fault current contribution on power system stability. The focus is on variable speed wind power plants. The study covers the impact on all three main categories of power system stability: voltage, frequency, and rotor angle stability. It focuses on long-term planning of the system. In addition to fault current contribution study, selected three parameters influencing this contribution are further analysed. First parameter is the priority of fault current contribution which is divided into active and reactive current. Second parameter is the reactive fault current gain of the

contribution. Last parameter is the active power recovery time of the contribution.

The simulations are implemented with a power system planning software PSS/E (Power System Simulator for Engineering). The wind power plants are modelled in the western coast area of Finland as a part of the Nordic power system scenario. Based on this scenario, the base-cases with certain power system operation situation are created. These operation situations vary from winter day to summer night.

The remainder of this thesis is divided into six chapters. Chapter 2 presents the power system stability and the characteristics having an influence on it. The stability is reviewed in all three main categories: voltage, frequency, and rotor angle stability. Chapter 3 introduces the concept of converter based power plant. First, the common variable speed wind turbines technologies are discussed in detail. Second, the operation principles of a wind power plant related to network connection requirements are illustrated. Last, the dynamic modelling principles of a variable speed wind turbine are presented.

Chapter 4 presents the concept of fault current contribution of wind power plants from multiple perspectives. In the beginning of this chapter, the common network connection requirements related to the fault current contribution are discussed. Furthermore, some research related to the current contribution is reviewed. In addition, the new regulation 2016/631 is shortly described and the requirements for fault current contribution in it are illustrated in detail. Last section of this chapter presents a detailed look at the fault current contribution requirements for wind power plants from selected transmission system operators.

Chapter 5 introduces the wind power plant models used in the simulations of this thesis. The chapter also discusses the dynamic modelling logic of the fault current priority, the reactive current gain, and the active power recovery time. Moreover, this chapter presents the methods for analysing the power system stability. Last, the chapter presents the Nordic power system scenario used in the simulations. Chapter 6 presents the results of this study. Chapter 7 completes this thesis with the evaluation of the results and with the conclusions.

2 Power System Stability

This chapter introduces the definition and basic concept of power system stability relevant to this thesis. The power system stability can be defined as the ability of a power system to remain in an equilibrium state. The equilibrium state can be either a normal operation condition state or an acceptable altered state subsequent to being subjected to a disturbance. [9]

A disturbance is an unplanned small or large event that divers the state of the power system from operating equilibrium state. Small disturbances, such as small load changes, take place continuously and the system begins adjusting to the altered state. However, less common large disturbances, such as a loss of a large generator or load, require more complex adjusting to keep the system stable. A stable power system must remain within operating equilibrium. This equilibrium requires the balance between the power supply and its demand. When this condition is met, the system will continue operating within its new state. [9]

Even though power system stability is a narrowly defined problem, its complexity in terms of its different forms and influenced factors makes it impractical to study it as such. Thus, the stability is classified into appropriate categories. Namely, the main categories are voltage stability, frequency stability and rotor angle stability. The subcategories for voltage stability are large-disturbance voltage stability and small-disturbance voltage stability. For rotor angle stability, the subcategories are small-disturbance angle stability and transient stability. Frequency stability is solely studied, and thus, it does not have any subcategories. Furthermore, the stabilities can be divided into short and long term stability phenomena within voltage and frequency stability, whereas rotor angle stability issues are all short term. The categories are shown in Figure 2.1. [9]

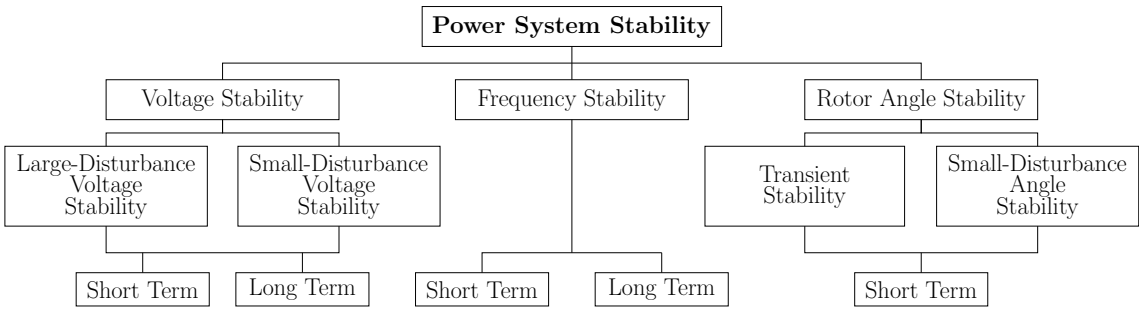

Figure 2.1: The classification of power system stability. Adapted from [9].

The classification of these categories requires different considerations. These considerations vary from the characteristics of the instability to methods for solving it. In addition, different instability types have also variation in the measuring and calculating of the instability. The categories and their individual impacts on the power system stability are discussed next in Sections 2.1, 2.2, and 2.3. [9]

2.1 Voltage Stability

Voltage stability can be defined as the capability of a power system to preserve steady voltages. The voltages are measured from the buses of the system. The stability must be maintained under normal operation and subsequent to being exposed to a disturbance. Steady voltages are preserved if the system has the ability to maintain or restore equilibrium between the load demand and the load supply within the network. The possible instability is a result of either a rise or a fall of voltage at some of the buses under the influence of a disturbance. The consequences may include the loss of loads and tripping of transmission lines or other network elements. [9]

As it was seen in the Figure 2.1, voltage stability is additionally classified into two subcategories: large-disturbance voltage stability and small-disturbance voltage stability. Large-disturbance voltage stability involves the study of large disturbances, such as system faults, contingencies of a circuit, a loss of a generator, or of a load. The ability to maintain steady voltages subsequent to a disturbance is determined by the network and load characteristics. These characteristics interact with the continuous and discrete controls and protections of the system. To determine this type of stability, examination of the dynamic performance of the system is required. Due to the different dynamic performance and interaction times of the devices (e.g., motors, the tap changers of transformers, and generator current limiters), the examined time period should be long enough to include them all. Thus, the time period taken into account can vary from a few seconds to tens of minutes as was presented in Figure 2.1. [9]

In contrast to large-disturbance voltage stability, small-disturbance voltage stability involves small disruptions such as progressive changes in the loads of the system. The disturbances and their effect on the voltage stability of the system can be examined with a steady-state approach with proper assumptions made. The assumptions are needed to linearise the dynamic equations of the system. However, the linearisation cannot present the non-linear effects such as tap changer controls. [9]

2.1.1 Characteristics Influencing Voltage Stability

Supporting the voltage depends on the active and reactive power flow on the transmission lines. A mismatch between the supply and the demand for reactive power results in a voltage change in the system. When the system is lagging (e.g., the current phase is behind the voltage phase), the deficit of reactive power results in a decrease of the voltage. Conversely, the surplus of reactive power results in an increase in the voltage. The system operator sets the range of voltage that determines whether the system operates within normal or exceptional range. The range differs according to the voltage level. [9]

One of the main contributors to the voltage stability is the relationship between the active and reactive power and the voltage level of the system. More prime contributors include the generator reactive power or voltage control, and load and reactive compensation device characteristics. In addition, the performance of voltage control devices, for instance transformer under-load tap changers, contribute to the stability. These prime contributors are discussed next. [9]

Generator automatic voltage regulators (AVRs) are used for controlling the voltage within the power system. In normal conditions of the network, the terminal voltages of the generators are kept constant. When the system experiences a low voltage condition, generators begin to feed more reactive power to the network to sustain the voltage. If the demand for the reactive power exceed the field current and/or the armature current limit of the generator, the terminal voltage begins to fall. Both the field and armature current limit are set to prevent the excess heating of the generator. The field current limit is automatically limited by an overexcitation limiter, whereas the armature current is usually limited manually. Thus, the generators have a certain limit for the voltage stability support. [9, 10]

Load characteristics depend on the type of load. These include but are not limited to small and large motors, static loads, and thermostat controlled loads. Loads having a varying active and reactive component with voltage interact with the transmission network. This interaction is caused by the altering power flow of the loads in the system. The power consumed by the loads tends to be restored in response to a disturbance. The recovery can be an action of motor slip adjustments, distribution voltage regulators, tap-changing transformers or thermostats. Maintaining the power consumption during the disturbance increases the stress on the network. The increased stress is due to the increased reactive power consumption causing further voltage reduction. Overall, the combined characteristics of the transmission system and its loads are part of the determination of the voltage where the system settles. [9]

Reactive compensation devices such as shunt capacitors, regulated shunt compensation, and series capacitors also provide reactive power and voltage support. Shunt capacitors can correct the receiving end power factor. This feature increases the voltage stability limit to some extent. On one hand, shunt capacitor can be used as a substitute for the reactive power reserves within some generators. On the other hand, an abundantly compensated network with shunt capacitors tends to have a weak voltage regulation. In addition, subsequent to a certain level of compensation, shunt capacitors solely do not have the characteristics to sustain a stable operation of the network. [9]

Regulated shunt compensation, such as a static var compensator (SVC), will regulate the voltage up to its predetermined maximum capacitive output. The regulation range within the limit does not compromise the voltage control or the instability problems. However, when the SVC is regulated at the limit, it becomes a pure capacitor. The pure capacitor does not provide voltage control and the reactive power support decreases with the square of voltage. Counterpart to a SVC, a synchronous condenser has an internal voltage source. The synchronous condenser promotes a more stable voltage regulation. Also, it has ability continue supplying reactive power at rather low voltages. [9]

Last, the series capacitors are self-regulating reactive power suppliers. The reactive power supplied is proportional to the square of the line current. Unlike in the reactive compensation devices mentioned above, the supplied reactive power of the series capacitor is independent of the bus voltages. Thus, series capacitors improve the voltage regulation. However, series capacitor compensation may cause subsynchronous resonance complications. In addition, they are not in principle used

in voltage control. Moreover, the protection of the line containing the capacitor requires special care. [9]

As it was discussed in the beginning of this chapter, it is clear that voltage stability cannot exclusively illustrate all the aspects of power system stability. Thus, another category is reviewed in the next section.

2.2 Frequency Stability

To maintain a stable frequency of the system, and thus maintaining power system stability, the system requires a balance between the generation and the electrical load of the system. If this active power balance is interfered, the frequency begins to decrease in a case of generation deficiency, and to increase in a case of generation surplus. The system should maintain or restore this imbalance without an unintentional loss of loads. Conversely, if the stability is not sustained, the frequency instability results in the tripping of generators and/or loads. At worst, the instability results in a collapse of the entire system. Commonly, a lack of frequency stability is associated with inadequacies in equipment responses. Also, coordination between control and protection equipment play a major role. Finally, the lack of generation reserve may also lead to instability. [9]

2.2.1 Characteristics Influencing Frequency Stability

The load-generation imbalance is a result of a severe system deviation. This upset usually leads to fluctuation of frequency, voltage and power flows. Furthermore, the fluctuation activates certain processes in the system. These processes are used to reduce the deviation of the frequency. An example of a control process is the additional power output response of a generator with speed governor to a load change. This response contributes to the frequency stability, and is better known as the spinning reserve response. Another control process is the use of supplementary reserve where reserve generators, commonly known as prime movers, are started in a case of major generator loss. As a protection process, certain loads or generators can be disconnected from the system to stable the frequency. Also, some loads can reduce their load as a function of frequency drop. [9]

The frequency deviation subsequent to a sudden imbalance is additionally dependent on the spinning generation of the system, better known as the system inertia. The more rotating masses exist in the system, the slower is the frequency deviation. The inertia is dependent on the inertial response of the individual generators in the system. A generator contributes an inertial response to the system inertia if a change in the frequency of the system causes a change in the rotational speed of the generator. Thus, the power related to the kinetic energy stored in the change of the rotational speed is then either fed to or taken from the power system. [9]

As it was shown in the Figure 2.1, frequency stability can be divided into short term and long term subclasses. The short term characteristics are mainly the underfrequency load shedding, generator controls, and generator protections. These characteristics last a fraction of seconds. Whereas, long term frequency stability

characteristics consist of the activation of reserve generators and the load voltage regulators. These processes take minutes to activate. To complete the description of the power system stability phenomena, the last main category contributing to the stability is discussed next. [9]

2.3 Rotor Angle Stability

Rotor angle stability represents the ability of a power system to prevent the synchronous machines from losing their synchronism with other generators. A disturbance in the power system can cause loss of synchronism. The maintain of synchronism depends on the ability of the system to sustain or restore equilibrium state between the electromagnetic torque and the mechanical torque of synchronous machines involved in the network. It is also possible that rotor angle instability occurs between two groups of machines. The instability is a result of increased rotor angles of some synchronous machines. Eventually this increment leads to the loss of their synchronism with other generators. Studying the rotor angle stability problem requires understanding of the relationships between the power outputs and the rotor angles of the synchronous machines. Thus, electromechanical oscillations of the power system are presented next. [9]

Consider a simplified power system consisting of a generator producing power to a motor shown in the Figure 2.2. The motor represents the large power system. In this case, all the resistances and generator speed governor effects are neglected. The rotor of the generator leads the rotor of the motor in this scenario. The stator field voltage of the generator E_{G} leads the stator field voltage of the motor E_{M}. This angle difference is presented as δ in the figure. [9]

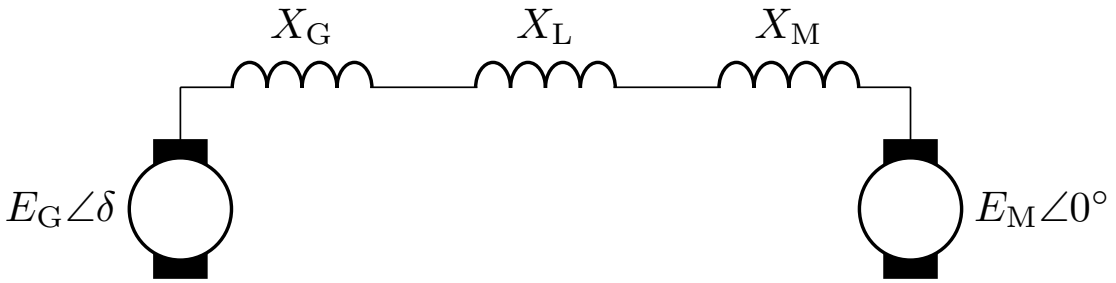

Figure 2.2: A simplified single-line diagram of the power system. Adapted from [9].

The power output of the generator to the motor is given by Equation (1):

$$P_{\mathrm{e}} = \frac{E_{\mathrm{G}} E_{\mathrm{M}}}{X_{\mathrm{T}}} \sin\delta \tag{1}$$

where X_{T} is the transient reactance; a summation of the reactance of the generator X_{G}, the motor X_{M}, and the transmission line X_{L} of the system. This equation can be plotted to present the power–rotor-angle relationship of a generator. The result is illustrated in the Figure 2.3. [9]

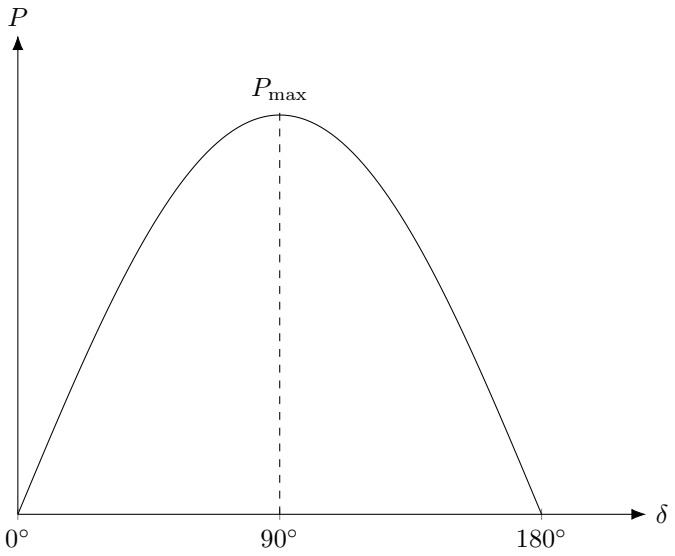

Figure 2.3: The power–rotor-angle relationship of a generator. Adapted from [9].

As it can be seen in Figure 2.3, due to the rough simplification of the system, the power output of the generator varies as a sine function of the angle. This is a highly nonlinear relationship. When the rotor angle is at 0°, the machine provides no power. When the angle increases, the power output also increases up to a certain maximum point, namely 90°. After the rotor angle passes the 90° angle, the power output begins to decrease. This state is unstable in a steady state, but in a transient state, the angle can go further than 90° without losing the stability. In practice, the maximum power angle enabling a stable power system subsequent to a disturbance is 30°. In a more accurate modelling of the machine, the corresponding figure would differ from the sinusoidal relationship. However, the general form of the plot would appear similar. [9, 10]

The transient stability phenomena can be studied with the power–angle relationship and the equal area criterion. The equal area criterion is illustrated in Figure 2.4. When a short-circuit fault occurs near the generator, the operating point of the generator shifts from point a to point b. At the same time, the operation of the generator is shifted to another power–angle curve determined by the fault conditions. Neglecting the resistive losses causes the active power P_e of the generator to be zero during the fault. Since the mechanical power P_m is now greater than the active power, the rotor of the generator begins to accelerate. The acceleration continues until the operating point reaches c; the fault clearing point. At the fault clearing point angle δ_1, the fault is cleared and the operating point shifts rapidly to d. This causes the rotor to begin deceleration, due to the active power output P_e being higher than the mechanical power. The angle still increases as a result of the kinetic energy gained during the acceleration period. This phenomenon shifts the operating point from d to e. At the point e, the excessive energy has been consumed by the system and the rotor angle has reached its final value δ_2 in its postfault power–angle curve. [9]

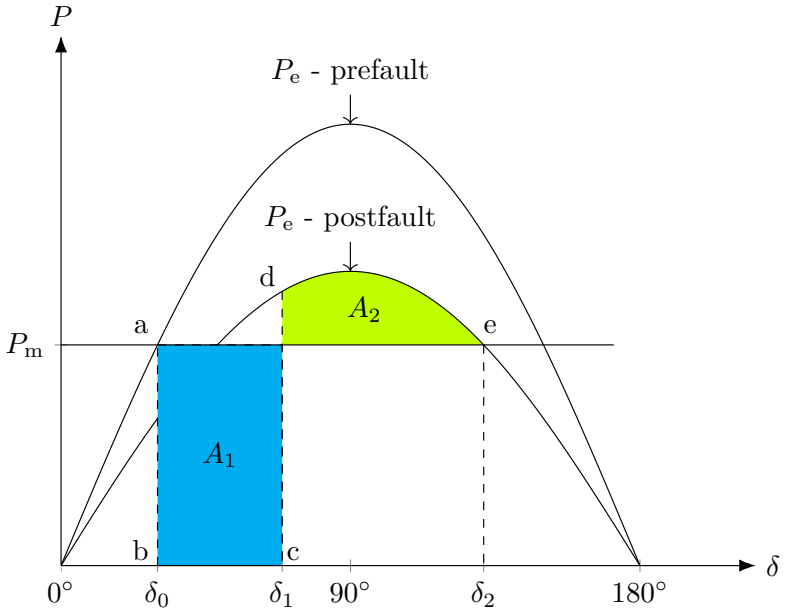

Figure 2.4: Equal area criterion during transient stability phenomena. Adapted from [9].

If the kinetic energy gained during the acceleration period, shown as area A_1 in the figure, is smaller than the deceleration area A_2, the stability will be preserved. If the area A_1 is larger, the synchronism loss of the generator leads to transient instability. The characteristics influencing the rotor angle stability are discussed next. [9]

2.3.1 Characteristics Influencing Rotor Angle Stability

Steady-state conditions always have an equilibrium between the mechanical torque input and the electromagnetic torque output of every machine. Also, the speed of machines remains constant. When a power system is interfered from its initial synchronized conditions, the rotors of the interconnected synchronous machines begin to either accelerate or decelerate. As a consequence, if one of the generators begin to rotate faster than another, the rotor angle position of that generator shifts compared with the slower one. [9]

The angular deviation results in a partial load transfer from the slower machine to the faster one. This transfer strives for the reduction of the speed difference, and thus, the reduction of the angular difference. Conversely, the power of the machine starts to decrease, if the angular difference is beyond the maximum point of the power–angle relationship shown earlier. This phenomenon results in a decreased power transfer and further increased angular separation eventually leading to instability, if the braking force is less than the exciting force. As was discussed, the sustenance of the stability in this situation depends on whether the angular positions of the rotors provide sufficient amount of restoring torques. To understand how the restoring torques affect the stability, the concept of change in electrical torque of a synchronous machine is introduced. [9, 10]

The change in the electrical torque ΔT_e of a synchronous machine after this machine has been exposed to a disturbance can be divided into two components:

$$\Delta T_\mathrm{e} = T_\mathrm{S}\Delta\delta + T_\mathrm{D}\Delta\omega. \tag{2}$$

Component $T_\mathrm{S}\Delta\delta$ describes the synchronization torque relating to the change of phase with the rotor angle deviation $\Delta\delta$. Conversely, component $T_\mathrm{D}\Delta\omega$ describes the damping torque relating to the change of phase with the speed deviation $\Delta\omega$. Terms T_S and T_D are the synchronizing and damping torque coefficients respectively. [9]

Existence of the above-mentioned components in the synchronous machines determines the system stability. If the restoring torque of damping is insufficient, the instability is due to oscillation. On the contrary, if the restoring torque of synchronizing is insufficient, the instability is caused by aperiodic drift. An example of oscillatory (a)) instability, non-oscillatory (b)) instability and oscillatory stability (c)) are shown in Figure 2.5. [9]

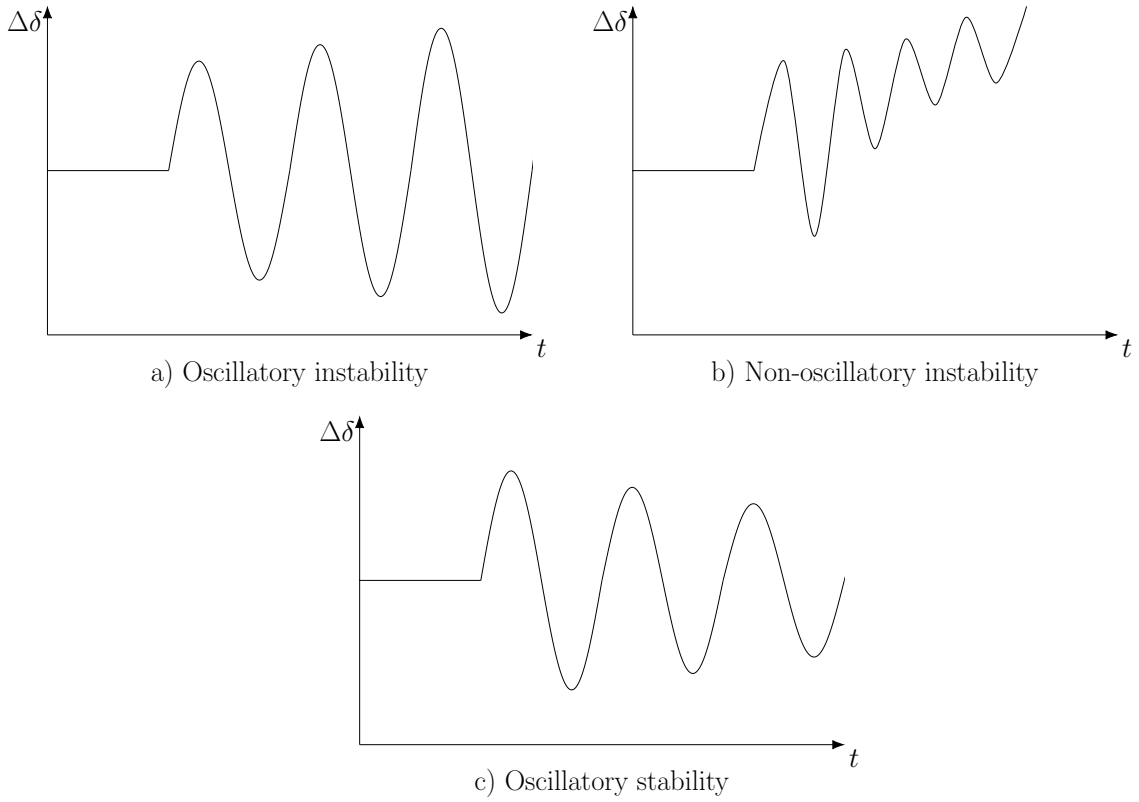

Figure 2.5: The impact of restoring torques of a synchronous machine on rotor angle stability. Adapted from [9].

As shown in the figure, the lack of restoring torque of synchronization increases the amplitude of the oscillation in every period, whereas the lack of restoring torque of damping constantly increases the rotor angle. In the oscillatory stability, both restoring torque of synchronization and restoring torque of damping are sufficient. Thus, the amplitude of the damping decreases. [9]

Similar to voltage stability, rotor angle stability can be divided into subcategories. These are small-disturbance angle stability and transient stability. Small-disturbance angle stability depends on the restoring torques: lack of synchronization torque leads to non-oscillatory instability, while lack of damping torque leads to oscillatory instability. The oscillatory instability is more common. The aperiodic drift can be properly eliminated with the voltage generator regulators mentioned previously. Small-disturbance stability study includes the first 10 to 20 seconds of dynamic behaviour followed by the occurred disturbance. [9]

Alternatively, large-disturbance rotor angle stability, better known as transient stability, involves less than 10 second the study of the outcome of the disturbance. Thus, both of the rotor angle stabilities occur in short terms. The transient instability results from a severe disturbance, such as a short-circuit on a transmission line. In contrast to the small-disturbance angle instability, transient instability is usually due to the deficient of synchronizing torque. The stability can be preserved if the power system maintains the synchronism of the severely deviated generators. With the different power system stabilities kept in mind, the converter based power plants and their adaptation to the power system are presented in the next chapter. The chapter summarizes the characteristics and operation principles of converter based power plants relevant to this thesis. [9]

3 Converter Based Power Plants

Converter based power plants are connected to the grid through a power converter. In wind turbine technologies, the connection of the generator can be partly or completely through a converter. The converter is used to control the generator speed, and thus, the output power of the generator. In solar photovoltaic (PV) power plants, the connection is completely through a converter. The power electronics in PV power plants are used to convert the generated direct current (DC) voltage into a suitable alternative current (AC) for the grid. Another task of a PV converter is to efficiently control the output power conditions similar to wind power plants. [11, 12]

Due to the unsubstantial share of power generation with PV power plants in the Finnish power system, this thesis will focus on variable speed wind turbine power plants. The variable speed wind turbine technologies are illustrated next.

3.1 Variable Speed Wind Turbine

This section presents the operating principle of a variable speed wind turbine. Secondly, currently the most used variable speed wind turbine generator technologies and their characteristics are reviewed.

3.1.1 Operation Principles of a Wind Turbine

The objective of a wind turbine is to generate electrical energy. This is achieved by utilizing the kinetic energy of air flow with rotor blades connected to a rotor hub shown in Figure 3.1. The rotor hub is connected to a low speed shaft of the turbine. Furthermore, the low speed shaft is connected to a gearbox. However, certain turbine technologies can also be gearless. In technologies including the gearbox, the gearbox of the drivetrain transforms the rotational speed of the low speed shaft into the higher rotational speed of a high speed shaft. Eventually, the high speed shaft drives the electrical generator and as a result the generator produces electrical energy. The turbine is designed in a way that with certain wind speeds maximum power output is attained. Therefore, electronic controllers are also required in the turbine to control the power output. [11]

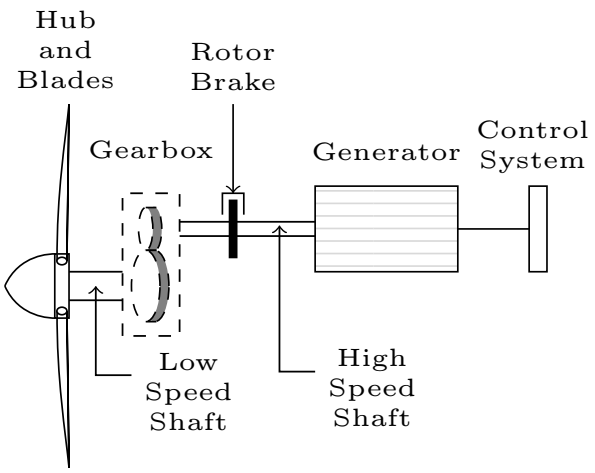

Figure 3.1: A simplified presentation of a wind turbine. Adapted from [11].

The electrical power P_{wt} produced from the air flow by a wind turbine is given by Equation (3):

$$P_{\text{wt}} = \frac{1}{2}\rho_{\text{air}} v_{\text{wind}}^3 A_{\text{r}} C_{\text{p}}(\lambda) \tag{3}$$

where ρ_{air} is the density of moving air, v_{wind} is the perpendicular velocity of the wind towards the swept area A_{r} of the rotor blade, and $C_{\text{p}}(\lambda)$ is the coefficient of efficiency. Therefore, the only parameter that can be controlled by the wind turbine is the efficiency coefficient. [11, 13]

With a certain rotor blade angle β and rotation speed ω_{t}, $C_{\text{p}}(\lambda)$ is non-linearly dependent on the wind speed. Thus, the coefficient will peak at a given tip-speed ratio λ. The tip-speed ratio is defined as the ratio of the blade tip speed and the wind speed. This ratio is expressed in Equation (4):

$$\lambda = \frac{\omega_{\text{t}} R_{\text{t}}}{v_{\text{wind}}} \tag{4}$$

where ω_{t} denotes the rotational speed of the rotor, R_{t} the radius of the blade, and v_{wind} the speed of the wind. [13]

In order to maximize the output of the turbine and to avoid excess stress on it on very high wind speeds, certain wind speeds depending on the turbine rating are in favour. An example of a turbine power–speed curve is shown in Figure 3.2. As it can be seen in the figure, maximum power output is achieved with a wind speed of around 13 m/s and above. The cut-out speed is at 25 m/s. At this wind speed, the turbine shuts down and stops producing energy. To restart the turbine, the wind speed must drop 3 to 4 m/s from the cut-out speed. This hysteresis effect is shown as a dashed line at 22 m/s. [14]

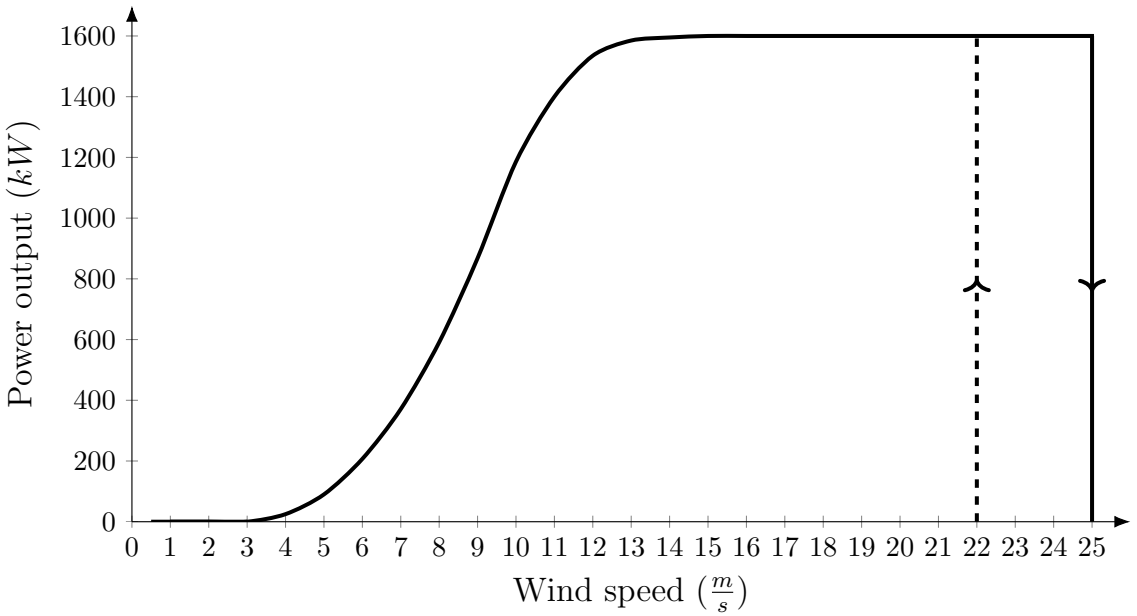

Figure 3.2: A typical power-speed curve of a wind turbine. Adapted from [14].

To allow the turbine to follow the power-speed curve, a mechanism is required to control the turbine output power. This is achieved with either pitch control, stall control or active stall control. In double fed induction generator and full converter generator, the management of output power is achieved with pitch control. [13, 14]

The pitch control approach involves the usage of electronic controllers of a turbine. The controllers measure the power output of the turbine several times per second. When the measured power output is over the predefined power-speed curve, the controller sends a signal to the yaw mechanism of the blade. The mechanism pitches the rotor blades slightly away from the wind. Thus, the tip-speed ratio is decreased. In a reverse situation when the power output is less than the maximum capable output, the blades are pitched again, but now towards the wind. In both cases, the utilization of the kinetic energy is maximized by keeping the coefficient of efficiency relatively constant. Thus, the overall efficiency of the turbine is improved. An example of the pitching of the blade and its effect on the power coefficient C_p can be seen in the coefficient curves in Figure 3.3 shown below. [11, 13, 14]

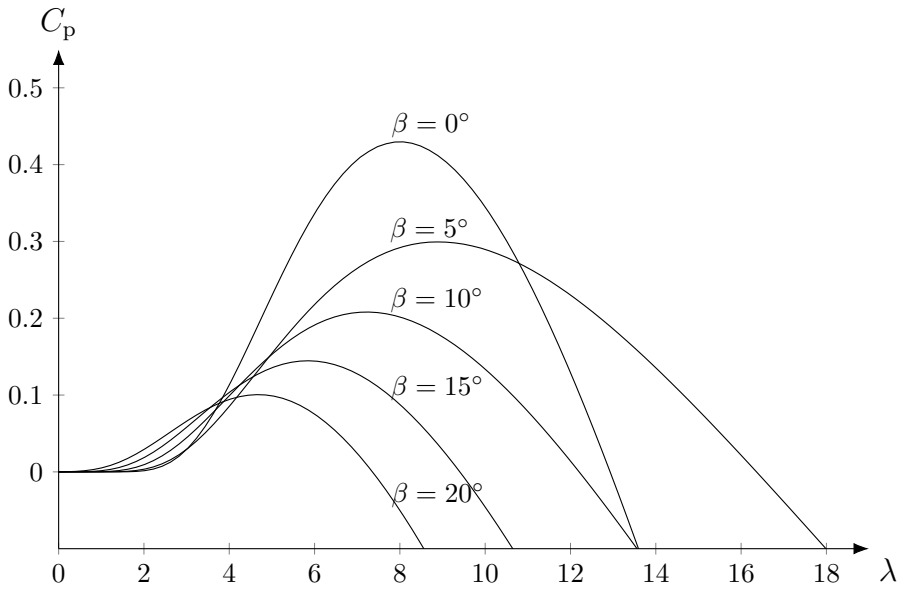

Figure 3.3: Coefficient of efficiency curves with different pitch angles β and tip-speed ratios of a wind turbine. Adapted from [11].

As the figure illustrates, the maximum value of the coefficient is obtained with a certain pitch angle β and tip-speed ratio λ. In the illustrated example, the highest coefficient was achieved with the pitch angle of 0° and tip-speed ratio of approximately 8. However, the coefficient has a theoretical maximum of 0.593 given by the Betz limit. [11]

3.1.2 Main Components and Characteristics of a Wind Turbine Generator

The most common generator types in current wind turbines are variable-speed wind turbine generators such as a double fed induction generator (DFIG) and a full converter (FC) generator. Prior to these technologies, fixed speed generators were used. The fixed speed generators are based on squirrel cage induction machines directly connected to the grid. These generators are no further reviewed as the focus of this thesis is on newer technologies. Thus, next sections present the characteristics of a DFIG and a FC generator. [11]

Double Fed Induction Generator

Figure 3.4 presents a simplified example of a double fed induction generator. As it can be seen in the figure, the stator of the machine is directly connected to the grid, while the wound rotor is connected to the rotor-side voltage-source converter (VSC). This rotor-side converter is connected to the grid-side converter through a DC-link. Furthermore, the grid-side VSC is connected to the network. With this setup, the stator operates synchronously at network frequency, whereas the rotation frequency of the rotor is decoupled from the power system frequency, and controllable by the converter. [11]

In this graph 3.4, the generator is coupled with a gearbox, but alternatives such as synchronous generator without a gearbox or induction generator with a gearbox are also possible. The advantage of the gearless generator is the avoidance of the complex gear and hydraulic mechanisms. The generator may also rotate at any suitable velocity. However, a gearless generator is a multipole low-speed generator with larger rotor diameter. [13, 15]

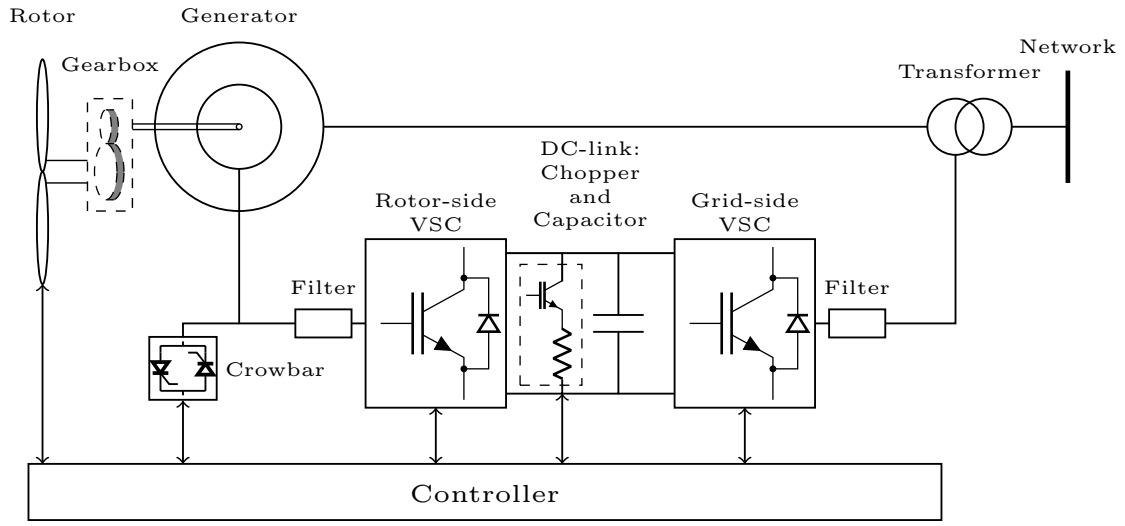

Figure 3.4: A simplified graph of a double fed induction generator connected to the network grid. Adapted from [15].

Typically, a VSC consists of multiple voltage-fed current regulated inverters. These inverters enable the two-directional power flow. The converter also enables the operation of the rotor machine at variable alternative current frequency as was mentioned. Thus, with the operation of the converter, the mechanical speed of the machine can be controlled. The filters provided on both sides of the converter are meant to reduce the switching harmonics and protect the machine from harmful effects, such as harmonic distortions of the VSC. The capacitor of the DC-link between the converters operates as energy storage. This holds the voltage variation in the DC-link voltage relatively low. In addition, the chopper between the converters operates as a braking resistor. [11, 16, 17]

The control of a DFIG plays an important role in proper and effective generation of energy in the turbine. The important magnitudes of a rotor-side converter are torque and active and reactive power. In contrast, reactive power and DC-link voltage are important in the grid-side converter. To keep the DC-link voltage constant, the grid-side converter measures the active power exchange between the rotor and the DC-link. The magnitudes of both rotor-side and grid-side converter are controlled by the generator. [11, 16, 17]

The generator can operate at either supersynchronous or subsynchronous mode. The mode depends on the relative speed of the rotor over the synchronous speed and the power flow direction in the converter. Active power is fed in supersynchronous

mode from the rotor through the converter into the system. Respectively, in sub-synchronous mode the rotor absorbs the active power from the system. When the unit operates at the synchronous mode, the voltage on the rotor is in principle direct current. Thus, only a remote net power exchange exists between the system and the rotor. Eventually, the total net electrical power flow from the machine to the system is a combination of the stator power directly fed into the system and the rotor power fed through the converter into the system. [15]

Full Converter Generator

Figure 3.5 presents a simplified schematic figure of a full-converter generator. As was discussed in the presentation of a DFIG, a full converter generator can also be gearless. The operation of the VSC and the DC-link are similar to that of the DFIG. The machine is connected to the network through a full size bidirectional converter. Therefore, the frequency of the generator is decoupled from the frequency of the grid. Because of this complete frequency detachment, the FC generator provides a better fault response compared with the DFIG. This response is later explained in detail. [15]

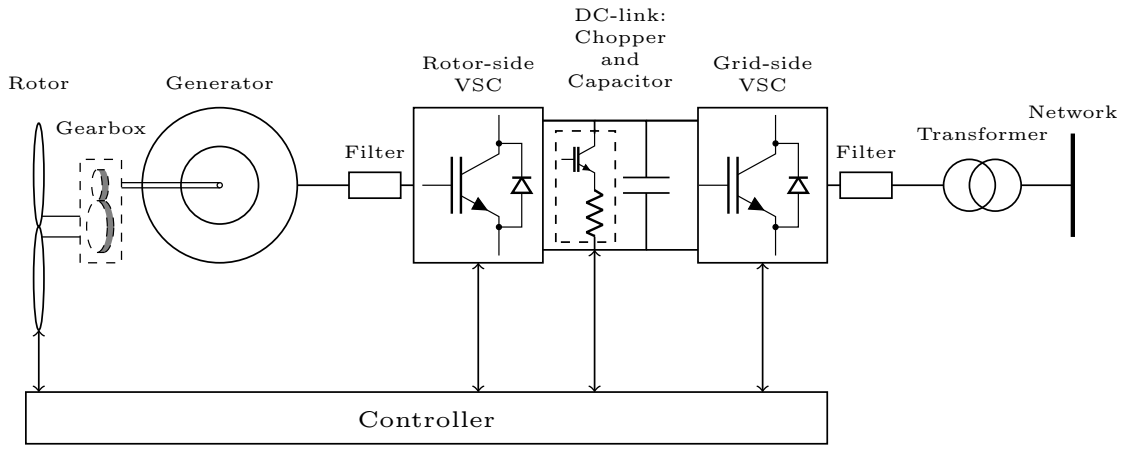

Figure 3.5: A simplified graph of a full converter generator connected to the network grid. Adapted from [15].

Another advantage of the converter is the wider operating speed range for the turbine. This improves the power performance of the turbine as was discussed in Section 3.1.1. In addition, with the full size grid-side converter, more reactive power can be fed into the network. However, as a disadvantage, the full size converter has higher power losses as a result of all the power flowing through the converter. [15]

Depending on the type and technology of individual wind turbines at a wind power plant, the network connection requirements are realised with different operation principles. The operation principles of wind turbines related to these requirements are discussed next in Section 3.1.3.

3.1.3 Operation Principles Related to Network Connection Requirements

The most common network connection requirements of a wind power plant can be divided into five categories:

- active power control and frequency regulation,
- reactive power control and voltage regulation,
- voltage and frequency operation range,
- fault ride through, and
- active and reactive current response under a disturbance.

As was explained earlier, the operation principles of a DFIG and a FC generator differ from each other. The operation principles related to the above-mentioned network connection requirements in both of these technologies are discussed next. [11]

Double Fed Induction Generator Operation Principles

The active power control and frequency operating range can be managed with the aerodynamic control system properties of a wind turbine. As it was mentioned earlier, the turbine is capable of varying the power output with the pitch control strategy. This is possible due to the ability of the generator to vary the speed of the rotor. Depending on whether the desired active power output is more or less than the prevailing power output, the turbine can operate either with the overspeeding mode or with the pitching mode. Thus, in both cases the optimal operation point of the power–rotor-speed curve is being compromised to meet the need. In case of low or medium wind speed levels, the rotor does not reach the rated speed of the turbine. As a consequence, the overspeeding method is preferred. In contrast, with high wind speeds the pitching control is preferred. The pitching control can be used for both limiting the rating of the power and to ramp the power up and down. An example of six different active power operation methods of a wind turbine are shown in Figure 3.6. [18, 19]

When the wind turbine is operated with the balance control method, the active power output is reduced/increased rapidly with a certain constant level steps shown in the figure a). On the other hand, in the delta control method in the figure b), the power production is limited by a fixed amount from the possible available power output. This method allows the turbine to participate in the frequency control by having the capacity to increase its power output in case of a frequency drop. In the third control method in the figure c), the frequency in the PCC is constantly measured. The active power output is then controlled depending on the measured frequency. The power gradient limiter, shown in the figure d) determines the maximum speed by which the active and reactive power of the turbine can change when the initial conditions, e.g. wind speed or the setpoint of the plant, are changed. This is used to keep the balance between the wind farms and the conventional plants. The fifth

control method is the system protection shown in the figure e). In this control the power output is rapidly reduced by the request of the system operator in case of a overload in the grid. The last control method in the figure f) limits the maximum power output of the wind turbine to a certain level from the available power. [11, 19]

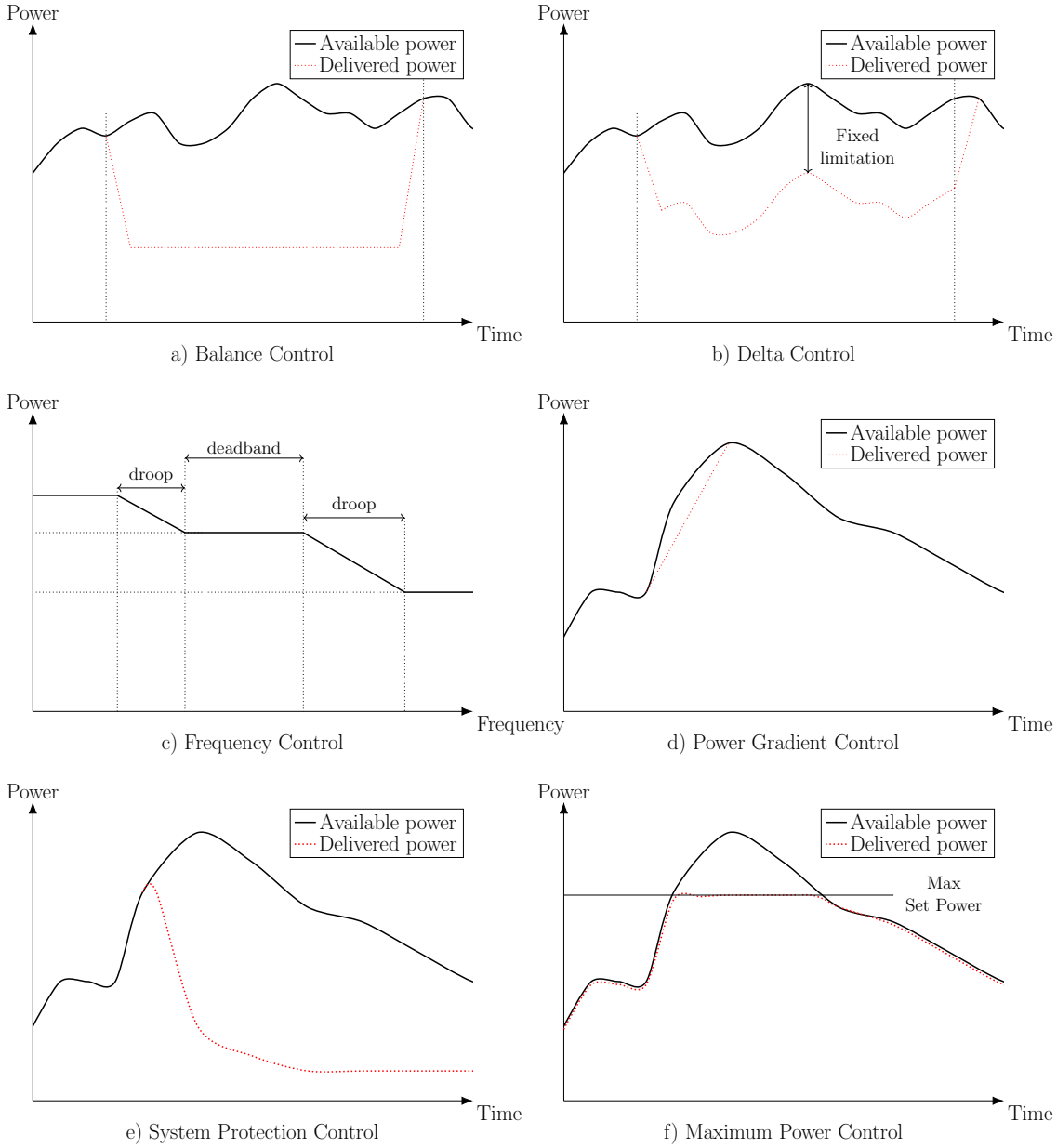

Figure 3.6: Active power control methods: a) balance control, b) delta control, c) frequency control, d) power gradient control, e) system protection control, and f) maximum power control. Adapted from [11, 19].

Supporting voltage regulation by supplying reactive power to a power system is usually achieved through the stator of the double fed induction generator. The supply is operated by changing the d-axis excitation on the rotor. The d-axis excitation illustrates the flux production component of the rotor current, whereas the q-axis

presents the torque production component. The division of rotor current to d- and q-axis's is called the vector control strategy. This strategy enables individual control of both the components. Thus, the d-axis component can be controlled to regulate the power factor of the generator, whereas the q-axis component can be adjusted in a way that the electrical torque of the machine is kept constant. [13, 20, 21]

DFIG is also able to provide the feeding or absorption of reactive power through the four-quadrant voltage source converter. With the operation of the grid-side converter of the wind turbine, the converter can act as a static synchronous compensator (STATCOM). In some cases STATCOM allows reactive power output or input even if the wind turbine generator would be disconnected from the network. Although a costly option, STATCOM can improve the voltage stability of the system. [13, 21–23]

The fault ride through requirement of a wind turbine can be managed with an active crowbar of the generator shown in Figure 3.4. The crowbar activates when the rotor current or the DC-link voltage increases above the given limit subsequent to a symmetrical three-phase voltage dip. Thus, the current is enforced to flow through the crowbar consisting of diode bridge, a certain size external resistance and a semiconductor switch. The shut-down of the rotor-side converter and the passing of current is implemented to protect the rotor and the DC-link capacitor from excess voltages and currents. [13]

During the fault ride through, the conduction of the crowbar causes the generator to shortly operate much like an asynchronous induction generator. Hence, the generator begins to consume reactive power. Depending on above-mentioned operation modes of the generator, it either consumes or produces active power. However, the quantities of these powers are relatively low due to low stator voltage. Typically 60 to 100 millisecond (ms) subsequent to the incidence, the generator voltage and currents have been stabilized. Thus, the crowbar is deactivated and the rotor current begins to flow through the converter again. Even though the transistors of the rotor-side converter are still closed, the current can flow through the parallel diodes of the transistor. If this current flow would result in a rapid decrease of the rotor current to zero for a certain time, the rotor-side converter would be started. If not, the crowbar would be activated again. After the successful attempt to restore the rotor-side converter, the control of gradual active and reactive power support of the generator can begin. This usually occurs within 100 ms of the voltage dip. [13, 21]

Another method for coping with the voltage dips and to gain a quick response to reactive power injection is the usage of stator switch. The stator breaker disconnects the stator for a short period of time and the rotor is demagnetised. Next, the operation of the rotor-side converter is resumed and the stator is reconnected. This allows the operation to be resumed. The advantage of this particular method is that during the stator disconnection time, the grid-side converter stays in operation. This allows the reactive power injection to the grid. With proper control settings of the rotor- and the grid-side converter, the requirement for reactive power response during a disturbance can be satisfied. [11]

Third method for diverting the induced rotor current is the usage of a chopper in the DC-link. Using the chopper instead of the the active crowbar allows a continuous operation and controlled fault ride through of the DFIG. This is in detail explained

in the next section of full converter generator characteristics. [24]

Similar to a DFIG, a FC generator can operate at a wide range of different speeds. This operation provides active power and support to the frequency regulation. This practice is similar with a DFIG. However, a full converter coupling of the generator has differences in the fault ride through and the reactive power support requirement which will be further illustrated. [24, 25]

Full Converter Generator Operation Principles

The FC generator allows greater flexibility and easier control of fault ride through and reactive power response with the complete decoupling of the generator from the network. Since the converters are situated between the generator and the network, the synchronous machine does not see the occurred voltage dip subsequent to a disturbance. Thus, no large transient rotor or stator currents are produced in the machine. As a result of the voltage dip, the maximum power output of the turbine is reduced. This output reduction is proportional to the magnitude of the voltage dip. [24, 25]

In a case of a voltage dip seen by the generator, the rapid operation of the grid-side converter quickly reduces the output power, whereas the power extracted by the rotor blades is not reduced. Hence, an imbalance between the energy extracted from the wind and the output energy is formed. The pitch control limits the overspeeding of the rotor and consequently the mechanical energy trying to be fed to the system. The excess energy that cannot be fed to the grid is flown to the DC-link and its capacitor, causing the capacitor voltage exceed the limits. This is prevented by the blocking of the rotor-side converter with the DC-link chopper and its braking resistor. The power electronic switch associated with the braking resistor feeds short-circuit current into the DC-link resistor. Therefore, the resistor dissipates the excess energy absorbed by the DC-link during the fault. During the voltage dip, the grid-side converter can continue its operation as a STATCOM. This operation provides reactive current support up to the rated capacity during the fault period. [24, 25]

After the fault has been cleared and the voltage level of the grid settled to a new stable state, the generator side converter is reconnected. The switching of the transistors can begin and the grid-side converter is able to feed active power again. The input power determined by the pitch control can also be set back to follow the predetermined power–speed curve. The ramping rate at which the active current recovers to the prefault state is determined by the power ramp of the generator and the error signal of the DC-link voltage. [24, 25]

Both DFIG and FC generators are complex facilities with complex control techniques. These facilities can be dynamically modelled up to a certain functional level. These dynamic models of the turbines are required in the emulation of the real-life behaviour of the wind power plants. The modelling principles are presented further in the next Section 3.2. [13]

3.2 Dynamic Modelling of Variable Speed Wind Turbine

This chapter presents common dynamic modelling principles and the main modelling characteristics of variable speed wind turbines equipped with either a DFIG or a FC generator. Wind power plants associated with multiple wind turbines are large generation facilities. These facilities connected to either a transmission or a distribution network can have a significant impact on the power system stability. Thus, an explicit dynamic modelling of the turbines is needed. With the dynamic models, the continuous behaviour of the generator variables can be simulated with different power system simulation programs. Furthermore, the simulation programs can be used with the important model components of the plant when planning a power system. [13]

The variables in the dynamic models are associated with certain wind turbine component. The different components are shown in Figure 3.7. As it has been illustrated in the figure, the control of a wind turbine and further a wind power plant is comprised of interaction between different models. These models can be classified as the aerodynamic, the mechanical, the generator system, the electrical equipment and the grid protection model. They are further explained in detail. [13]

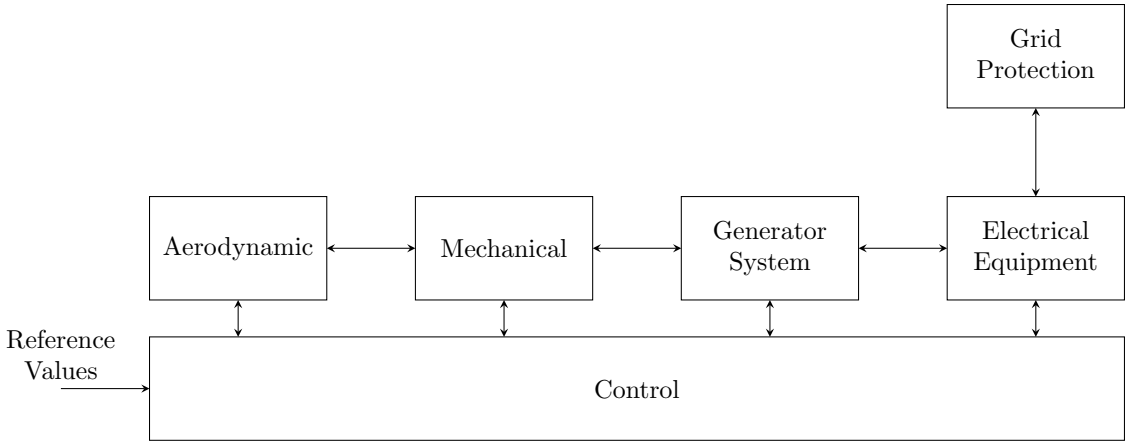

Figure 3.7: Components of a wind turbine contributing to the dynamic behaviour. Adapted from [13].

One must note that generic models based on generic physical principles of wind turbines are commonly used to simulate the overall picture of a power system study. Although the models are simplifications, the view usually covers the most important dynamic aspects of the system. Thus, the emulation of different manufacturer designs is possible with a change of the parameter values. However, a detailed 3-phase component level modelling may be needed for improving or assessing more detailed equipment design. Also, the following control schemes of the modelled components can be completely different depending on the type of the turbine, the amount of simplification made, or the controllers used. In addition, different stability simulation programs may have different inputs. [13]

3.2.1 Modelling the Individual Components

One example of modelling the turbine aerodynamics is shown in Figure 3.8. The modelling can be achieved with a proportional-integral (PI) regulator. The regulator acts on the difference between the actual and reference speed of the rotor. This process is similar to the actual pitch control system of a wind turbine. The actual speed ω_{act} is measured from the generator output, whereas the reference speed ω_{ref} is defined by the user. The output is the pitch angle β fed to the next control system. This system operates the mechanical components of the turbine. [13]

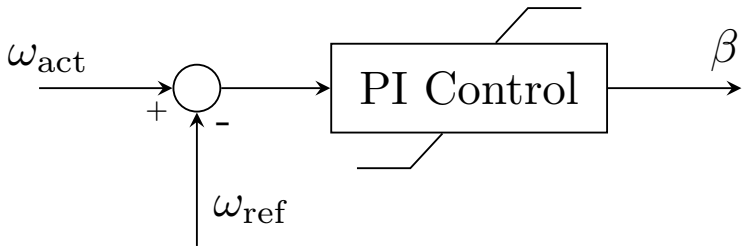

Figure 3.8: The aerodynamic modelling of a wind turbine. Adapted from [13].

Similar to the Equation (3), the mechanical power of the turbine is calculated with the given pitch angle β, the turbine rotor rotation speed ω_{t} and the wind speed v_{wind}. The calculated mechanical power P_{m} is then fed with the measured output electrical power P_{e} to the shaft dynamics as shown in Figure 3.9. [13]

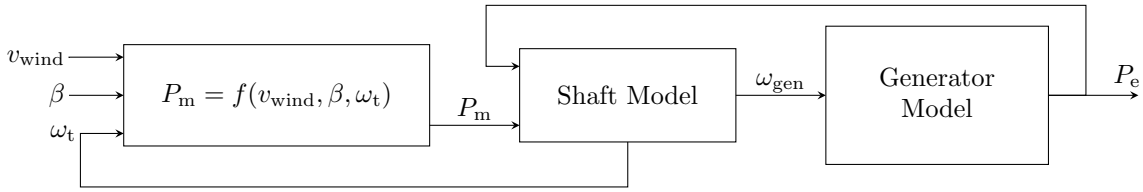

Figure 3.9: The mechanical modelling of a wind turbine. Adapted from [13].

Generally, the mechanical control is modelled as a two-mass equivalent in double fed induction generator. These two masses are the high speed mass of the turbine and the low speed rotor of the generator. This is due to precise modelling of the damping coefficient between these masses. In FC generator, the two-mass modelling is not required normally. This is a result of the decoupling of the generator from the grid. [13]

Subsequent to the calculation of the optimal generator speed in the shaft dynamics of the turbine, the generator rotor speed is then fed to the generator model. Up to this point the modelling of both DFIG and FC generator wind turbine have been fairly the same, except for the possibility to disregard the two-mass modelling in the FC generator. After the mechanical control, the dynamic modelling of the generator and controlling components related to it will differ. The generator models are individually specified next. [13]

Double Fed Induction Generator Dynamic Model

A DFIG is modeled as a simple wound rotor induction machine. The stator- and rotor-circuits of the machine are energized. Thus, both stator and rotor winding are involved in the process of electricity production. Therefore, the modelling of the DFIG is nearly the same as the modelling of an induction machine. The only difference is that the rotor voltages are supplied by the DFIG rotor-side converter. The technical details of the induction machine modelling and the reference frame theory can be found in the following literature [26–28]. The details are no further discussed in this thesis.

Alternatively, studies [29, 30] have also represented the DFIG as an equivalent controlled current source shown in Figure 3.10. This simplification neglects all the mechanical state variables of the generator rotor. Due to the need for a rapid response of the converter, the flux dynamics are also disregarded. The current source resembling the generator model calculates the needed injection of active and reactive current I_p and I_q respectively. The injection currents are calculated from the flux and active current commands received from the electrical control. The reactance X'' illustrated in the figure describes the subtransient reactance.

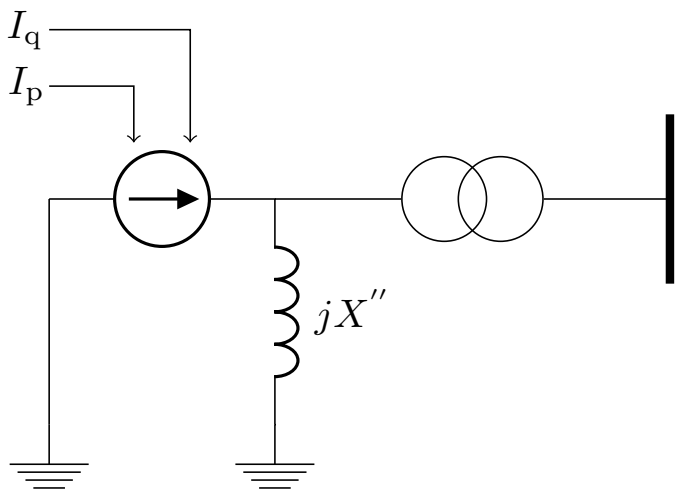

Figure 3.10: The alternative dynamic model of a double fed induction generator. Adapted from [29].

The control system of the generator includes the control systems of the rotor-side and the grid-side converters. Simplified block diagram of the control system of rotor-side converter is presented in Figure 3.11. In this generic control scheme, the active power P_G and reactive power Q_G of the generator are controlled separately in the rotor-side converter. In addition, the converter controls are tuned with certain control loops in order to reach the controlled parameters to the reference values. The loops can be achieved with PI controllers shown in the figure. The first PI controller from the left defines the reference current values i_dR and i_qR while the second PI controller defines the dq-axis modulation indices V_dR and V_qR of the rectifier. [31]

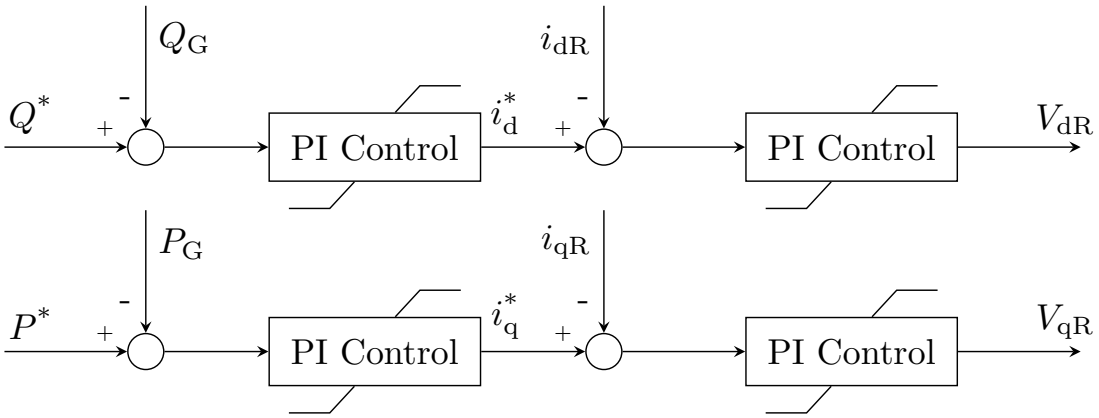

Figure 3.11: The block diagram of the rotor-side converter controls of a DFIG. Adapted from [31].

Respectively, in the grid-side converter shown in Figure 3.12, the DC-link voltage V_{dc} and the reactive power Q_{T} are controlled. Similar to the rotor-side converter, the first PI controller from the left defines the reference current values i_{dI} and i_{qI}. The second PI controller defines the modulation indices P_{mdI} and P_{mqI} of the inverter. [32]

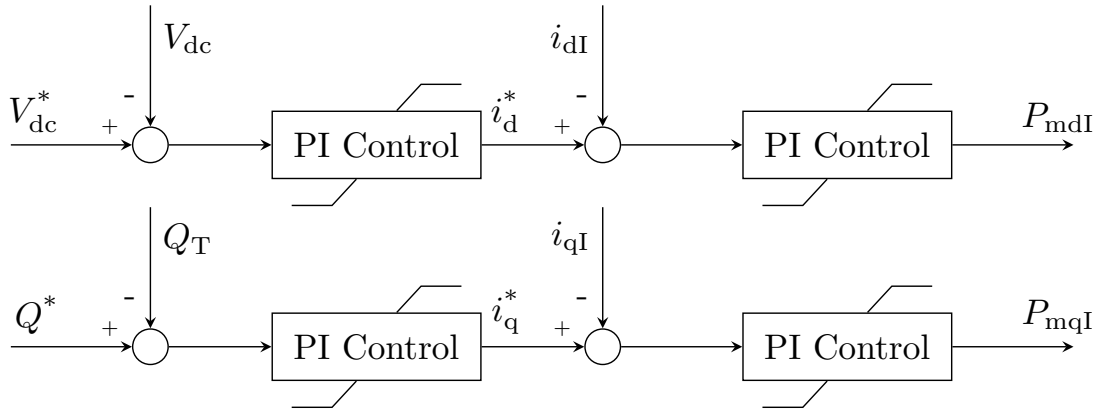

Figure 3.12: The block diagram of the grid-side converter controls of a DFIG. Adapted from [32].

Full Converter Generator Dynamic Model

In contrast to a DFIG, a full converter generator is commonly modelled as a synchronous generator. Models with an asynchronous, a permanent magnet synchronous (PMSG) or an electrically excited synchronous generator are also possible. Alternatively, as was introduced in the DFIG modelling, the FC generator can be modelled as a current source as well. [29, 30, 32]

The rotor-side converter is used to control the generator voltage and the output active power illustrated in Figure 3.13 for a full converter PMSG. The controlled parameters are the AC voltage of the generator V_{acG} and the active power output P_{G}. Similar to DFIG controlling, the outer PI controller defines the reference current

values i_{dR} and i_{qR} while the inner PI controller defines the dq-axis modulation indices P_{mdR} and P_{mqR} on the rectifier side. [32]

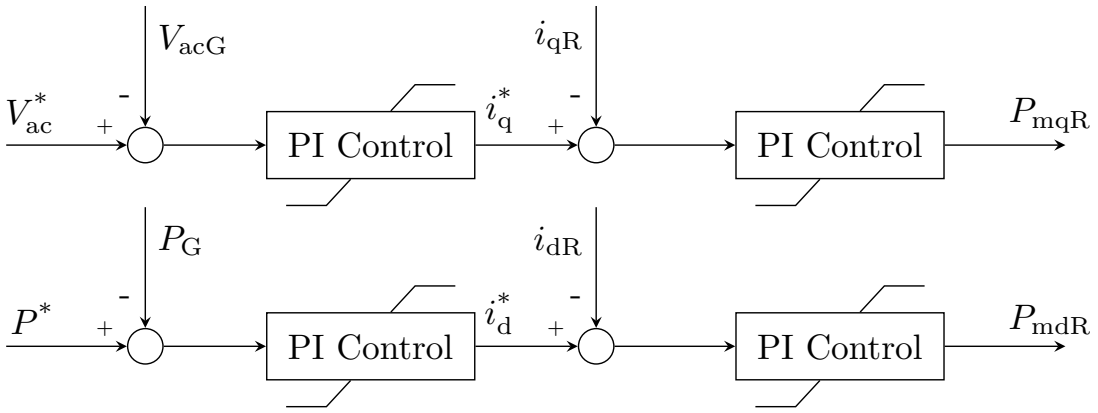

Figure 3.13: The block diagram of the rotor-side converter controls of a FC generator. Adapted from [33].

The grid-side converter of a FC generator controls the same parameters as the DFIG grid-side converter: DC-link voltage and reactive power output of the generator. The control method has already been illustrated in Figure 3.12. [32]

Modelling the Protection Schemes

The protection scheme of the turbine dynamic model can be implemented as logic statements. With the measurements of the terminal voltage and network frequency at the terminals of the machine, the statements can be set as such that the operation follows the given conditions. When a certain minimum or maximum value is reached, the logic statement activates the protection schemes. This protection scheme is used for example in the DC-link braking resistor mentioned in Section 3.1.3. [13]

3.2.2 Aggregation of Multiple Wind Turbines

It is common to model wind farms as a single equivalent machine in dynamic modelling. This is because modelling and simulating dozens of individual units can be inconvenient. In addition, a system represented in per unit values can be scaled straightforward. In the aggregation of multiple wind turbines, a single wind turbine generator model can be scaled to represent the complete power plant. One must note that the aggregated single equivalent generator model might not adequately correspond the actual wind farm. A wind farm with multiple feeders with various lengths, the response of each individual turbine or turbine group is likely different in a system disturbance. Also, the wind farm may include different generator technologies having different characteristics as was discussed in Section 3.1.2. [13]

The aggregation can be divided into three different methods: the single unit presentation, the cluster presentation, and the compound presentation. The single unit presentation is the method mentioned at the beginning of this section. All the

wind turbines in a wind farm are presented as a single equivalent wind turbine. The equivalent wind turbine power output and the rating have been multiplied by the number of wind turbines in the farm. This type of aggregation requires that the wind speed, and thus the power output, is assumed to be the same for every turbine. If the wind speed differ between individual turbines, the cluster aggregation method can be used. [15, 34]

The cluster presentation separates the turbines with different wind speed. Thus, the model has as many aggregated turbines as there are different wind speeds. The third method is somewhat a mixture of the other methods. It involves the aggregation of the electrical system, consisting of the electrical controls and the electrical parts of the generators. The mechanical characteristics are individually modelled. Generally, in transient stability studies the wind speed is assumed constant. Also, the mechanical behaviour has neither a large impact on voltages nor on power flows at the connection point. Therefore, it is justified to use the single equivalent representation in most studies. [15, 34]

As it has been discussed in the earlier chapters, the preservation of the power system stability necessitates certain requirements from the power plants connected to the grid. These requirements include the fault ride through of the power plants. Also, to provide addition stability to the system, fault current contribution can be requested from the converter based power plants. Therefore, the fault current contribution of wind power plants is presented next in Chapter 4.

4 Fault Current Contribution of Wind Power Plants

The following chapter presents the fault current contribution of wind power plants from multiple perspectives. First, the network connection requirements for the wind power plants related to the fault current contribution are discussed in Sections 4.1 and 4.2. Secondly, research related to the fault current contribution is reviewed in Section 4.3. Thirdly, in Section 4.4 the new regulation on the requirements for the grid connection of a generator is shortly presented. Last, fault current contribution requirements in selected countries are illustrated in detail in Section 4.5.

4.1 Requirement for Fault Ride Through

To secure a reliable operation of the network, a loss of a considerable amount of wind power supply is not acceptable in terms of power system stability. The disconnection of several wind power plants would deviate the load and generation balance. This would have an impact on the frequency of the system. Eventually, more spinning generation reserves would be needed. To prevent this need for new spinning reserves, it is required that the wind power plants remain in operation and connected to the system throughout the fault. The technical details regarding to how different variable speed wind turbine types manage this was explained in Section 3.1.3. [19]

The fault ride through requirement for a wind turbine can be represented with a voltage dip curve as a function of time. According to the IEC standards, a voltage dip is defined as ”a sudden reduction of the voltage at a particular point on an electricity supply system below a specified dip threshold followed by its recovery after a brief interval”. The dip is primarily caused by a short-duration increase and termination of short-circuit current in the network. Thus, the magnitude of the current and the measured location determines the voltage magnitude of the dip. [35]

Figure 4.1 represents an example of how the fault ride through can be requested. This figure is taken from the grid code of Finnish transmission system operator (TSO) Fingrid Oyj. The given example is determined for power plants with a rated capacity of at least 100 MW. The line indicates the voltage dip occurring at the VJV Reference Point. In some grid codes, this reference point is called the point of common coupling (PCC). The VJV Reference Point is the point where the network requirements must be fulfilled. In wind power plants connected to high voltage network, the location of VJV Reference Point in this grid code is defined as the high voltage side of that step-up transformer, which is electrically closest to the connection point of the plant. During and after this sort of fluctuation of voltage at the VJV Reference Point, the power plants are required to stay connected to the grid and continue operation. [8]

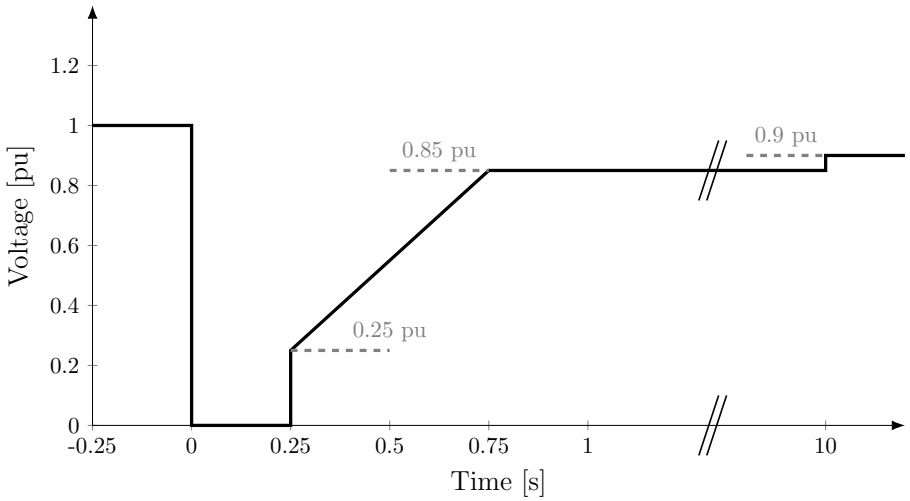

Figure 4.1: An example of a voltage dip occurring at the VJV Reference Point in Fingrid Oyj grid code. The wind power plant is required to continue operation normally at and above the shown line. Adapted from [8].

The duration of the voltage dip depends on the network conditions and the response time of the protection system clearing the fault. In addition, the curve form can be different in certain national grid codes according to the reference measure point. One must take into account that both asymmetrical and symmetrical faults can occur in the network. Therefore, different fault type can have different requirements. The requirements for a wind farm can also vary according to the voltage level and the rated power of the plant. [36]

During the voltage deviation, wind power plants can also provide fault current support to the grid. As it was discussed in Section 3.1.3, wind turbines equipped with converters can control both active and reactive current output to the system. This useful characteristic can be exploited in the active and reactive current contribution represented next in Section 4.2.

4.2 Requirement for Active and Reactive Current Contribution Under Disturbances

Similar to synchronous machines discussed in Section 2.1, the main concept of active and reactive current response of a wind turbine is to provide voltage and frequency stability to the network in normal conditions and after disturbance. In addition, the recovering time from the disturbance plays an important role. Thus, active and reactive current responses can be requested to provide enhanced stability to the system. This requirement can be managed with the wind turbines equipped with converters. [36]

To maintain the voltage stability of the power system, the support and rapid restoring of voltage subsequent to a disturbance is crucial. Without proper voltage control and rapid response times, both voltage and transient stability can be lost. Thus, active and reactive current contribution is commonly required in relation

to the voltage drop seen by the wind power plant. The technical details and the difference between the active and reactive current response of individual generator types were illustrated in Section 3.1.3. The fault current contribution and power recovery requirements in the individual grid codes of selected countries are later discussed in detail in Section 4.5. [36]

This requirement has attracted more attention in recent years due to the growing capacity of wind power plants in power systems. Especially the reactive current injection during the fault has been widely researched. Also, various injection requirements have been implemented in the grid codes. The requirement for a certain active power recovery time subsequent to a disturbance has also become more common in the national grid codes. Prior to the presentation of the requirements in certain countries, some of the research related to the fault current contribution are reviewed next in Section 4.3. [36–40]

4.3 Research Related to Fault Current Contribution of Wind Power Plants

The fault behaviour of wind turbines was analysed in [36]. One of the sections reviewed the voltage support from wind power plants in a weak network. This study indicated that the decision about a support scheme becomes more relevant in a weak network. The network was defined as weak when the ratio between the short-circuit power at the point of common coupling and the wind power plant capacity was far less than 10. The study illustrated that also with a low X/R (the reactance of the system in proportion to the resistance of the system) ratios, the coordinated injection of both active and reactive current is beneficial for voltage support during and shortly subsequent to the fault. In addition, fast active power recovery was said to be advantageous with a low X/R ratio.

The study in [37] presented the impact of different mitigation methods on transient instability with wind power plants. The study compared wind power plants with either limited voltage support, support with synchronous compensators, or support with either active or reactive current contribution. The results suggested that the most effective mitigation measure for transient instability issues was the prioritization of active current in proportion to retained voltage. Meanwhile, reactive current was provided up to the generator rating. The additional voltage support with the reactive current priority was said to be leading to incidental tripping of units.

The impact of reactive current contribution on PCC voltage and the rotor angles of nearby synchronous generators was evaluated in [38]. The traditional unity power factor operation was compared with the additional reactive current contribution. The results indicated that when the modelled wind power plants were providing 2 % (on a per unit base) of reactive current in proportion to 1 % voltage drop, the power system was improved during disturbances. In addition, the effect of increased reactive current contribution from 2 % to 4 % in proportion to 1 % voltage drop was studied. This increment resulted in even further improvements in the power system stability.

In [39], the effect of post-fault active power ramp rate on the transient stability of a power system was reviewed. This study declared that depending on the location of the wind power plants, the transient stability can be either improved or weakened. In areas with higher generation capacity, the impact of wind power plants on critical fault clearing time was relatively less when compared with the lower generation capacity area. In addition, when the active power ramp rate was reduced from 2 pu/s to 0.5 pu/s in the exporting areas, an improvement in the transient stability margins was seen. The faster deceleration of the synchronous machine was enabled by the provision of more kinetic energy to the local loads during the critical first swing.

The research in [40] compared the impact of different wind turbine technologies on power system stability. The comparison was between a DFIG and a FC generator. The DFIG operated with a constant power factor, whereas the FC generator operated with a variable power factor (e.g., additional active and reactive current contribution control). The results showed that the reviewed critical clearance time was increased, and the first rotor angle swing decreased, if the wind power plants were modelled as FC generators compared with DFIG generators.

4.4 Network Code on Requirements for Grid Connection of Generators Regulation

According to the European Network of Transmission System Operators for Electricity (ENTSO-E), the development of new and consistent network connection requirements is mandatory for ”a secure, competitive and low carbon European energy sector and a pan-European Internal Energy Market”. Thus, new network codes consisting of the grid connection, the system operation and the electricity market have been prepared during the past few years. These network codes also include the Network Code of Requirements for Generators (NC RfG). [41]

The development of the NC RfG was requested by the European Commission. The regulations were assessed by the Agency for the Cooperation of Energy Regulators (ACER) and was later submitted to the European Commission. The NC RfG was finalized and agreed by the Member States in the comitology procedure. The regulation 2016/631 with the implemented network codes was commissioned in 14th of April 2016. The Member States and their transmission and distribution system operators (DSOs) affected by this regulation have a three-year transition period. During this period, the operators are required to update their own network connection requirements according to the regulation. [41, 42]

The requirements in the NC RfG are said to be ”non-exhaustive”, meaning that the network codes are not meant for full harmonization all over the European Union. This partial freedom gives the relevant TSO or DSO judgement of own on the specifications and parametrising of those requirements. This regulation also includes the fault current contribution and active power recovery requirement. [41–43]

The fault current contribution requirement is declared in Article 20. The Article states that the relevant system operator in coordination with the relevant TSO has the right specify whether a power park module (non-synchronously connected or

connected through power electronics to the network) has to provide fast fault current at the connection point in case of a symmetrical (3-phase) as well as an asymmetrical (1-phase or 2-phase) fault. The fast fault current is presented as "a current injected by a power park module or HVDC system during and after a voltage deviation caused by an electrical fault with the aim of identifying a fault by network protection systems at the initial stage of the fault, supporting system voltage retention at a later stage of the fault and system voltage restoration after fault clearance". The actual details of the requirement are left to be specified by the system operator. [42]

The post-fault active power recovery requirement is also declared in Article 20. The details are left to be particularized by the relevant TSO. The Article denotes that the relevant TSO will specify when the post-fault active power recovery begins, a maximum allowed time for the recovery, and the magnitude and accuracy of the recovery. The latter two of the requirements are based on a voltage criterion. [42]

Even though the declared requirements are "non-exhaustive", the new regulations give a perspective on which requirements are, or are to become, important in the power system in terms of its robustness and stability. The following Section 4.5 gives a detailed review on the requirements under discussion in the present grid codes of selected TSOs.

4.5 Detailed Fault Current Contribution Requirements in Certain Countries

This section presents the fault current contribution and active power recovery requirements for wind power plants in certain countries. Every country has its own transmission system operator. Some countries have several operators. The transmission system operators are responsible for the grid code requirements for power plants connected to their transmission network. The countries selected for the fault current contribution requirement review, their TSOs, the grid code titles and the date of issues are shown in Table 1.

Table 1: The transmission network grid codes from the selected countries

Country	TSO	Title of the grid code	Date of issue
Canada	Hydro-Québec[1)]	*Transmission Provider Technical Requirements for the Connection of Power Plants to the Hydro-Québec Transmission system [1]*	February 2009
Denmark	Energinet.dk	*Technical regulation 3.2.5 for wind power plants with a power output above 11 kW [2]*	10th of June 2015
Germany	Multiple[2)]	*TransmissionCode2007 Network and System Rules of the German Transmission System Operators [3]*	August 2007
Great-Britain	National Grid	*The Grid Code Issue 5 Revision 15 [4]*	3rd of February 2016
Ireland	Eirgrid	*EirGrid Grid Code Version 6.0 [5]*	22th of July 2015
Norway	Statnett	*Functional Requirements for the Norwegian Power System [6]*	1st of September 2012
Sweden	Svenska Kraftnät	*Affärsverket Svenska Kraftnäts...*[3)] *[7]*	25th of October 2005

[1)] Hydro-Québec was selected from several TSOs in the region.
[2)] Due to having four separate TSOs in their region, the grid code reviewed is the TransmissionCode2007, which affects each of the TSO in Germany.
[3)] Affärsverket Svenska Kraftnäts Föreskrifter och Allmänna Råd om Driftsäkerhetsteknisk Utformning av Produktionsanläggningar.

As it has been explained in Sections 3.1.3 and 4.2, the reactive power response, and thus the reactive current contribution from the plants have become more common in the grid codes of transmission networks. These responses are needed for the voltage regulation and support of the system. As the new regulation proposes, more changes to the current grid codes are to become. In the German grid code, the following

Figure 4.2 illustrates the required behaviour from wind power plants for voltage support during a network fault. Y-axis determines the required reactive current injection. The value is calculated from the change in delivered current ΔI_{B} prior to the disturbance to during it. This value is proportioned to the maximum current capacity I_{n} of the plant. Furthermore, x-axis determines the change in voltage ΔU from prior to disturbance to during it. This is further proportioned to the nominal voltage U_{n}. [3]

The grid code *TransmissionCode2007* requires the additional reactive current to be supplied at the grid connection point during a more than 10 % of an effective value drop of the generator voltage. The required amount of reactive current should be at least 2 % of the rated current per percent of the voltage drop. This ratio is expressed with the slope of the line in the figure. The ratio is measured on the low-voltage side of the generator transformer. The control response time in which the reactive power must be fed into the network, should be less than 20 ms. The supply should also extend to 100 % of the rated current. These characteristics need to be maintained at least for an additional 500 ms after the voltage is returned to the deadband range. In addition, the active power supply must be recovered immediately subsequent to the fault clearance. The original value should be accomplished with a gradient of at least 20 % of the nominal capacity per second. [3]

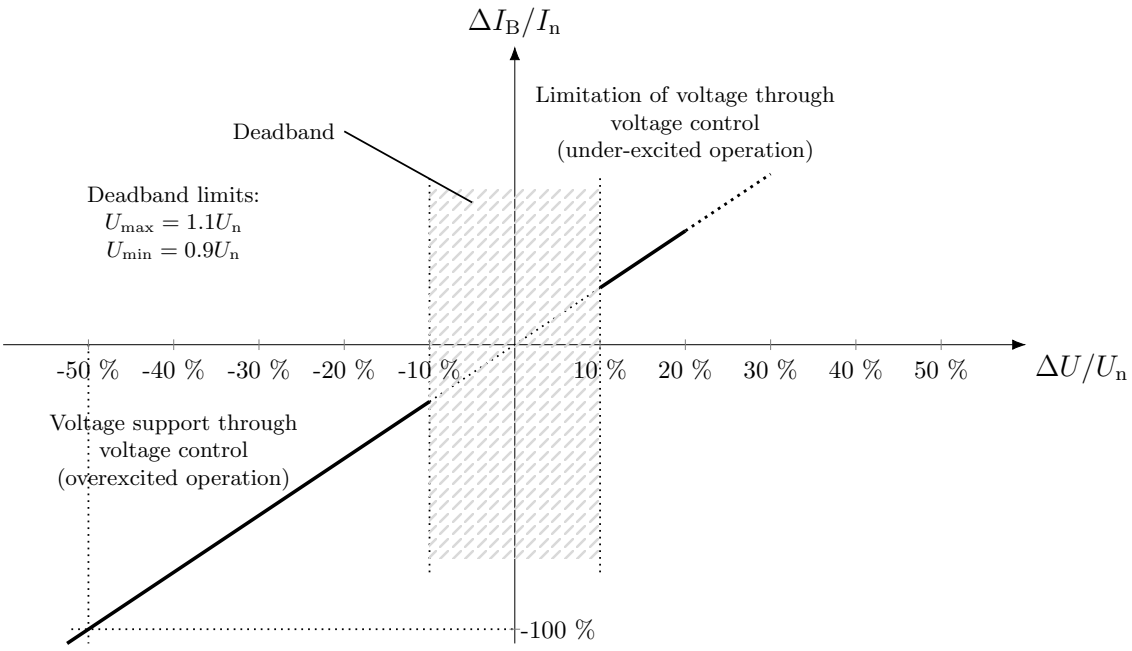

Figure 4.2: Required reactive current injection in proportion to the voltage drop from the renewable-based generating units in *TransmissionCode2007* Grid Code. Adapted from [3].

In contrast to *TransmissionCode2007*, in *EirGrid Grid Code*, the priority of disturbance support is given to the active current response. The controllable wind farm should provide at least 90 % of its maximum available active current, or maximum permitted active current set by the TSO, whichever is lesser. The injection

should be as quick as possible, but in any event within 500 ms when the voltage has been recovered up to 90 % of the nominal voltage in a fault clearing time of less than 140 ms. The injection should occur in less than 1 second when the fault clearing time is longer. It is said that the reactive current response must be within the rating of the wind farm with a rise time of no longer than 100 ms. Its amount should be at least proportional to the voltage dip. The settling time should be no longer than 300 ms. In addition, the pre-fault reactive control mode should be recovered within 500 ms of the voltage return to the normal operating range set by the TSO. According to the grid code, the reactive current response can be managed with either the actual wind generators or other dynamic reactive devices on the site. Also, a combination of both is allowed. Nevertheless, as stated in the grid code, first priority is given to the active current response. [5]

The Danish grid code determines different requirements for different rated power capacities of the wind power plants. The categories are A, B, C and D. In category A, the maximum power output is above 11 kilowatt (kW) up to and including 50 kW. In category B, the maximum power output is above 50 kW up to and including 1.5 megawatt (MW). In category C, the maximum power output is above 1.5 MW up to and including 25 MW. The remaining category D includes all the wind power plants with the maximum power output above 25 MW. [2]

According to the Danish grid code, category A and B wind farms have no requirements for current injection. Then again, category C and D wind farms are required to provide reactive current according to Figure 4.3. Y-axis determines the voltage drop in percentages on the wind turbine terminal from the normal operating voltage value U_{c}. In contrast, x-axis determines the required reactive current injection I_{Q} in proportion to the rated current I_{n}. The rated current I_{n} is the maximum continuous current designed to be delivered by the wind power plant. Area A determines the area in which the wind power plant must stay connected to the network and maintain normal production. Area B determines the required fault current priority. Area C determines the area in which the disconnection of the wind power plant is allowed. [2]

The reactive current control should follow the characteristics of the shown curve latest after 100 ms of the beginning of injection with a tolerance of ± 20 % within the design specifications of the unit. In area B of the figure, the first delivery priority is given to the reactive current, and the second to active current. The requirement is told to be valid in three-phase faults, and subsequent to the disconnection of all types of asymmetrical faults. In addition, the reduction in the active power is acceptable, but the power is encouraged to be maintained if possible. However, the farm should be able to provide active power no later than five seconds subsequent to the normalization of the operation at the point of connection. [2]

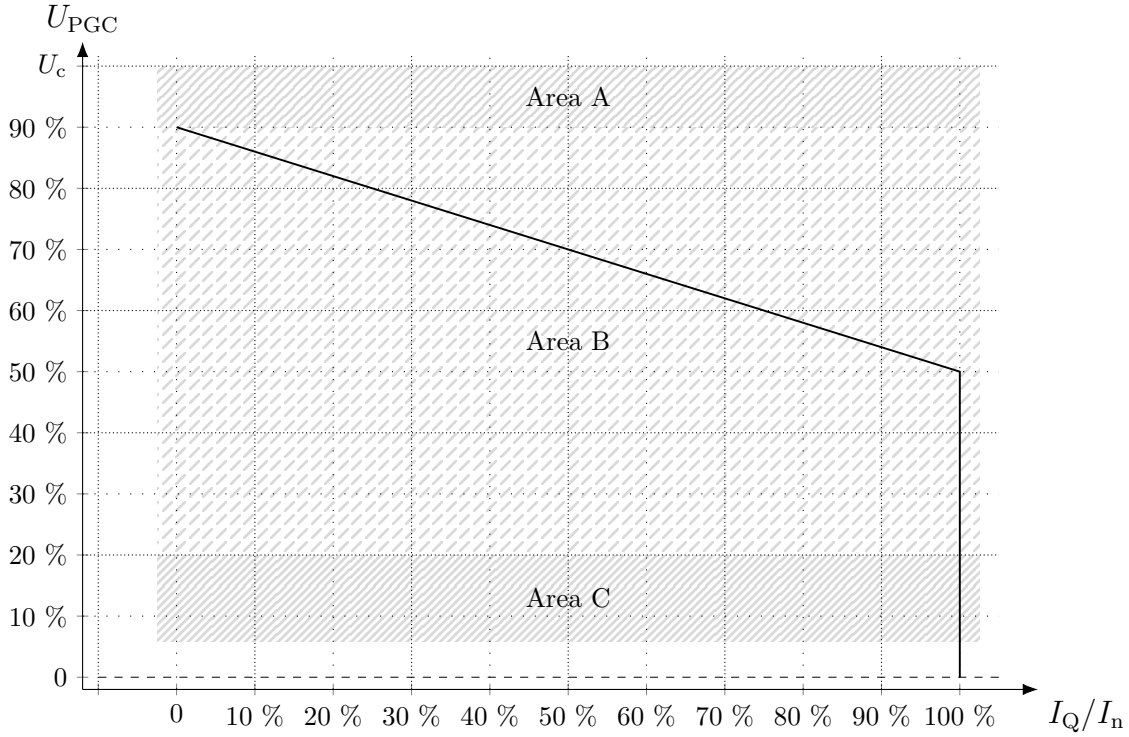

Figure 4.3: Reactive current injection required in case of a voltage drop for category C and D wind power plants in Energinet.dk grid code. Adapted from [2].

In the British grid code, the requirements are specified according to the fault duration. Wind farms are required to generate the maximum reactive current without exceeding the rating limit when the voltage dip exceeds the given normal operation limits. This requirement holds in case of the short-circuit fault lasts less than or up to 140 ms. In addition, the active power output should be restored at least up to 90 % of the pre-fault level no later than 500 ms subsequent to the stabilization of the voltage to the range of normal operation. On the contrary, if the fault lasts longer than 140 ms, wind farms are required to restore their active power output in no less than 1 second subsequent to the restoration of the voltage. This requirement holds for both on- and offshore wind farms. Exceptions for active power restoring are given to the units that have needed to reduce their active power output. [4]

Canadian, Swedish and Norwegian grid codes do not contain any specific current injection requirements nor any active power recovery times for wind power plants. However, they do require, as all the other grid codes, the wind farms to stay in service up to the given limits, and contribute to the voltage and frequency regulation of the grid. [1, 6, 7]

5 Designing the Simulations

In this chapter, the wind power plant models used in the simulations of this thesis are presented in Section 5.1. Secondly, the impact of parameter variation on the behaviour of the wind power plant models is discussed in Section 5.2. Thirdly, in Section 5.3 the methods for analysing the power system stability are described. Last, the adapted cases for the simulations are shortly reviewed in Section 5.4.

5.1 Wind Power Plant Models

The following section presents the wind power plant models used in the simulations. In addition, some of the parameters related to these models are presented.

5.1.1 Wind Power Plant Models From Western Electricity Coordinating Council

The following sections illustrate two generic wind turbine models from Western Electricity Coordinating Council (WECC). First section presents the double fed induction generator dynamic model and second the full converter model. The Electric Power Research Institute (EPRI) has prepared the reviewed models, whereas the guideline has been created by the Renewable Energy Modeling Task Force of WECC. The description of the parameters and the values used in the related models are found in Tables E.1, E.2, and E.3 of Appendix E. The model chosen for this study was the full converter model without the drive-train module. This model represents other converter power plants to some certainty as well. [44, 45]

These generic wind power plant models made it possible to variate selected parameters of the power plants related to this thesis. These parameters are occasionally hard-coded in the specific models of certain wind turbine manufacturers. In addition, manufacturer models are more complicated and include more parameters. Similarly modelled power plants can also cause less interaction complications. Nevertheless, too specific models are commonly not necessary in the long-term planning of the power system. It is not known what kind of wind power plants will be manufactured in the future. Thus, it is justified to use the generic models.

The parameter values were selected according to the guideline, the report, and earlier practices. Some of the values were altered to fulfil three network connection requirements for wind power plants in the grid code of Fingrid Oyj. First requirement is that the response time of reactive power injection of the plants is less than a second. This is calculated from zero to 90 % change in reactive power. Second requirement states that the overshoot of the reactive power response is less than 15 % from the overall change. Last one requires that the response should settle at the target value in less than three seconds from the beginning of the impulse. In addition to these requirements, certain control modes are presumed in the grid code. These control modes are later reviewed. [8]

Double Fed Induction Generator Dynamic Model

The model in Figure 5.1 presents the double fed induction generator dynamic model.

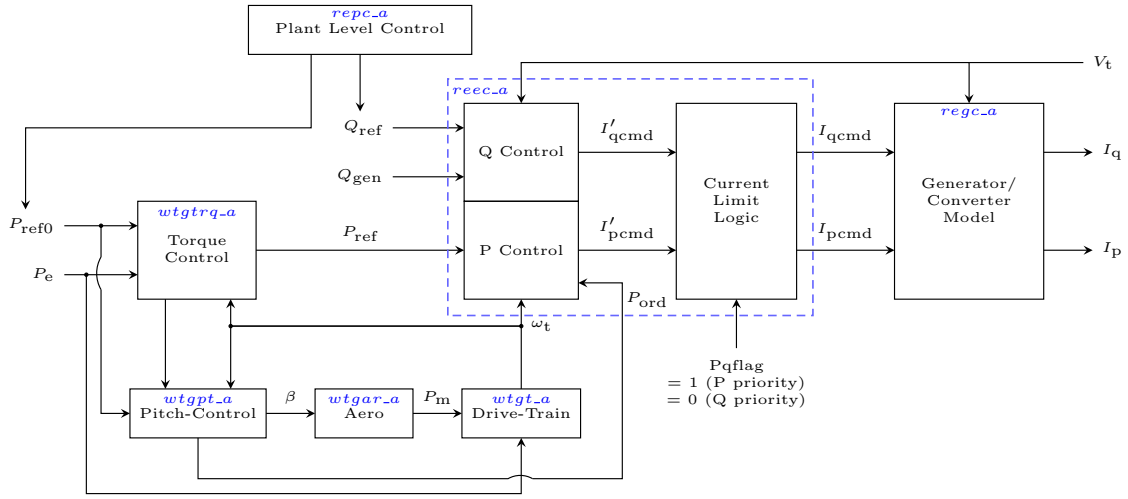

Figure 5.1: The generic wind turbine model of DFIG. Adapted from [44].

As the figure 5.1 illustrates, the model has been separated into modules presented with blue labels. The model consist of seven modules:

1. the wind power plant controller (repc_a),
2. the electrical control (reec_a),
3. the generator and converter (regc_a),
4. the torque controller (wtgtrq_a),
5. the pitch controller (wtgpt_a),
6. the aerodynamic (wtgar_a), and
7. the drive-train (wtgt_a) module.

Similar to the models presented in Section 3.2, these modules require certain inputs to have certain outputs. Since this thesis focuses on the fault current contribution of the wind turbines, the modules one to three representing the electrical controls are further discussed in next sections. [44, 45]

The Wind Power Plant Controller Model

The following Figures 5.2 and 5.3 present the power plant level controller module. The details of the parameters related to these modules are found in Table E.1 of Appendix E.

The module shown in Figure 5.2 is used to emulate the plant-level voltage or reactive power control. The control modes are either user specified bus voltage

control or user specified branch reactive power control. Thus, the controller has the inputs of either voltage reference V_{ref} and measured voltage V_{reg}, or reactive power reference Q_{ref} and measured reactive power Q_{gen} at plant level. The inputs depend on the switch $Vcompflag$ controlling the mode. In addition, the voltage control has an option for line drop compensation or droop and deadband, whereas the reactive power control has only deadband option. Nevertheless, the output reactive power command Q_{ext} is one of the input of the reec_a module as was shown in the complete model in Figure 5.1. [45]

In the simulations, the voltage control with the reactive droop mode was used. These modes were selected according to the required operation of the plants in the Fingrid Oyj grid code. This grid code requires that the wind power plant is able to operate the voltage of the reference point. In addition, the droop of the reactive power needs to be adjustable from 1 % to 10 %. Thus, in the model, the *RefFlag* switch was set to one and the *Vcompflag* mode was initialized as zero. In addition, the parameters related to the step response of the voltage control were set to constant, even though the connected power plants have different short-circuit powers. Although not optimized, it was found that the response was within the limits of the requirements for all the modelled wind power plants with the given constant values. All the parameter values of this model can be found in Appendix E in Table E.1. [8]

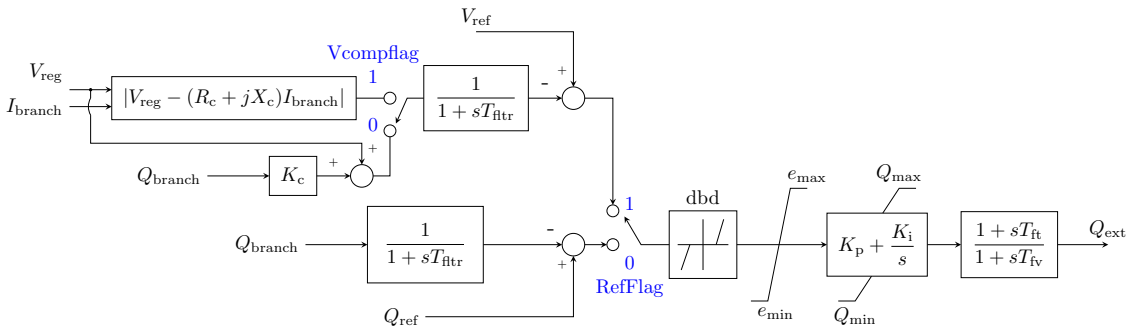

Figure 5.2: The DFIG wind power plant reactive power controller model. The parameters and their values related to the model are found in Table E.1 of Appendix E. Adapted from [44].

The controller module in Figure 5.3 emulates the active power control. This is achieved by the inputs of reference power $P_{\text{plant,ref}}$, measured generated power P_{branch} and both measured and reference frequency f and f_{ref} respectively. The output active power P_{ref} is connected to the reec_a module. However, this frequency control module was neglected in the simulations by setting the F_{flag} as zero. Thus, P_{ref} was initialized as a constant. [45]

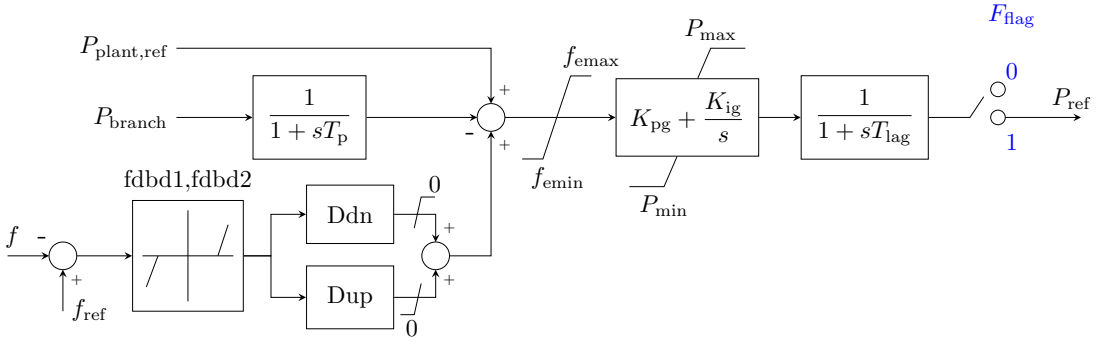

Figure 5.3: The DFIG wind power plant active power controller model. This module was neglected in the simulations. Adapted from [44].

The Electrical Control Model

The electrical control model is shown in Figure 5.4. The module has active power reference P_{ref} and reactive power reference Q_{ref} as inputs. These inputs can either be initialized as constants or fed by the power plant controller model. This model also has an feedback input of the generated reactive power Q_{gen}. [45]

There are three possible normal state control options are available for this model: a constant power factor, a constant reactive power, and an initialized reactive power from the power plant controller model. The fourth control option is the selection between active or reactive current contribution priority during a voltage dip. Desired settings are controlled by the switches *PfFlag*, *VFlag*, *QFlag*, *Pflag*, and *Pqflag* shown in blue in the figure. The outputs of the model are the active I_{pcmd} and reactive I_{qcmd} current command that are inputs of the generator and converter model presented in the next section. [44, 45]

In this thesis, the control mode of the electrical control model was the initialization of reactive power from the power plant controller model. This was selected due to the wanted voltage control of the plant. Thus, the *PfFlag* switch was set to zero. In addition, the *QFlag* switch was also set to zero. This mode was selected to bypass the interaction of having both generator level and power plant level voltage control. In addition to the above settings, the active power control was not set as rotor speed dependant. Therefore, the *PFlag* switch was set to zero as well. The fault current contribution mode at the uppermost part of the figure was set to activate when the controlled voltage was seen to fall below 0.9 pu. The freezing of this state for a certain time after the fault clearing was neglected. The *Pqflag* was varied according to the simulation. [45]

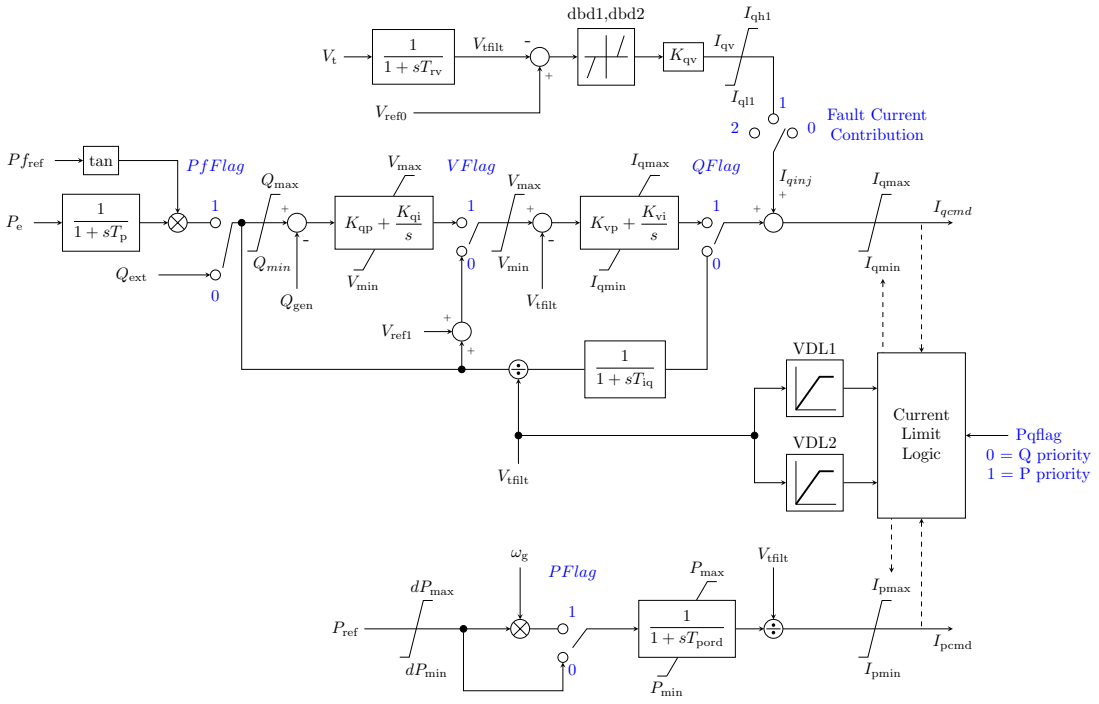

Figure 5.4: The DFIG electrical control model. The parameters and their values related to the model are found in Table E.2 of Appendix E. Adapted from [44].

The Generator and Converter Model

The following Figure 5.5 presents the generator and converter model of a wind turbine. The model processes the active I_{pcmd} and the reactive current commands I_{qcmd} and injects the active I_{p} and reactive I_{q} current into the grid model. The model contains two blocks named as the "high voltage reactive current management" (HVRCM) and "low voltage active current management" (LVACM). The HVRCM block can be set to limit the reactive current injection in high voltage conditions. In addition, the LVACM block can be set to limit the active current injection in low voltage conditions. The injection of active current in low voltage conditions can also be varied with the low voltage power logic *Lvplsw* switch. This switch was initialized as zero in the simulations. This mode was selected to let the maximum current limit logic determine the injection of both active and reactive current. The values of the other parameters are found in Table E.3 of Appendix E. [44, 45]

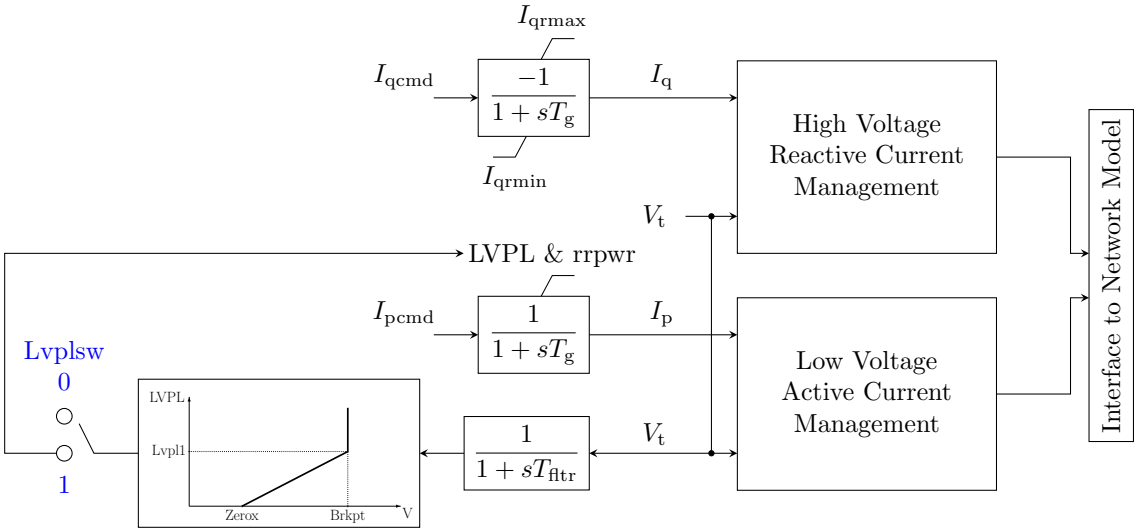

Figure 5.5: The DFIG generator and converter model. The parameters and their values related to the model are found in Table E.3 of Appendix E. Adapted from [44].

Full Converter Generator Dynamic Model

The model in Figure 5.6 illustrates the full converter generator model which is quite similar to the DFIG model. The only difference is that modules presenting the pitch control, torque control and aerodynamic control of the turbine are neglected. Thus, FC generator model has only four modules. Controls inside these modules are modelled the same as in the DFIG model. Therefore, they are not repetitively explained. [45]

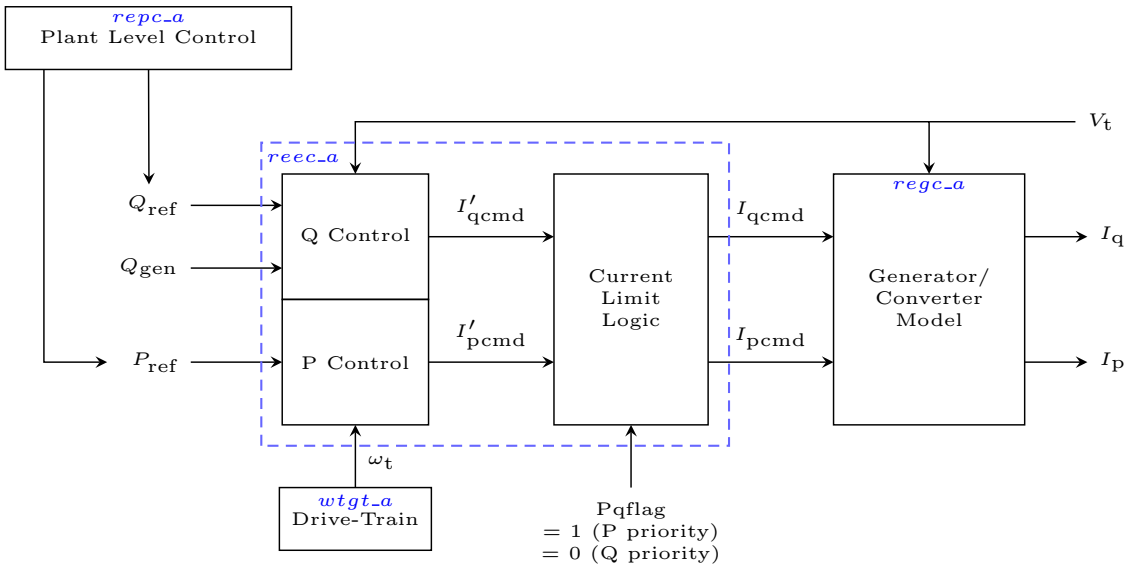

Figure 5.6: The FC generator wind turbine model. Adapted from [46].

Dynamic models shown in this section can be used to simulate the wind turbine characteristics with different simulation programs. In some countries wind power plant operators are forced to provide dynamic models of their power plants for system operators. These models can be used to emulate the real life operation behaviour of the turbines with certain resolution. The emulation can be used to determine whether the wind power plant can pass the common network connection requirements regulated by system operators. Also, the models are commonly used in the long-term power system planning. The variation logic of selected parameters as well as the analysing methods are presented next. [8]

5.2 Impact of Parameter Variation on the Behaviour of the Model

The following section illustrates how the variation of selected wind power plant parameters affect on their dynamic behaviour. First, the selection between active or reactive current contribution priority is discussed in Section 5.2.1. Then, the affect of reactive current gain variation on the behaviour of the plant is explained in Section 5.2.2. Finally, the impact of the active power recovery time variation is presented in Section 5.2.3.

5.2.1 Variation of Fault Current Contribution Priority

The selection between the active and reactive current contribution priority of the wind power plant is set by the electrical control model shown earlier in Figure 5.4. The current limit logic is defined with multiple functions depending on which current is prioritized. If reactive current prioritization is activated, the logic works as follows:

$$I_{\text{limits}}^{\text{Q-prio}} = \begin{cases} I_{\text{qmax}} = \min\{VDL1, I_{\text{max}}\} \\ I_{\text{qmin}} = -I_{\text{qmax}} \\ I_{\text{pmax}} = \min\left\{VDL2, \sqrt{I_{\text{max}}^2 - I_{\text{qcmd}}^2}\right\} \\ I_{\text{pmin}} = 0 \end{cases} \tag{5}$$

Alternatively, in active current prioritization the logic is following:

$$I_{\text{limits}}^{\text{P-prio}} = \begin{cases} I_{\text{qmax}} = \min\left\{VDL1, \sqrt{I_{\text{max}}^2 - I_{\text{pcmd}}^2}\right\} \\ I_{\text{qmin}} = -I_{\text{qmax}} \\ I_{\text{pmax}} = \min\{VDL2, I_{\text{max}}\} \\ I_{\text{pmin}} = 0 \end{cases} \tag{6}$$

Terms $VDL1$ and $VDL2$ are piecewise linear curves defined by the user. I_{max} is the maximum current output of the wind power plant given by the user. I_{pcmd} and I_{qcmd} are the parameters determined by the electrical control model. In the simulations, these terms were initialized so that the current limits were determined by the I_{max}, I_{pcmd} and I_{qcmd} parameters rather than the $VDL1$ and $VDL2$ parameters. Also, the

current contribution was set to begin after the voltage at busbar controlled by the wind power plant falls below 0.9 pu. [45]

As the equations demonstrate, the prioritization can limit the output of the opposite current. Consider an example of a wind power plant with 1 per unit (pu) nominal active power output. When the voltage of the plant is 1 pu, the active current feeding is 1 pu as well. When the plant operates in limits of network connection requirements, at 1 pu voltage the reactive current capability should be:

$$I_{\mathrm{q}} = I_{\mathrm{p}} \tan(\arccos(0.95)) \approx 0.33 \text{ pu},$$

and the total current capability:

$$I_{\max} = \sqrt{I_{\mathrm{p}}^2 + I_{\mathrm{q}}^2} \approx 1.05 \text{ pu}.$$

When the plant operates with active current prioritization, the fall of voltage from nominal value increases the amount of active current fed, to keep the active power nominal. Thus, according to Equation (6), the proportion of the reactive current will be less than that of the maximum current. However, if the reactive current is prioritized, the active current will drop from its nominal value and stay below the current limit set by the logic of Equation (5). Meanwhile, the reactive current will be limited by the maximum current capability of the plant. With the additional piecewise linear curves $VDL1$ and $VDL2$, the current limits can be set in a more specific manner according to precise voltage drop levels. [45]

5.2.2 Variation of Reactive Fault Current Gain

Reactive fault current gain value can be varied with the gain parameter K_{qv} in the electrical control model shown in Figure 5.4. In this thesis, the parameter was varied between 0.5 and 5 pu. The parameter changes the slope that determines the change in reactive fault current injection in proportion to the voltage drop. The following Figure 5.7 illustrates this slope with various K_{qv} parameters shortened to K in the figure. The area marked with dashes illustrates the deadband area where the operation of the power plant is determined by the normal voltage control operation requirements. [45]

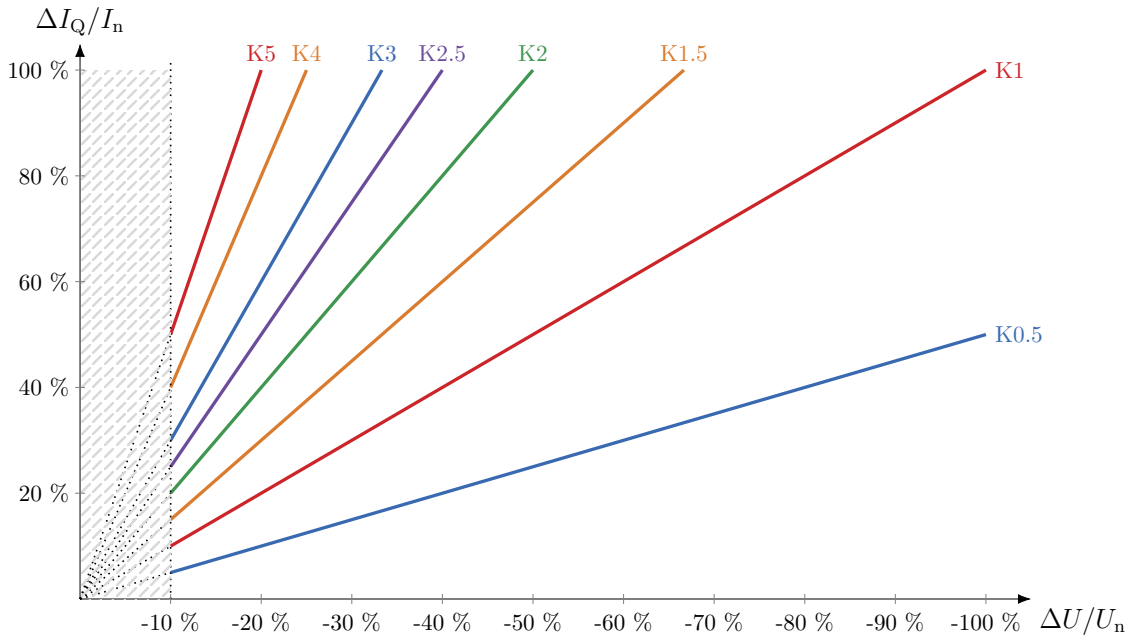

Figure 5.7: The effect of the variation of reactive fault current gain value K_{qv} (pu/pu), shortened to K in the plot. The deadband area marked with dashes is the area with less than -10 % change in the voltage. This area illustrates the range for normal voltage control operation of the plant.

As it can be seen in the figure, with a high gain, such as K4 and K5, the reactive current injection reaches its limit with even a low voltage drop. Then again, with a low gain value K0.5, the gain is not sufficient to boost the reactive current injection up to its limit even with a 100 % voltage drop. The default value of K_{qv} was decided to set to 2.5 pu in the simulations. This value was used in the cases where this parameter was not varied.

5.2.3 Variation of Active Power Recovery Time

The active power recovery time parameter *rrpwr* is set in the generator and converter model shown in Figure 5.5. The parameter has a unit of pu/s. In this thesis, the value of the parameter was varied between 0.2 and 1 pu/s. Conversely the times for active power recovery from zero to nominal value were from less than a second to five seconds. The following Figure 5.8 illustrates the variation of the parameter value *rrpwr* (shortened to R in the figure) and its effect on the time required for complete active power recovery from zero to nominal value. The default value of *rrpwr* was decided to set to 2 pu/s in these simulations. This value was used in the cases where this parameter was not varied. [45]

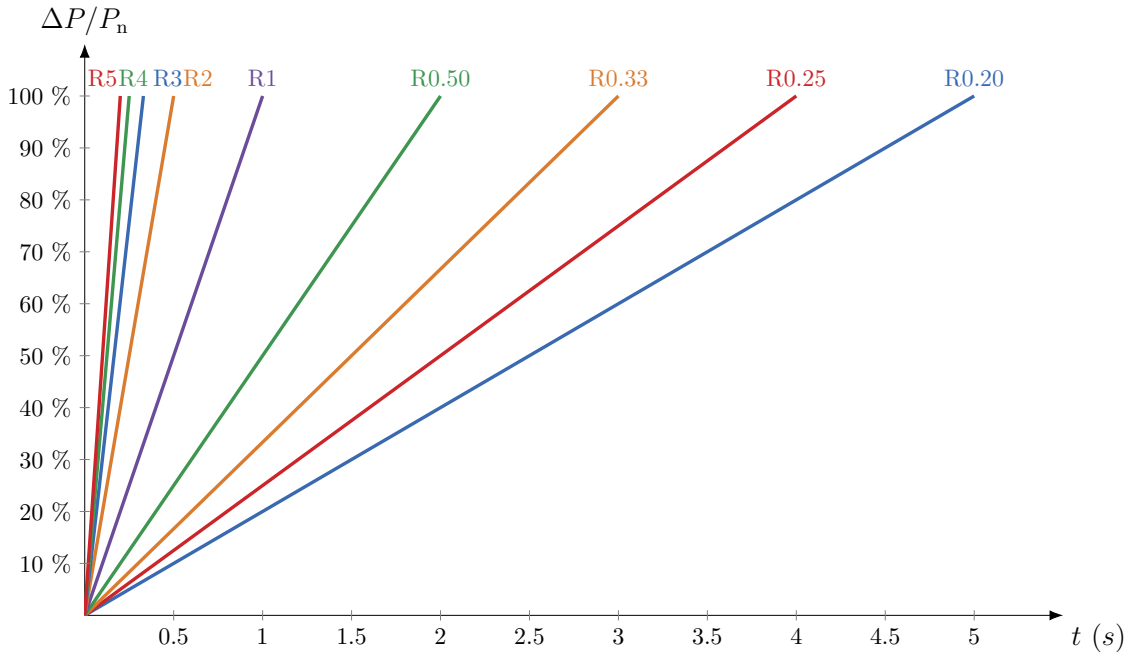

Figure 5.8: Different active power recovery times for a wind power plant. The recovery time illustrates the time required for complete recovery from zero to nominal active power output. The value of the parameter is indicated subsequent to the R (pu/s) letter in the figure.

5.3 Methods for Analysing the Power System Stability

This section illustrates the methods for analysing the power system stability. Power system stability studies and simulations related to it depend on the chosen perspective. Also, the level of detail of the model and its data differs according to the investigated phenomenon. In general, the simulations can be divided into two categories; electromagnetic transient and electromechanical transient simulation studies. [14]

Electromagnetic transient studies are simulated with special electromagnetic transients programs (EMTPs), such as Alternative Transient Program (ATP) and PSCAD/EMTDC. Above-mentioned programs include the exact phase representation of all the electrical components. Thus, the simulations can be used to determine both symmetrical and asymmetrical fault currents. For the coordination of the insulation, overvoltages in connection with switching and lightning surges can also be studied. Short term transient studies occurring in microseconds are studied with the EMTPs. In general, EMTPs are used to determine detailed performances of individual electrical components in the power system. [14]

Conversely, electromechanical transient studies are commonly simulated with transient stability programs (TSPs), such as PSS/E and Simpow. These programs have the phasor representation of all the electrical components. Some of the programs include only positive sequence phasor representation, whereas some programs also present the negative and zero sequences. As it was mentioned in Chapter 2, the dynamic stability phenomena occur between milliseconds and minutes. [14]

In the simulations of this thesis, PSS/E version 33.9.0 was used. PSS/E can be used to simulate both steady-state and transient power system phenomena. The program presents the results as a positive sequence root mean square values. Dynamic simulations use the steady-state results of the case as a base information. The dynamic models can be either internal models or external models programmed by the user. Including both type of models is also possible. The PSS/E base-cases used in this thesis included both internal and external models.

Analysing disturbances occurring in the power system is one of the essential parts of the long-term power system planning. Therefore, to study different stabilities, four different disturbances occurring in the power system were reviewed. First of them was the tripping of cross-border HVDC link between Finland and Sweden (Fenno-Skan2) with a 100 ms substation disturbance prior to the tripping. This disturbance was exploited in the rotor angle stability study. Second disturbance was the tripping of the largest power plant in Finland (Olkiluoto 3) with 100 ms busbar disturbance prior to the tripping. Third disturbance was the tripping of another power plant in Finland (Hanhikivi 1) with 150 ms busbar disturbance prior to the tripping. Last disturbance was 250 ms 400 kV substation busbar disturbance in selected substations.

In case of the tripping of Olkiluoto 3, certain amount of load is disconnected from the network immediately after the tripping of the generator. This is a protection scheme of the system. The tripping of a large generator and substation disturbances were exploited in both voltage and rotor angle stability issues. In addition, the tripping of a large generator invokes the imbalance between the production and consumption of the system. Thus, the tripping of Olkiluoto 3 was also utilized in the frequency stability study.

The voltage of 400 kV substations was analysed in voltage stability study of this thesis. It concentrated on the differences of the voltage fluctuation during and immediately after the fault clearing. In rotor angle stability study, the rotor angle oscillations of large synchronous machines were examined. The evaluation was on the first up- and down-swing of the rotor angle. Also, the damping of the oscillation was taken into account. In the frequency stability study, the frequency of 400 kV substation was reviewed. The fluctuation of the frequency during the fault and immediately after the clearance of it was analysed. The state at which the frequency settled was also reviewed.

The simulation was set up to last 30 seconds. During this time, commonly all the stability phenomena occurring in this research could be observed. However, in some cases a shorter time period was examined. Cases with a shorter time period mean that the state of the system had already been settled, or was near to be settled, to the new state. Therefore, a longer review was not necessary.

5.4 The Nordic Power System Scenario

This section presents the cases that were created and used in the simulation results in Chapter 6. The cases were prepared from the year 2025 Nordic power system scenario. This scenario included the Nordic power system and its dynamic models

from Finland, Sweden and Norway. The cross-border high voltage direct current (HVDC) links and high voltage alternative current (HVAC) lines were also modelled. The 2025 scenario contains the most significant investments up to the year 2025 in the Nordic countries.

Utilizing the above-mentioned scenario, 5 base-cases with load and generation differences were prepared. These base-cases reflect different power system operation situations ranging from a summer night to a winter day. The cases were solely prepared for a comparison study of different wind power plant operation mode. Hence, they did not take into account all the operation methods of the system, but were accurate enough for this study. The cases were further altered by substituting conventional power generation and/or cross-border capacity with wind power plant generation according to the below-mentioned wind power plant capacities. The cases and their characteristics are presented in Table 2. The modelled wind power plants were located geographically at the western coast area of Finland. These crude locations are shown in Figure 5.10.

Table 2: The base-cases used in the simulations

Case	Time of year	Consumption in the system	Modelled wind power plant capacity (MW)	Overall capacity[1)] (%)	Import/ Export[2)]
A	Mid-winter day	High	3000	23.6	Import
B	Early-winter day	Normal	2500	21.5	Import
C	Summer night	Low	1500	31.8	Import
D	Winter night	Normal	4000	31.3	Export
E	Summer night	Low	3000	35.2	Export

[1)] The overall capacity of the modelled wind power plants in percentage is calculated from the overall production in Finland in the reviewed case.

[2)] In case of import, the power flow is from Sweden to Finland, whereas in case of export, the power flow is from Finland to Sweden.

The wind power plants were connected to 110 kV network substations through a transformer. These substations were connected with either one or two transformers to 400 kV network substations. The placement of the aggregated wind farms is illustrated in Figure 5.9. Three wind power plants with line lengths of 20, 40 and 60

kilometres from the substation were modelled to six substations. In the remaining two substations, four wind farms were modelled. These substations had the fourth generator with the line length of 20 km. This generator is illustrated as in dotted form in the figure. The voltage of the busbar with PCC was controlled by the modelled generator connected to that busbar.

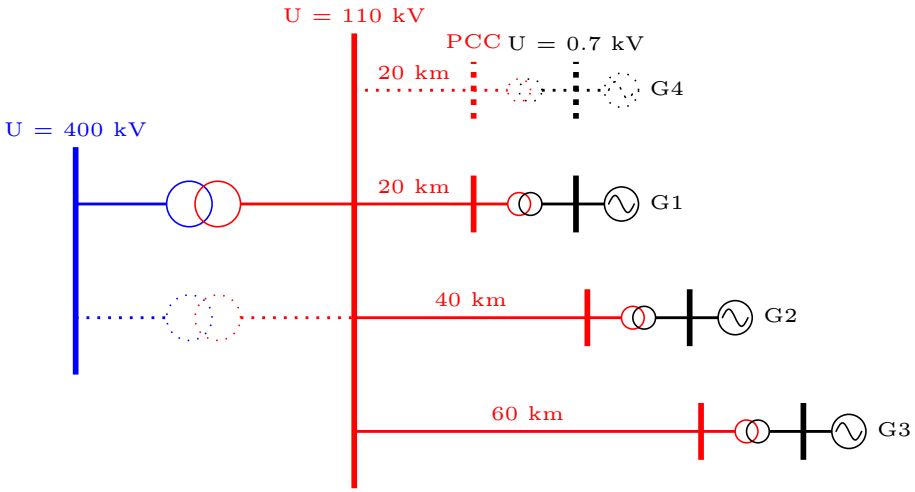

Figure 5.9: The positioning of the modelled wind power plants inside a substation. Each generator controlled the voltage of the PCC busbar.

Legends of the simulation result figures are using the given names of generators, meaning that generators G1 and G4 are the ones nearest to the substation, whereas generator G3 is the furthest. In addition, 400 kV substations with the connected plants were alphabetically named according to their geographical location in the network. These substations are illustrated in Figure 5.10. The names are presented in the legends of the results as well.

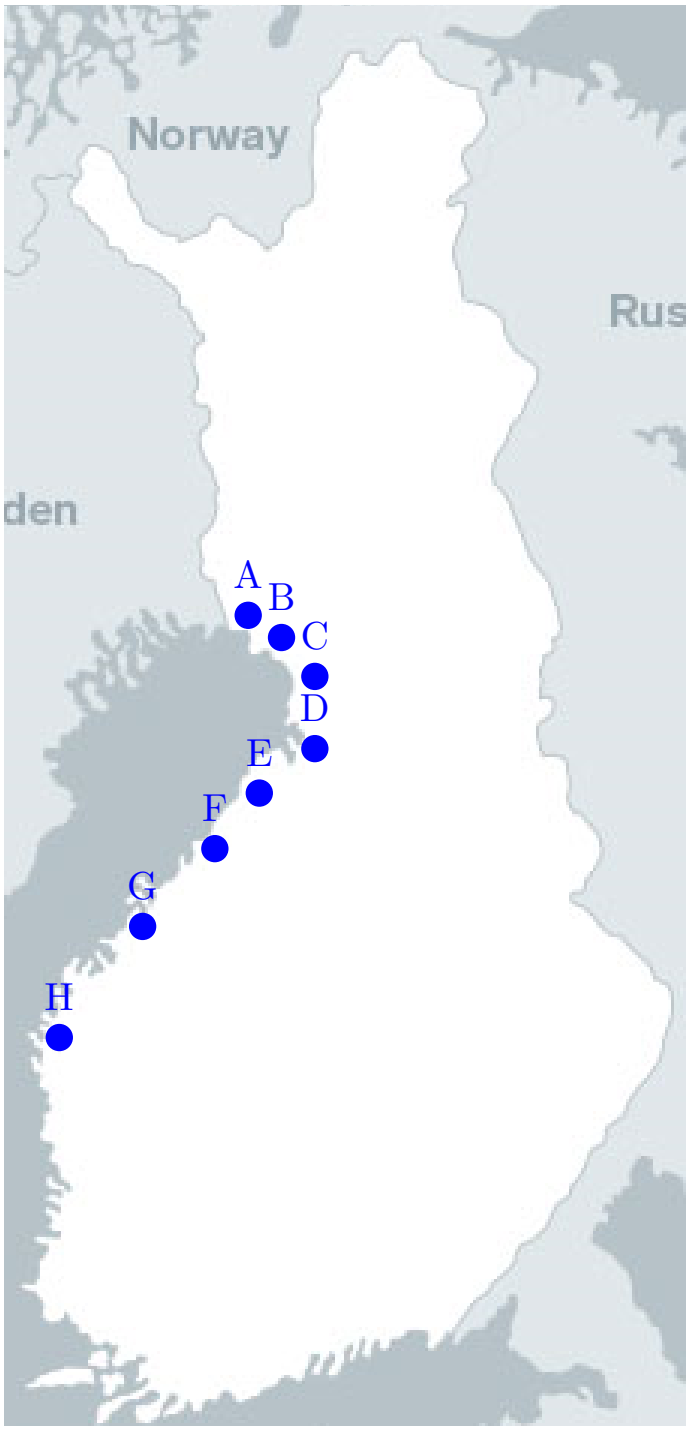

Figure 5.10: Crude geographical locations of the 400 kV substations where the wind power plants were connected to. Adapted from [47].

6 The Impact of Fault Current Contribution from Converter Based Power Plants on Power System Stability

Chapter 6 presents the simulation results of the studies conducted as a part of this thesis. This chapter is divided into four sections. In the first Section 6.1, the impact of zero fault current contribution is compared with the impact of set fault current contribution on power system stability. In the second Section 6.2, the impact of active fault current contribution priority is compared with the impact of reactive fault current contribution priority. Subsequent to the priority comparison, the impact of reactive fault current gain on power system stability is illustrated in Section 6.3. Finally, the impact of active power recovery time is explored in Section 6.4.

The information of the base-cases can be found in Table 2. The parameters and their values of the modelled wind power plants are shown in Appendix E in Tables E.1, E.2, and E.3. Most of the results are obtained without Hanhikivi 1 connected to the network. When introducing a result it is mentioned if the base-case was altered to include Hanhikivi 1 in the simulations.

6.1 Impact of Fault Current Contribution on Power System Stability

This section reviews the results obtained from the impact of fault current contribution on power system stability study. Wind power plants without any fault current contribution were compared with wind power plants having set current contribution. The zero fault current contribution resembles the disconnection of wind power plants during a disturbance. Prior to the disturbance, these plants fed nominal active power to the network. In this study, set fault current contribution means that during the fault, these wind power plants operated according to specified contribution. The contribution was set either active or reactive current. In addition, these power plants produced nominal active power to the network prior to the disturbance.

6.1.1 Impact of Fault Current Contribution on Voltage Stability

The following section illustrates the difference in voltage stability between wind power plants without any current contribution, indicated now and later as 0% in the legends of the figures, and wind power plants with set current contribution, indicated now and later as 100% in the legends of the figures.

Figure 6.1 presents the voltage of the 400 kV substation D. This substation was situated near another 400 kV substation C where 250 ms disturbance was applied at time 1.0 second. The base-case used to obtain this result was the mid-winter day of import. The wind power plants were modelled with reactive current contribution priority, indicated later as Q in the brackets at the legends of the figures. The voltage difference grew to 0.06 pu during the disturbance, whereas immediately after the

disturbance the difference was 0.12 pu. The higher voltage was obtained with the reactive current contribution priority.

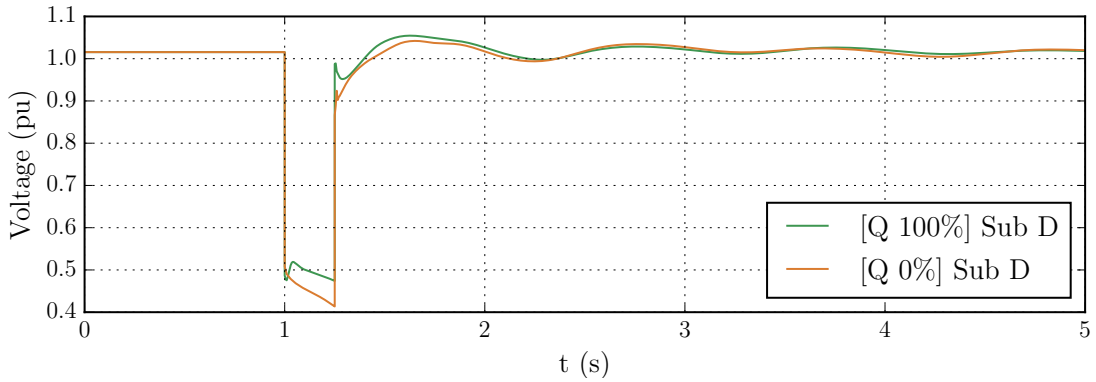

Figure 6.1: The voltage fluctuation at the substation D in case of 250 ms disturbance in a nearby substation C. The base-case of the simulation was the mid-winter day of import. The comparison is between reactive fault current contribution priority ([Q 100%]) and without any fault current contribution ([Q 0%]). Wind power plants operated at nominal active power production prior to the disturbance in both cases.

Figure 6.2 illustrates the behaviour of a wind power plant during the disturbance. In the plot, the additional reactive current injection begins as soon as the plant sees the voltage drop in case of set fault current contribution. Due to the limit of the converter maximum current, the active current injection decreases at the same time. On the other hand, the zero contribution of fault current can be seen as a rapid decrease of both active and reactive current shown with orange plots in the figure. The voltage difference of the substation is clearly affected by this current contribution difference.

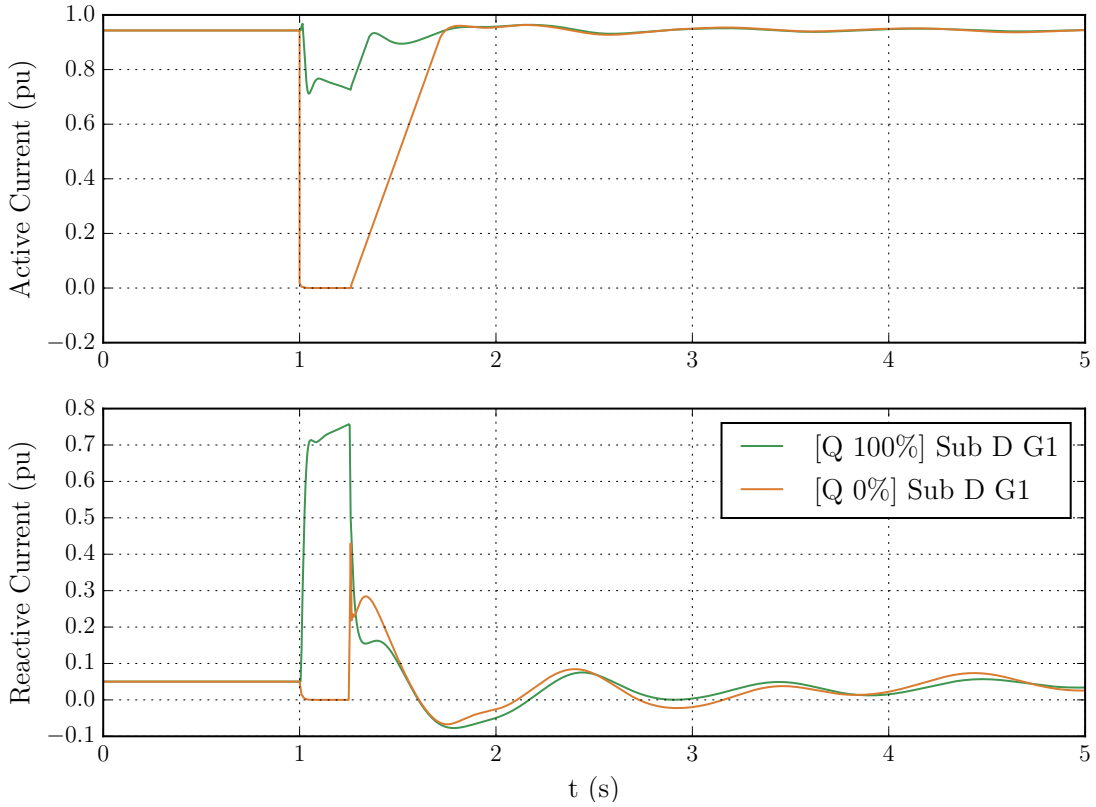

Figure 6.2: The injection of active and reactive current of wind power plant G1 connected to the substation D in case of 250 ms disturbance in a nearby substation C. The base-case of the simulation was the mid-winter day of import. The comparison is between reactive fault current contribution priority ([Q 100%]) and without any fault current contribution ([Q 0%]). Wind power plants operated at nominal active power production prior to the disturbance in both cases.

The active and reactive current injection from a wind power plant can also be shown with active and reactive power feeding of the plant. This takes into account the voltage of the generator. As the Figure 6.3 demonstrates, the power feeding is graphically similar to the current injection. Active and reactive power are both fed in case of set fault contribution. Whereas, with zero current contribution both of the injections fell to zero during the fault. This is understandable, since the value of the current was also zero.

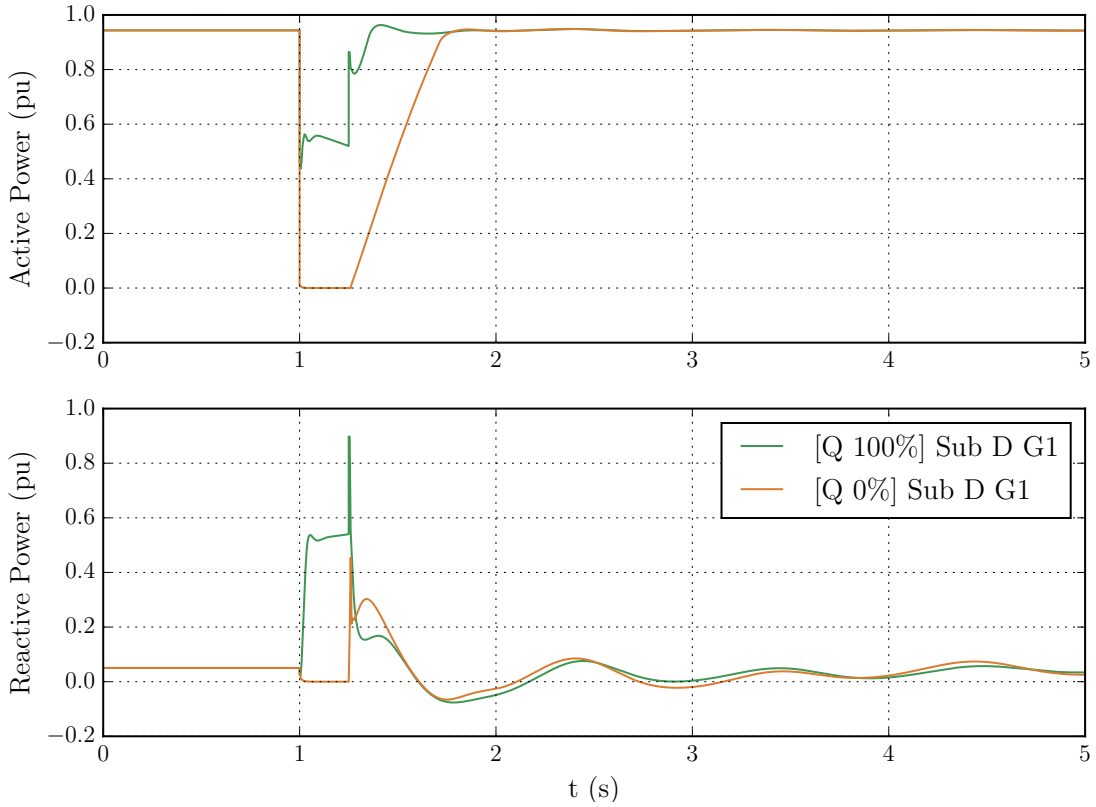

Figure 6.3: The injection of active and reactive power of wind power plant G1 connected to the substation D in case of 250 ms disturbance in a nearby substation C. The base-case of the simulation was the mid-winter day of import. The comparison is between reactive fault current contribution priority ([Q 100%]) and without any fault current contribution ([Q 0%]). Wind power plants operated at nominal active power production prior to the disturbance in both cases.

Another voltage fluctuation difference in a substation disturbance, but with active current prioritization, indicated later as P in the brackets of the legends of figures, is shown in Figure 6.4. The fault was applied at the same substation as in the earlier situation. The reviewed substation in the figure was also the same. With active current priority, the voltage difference is 0.02 pu between the set fault current contribution and the zero fault current contribution. This difference is in favour to the latter one. The higher voltage at the substation during the fault is caused by greater contribution of other devices in the network.

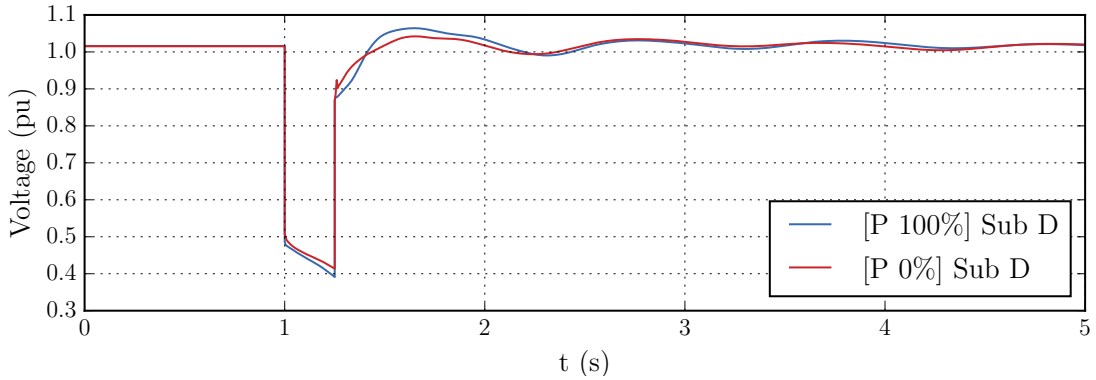

Figure 6.4: The voltage fluctuation at the substation D in case of 250 ms disturbance in a nearby substation C. The base-case of the simulation was the mid-winter day of import. The comparison is between active fault current contribution priority ([P 100%]) and without any fault current contribution ([P 0%]). Wind power plants operated at nominal active power production prior to the disturbance in both cases.

A wind power plant connected to the substation increased its active current and reactive current injection as it can be seen in Figure 6.5. In this case, the reactive current injection was limited by the maximum current due to the active current priority, and its amount was considerably less than in the case of reactive current contribution priority. Hence, the voltage value of the substation was lower compared with the reactive current contribution case. In addition, the difference in the voltage of the substation between the zero injection and set injection with active current priority was also smaller.

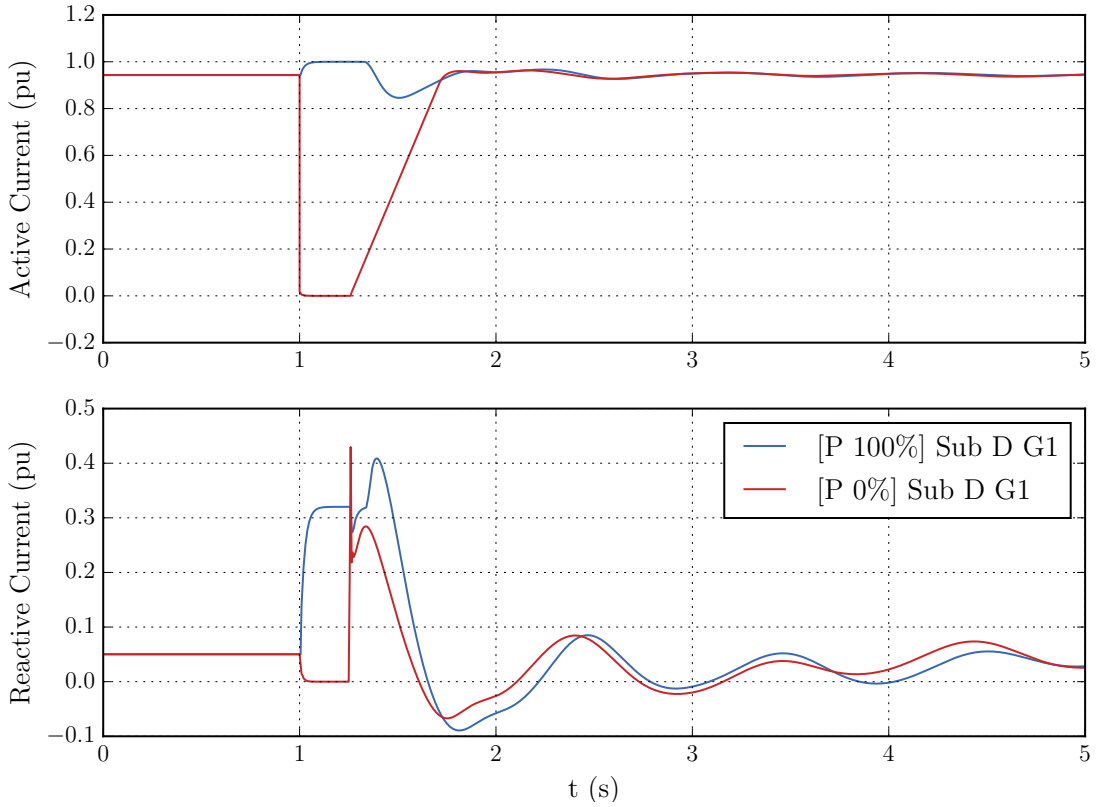

Figure 6.5: The injection of active and reactive current of wind power plant G1 connected to the substation D in case of 250 ms disturbance in a nearby substation C. The base-case of the simulation was the mid-winter day of import. The comparison is between active fault current contribution priority ([P 100%]) and without any fault current contribution ([P 0%]). Wind power plants operated at nominal active power production prior to the disturbance in both cases.

Similar to the first case in this section, the injection of active and reactive current of the plant can be plotted as active and reactive power feeding. The power flow of the plant G1 connected to the substation D is shown in Figure 6.6. As it was already noted in the first case, the power feeding follows the characteristics of the current injection. However, it was noticed that some of plants without fault current contribution had a greater reactive power output immediately after the fault clearance compared with the plants having active current contribution priority.

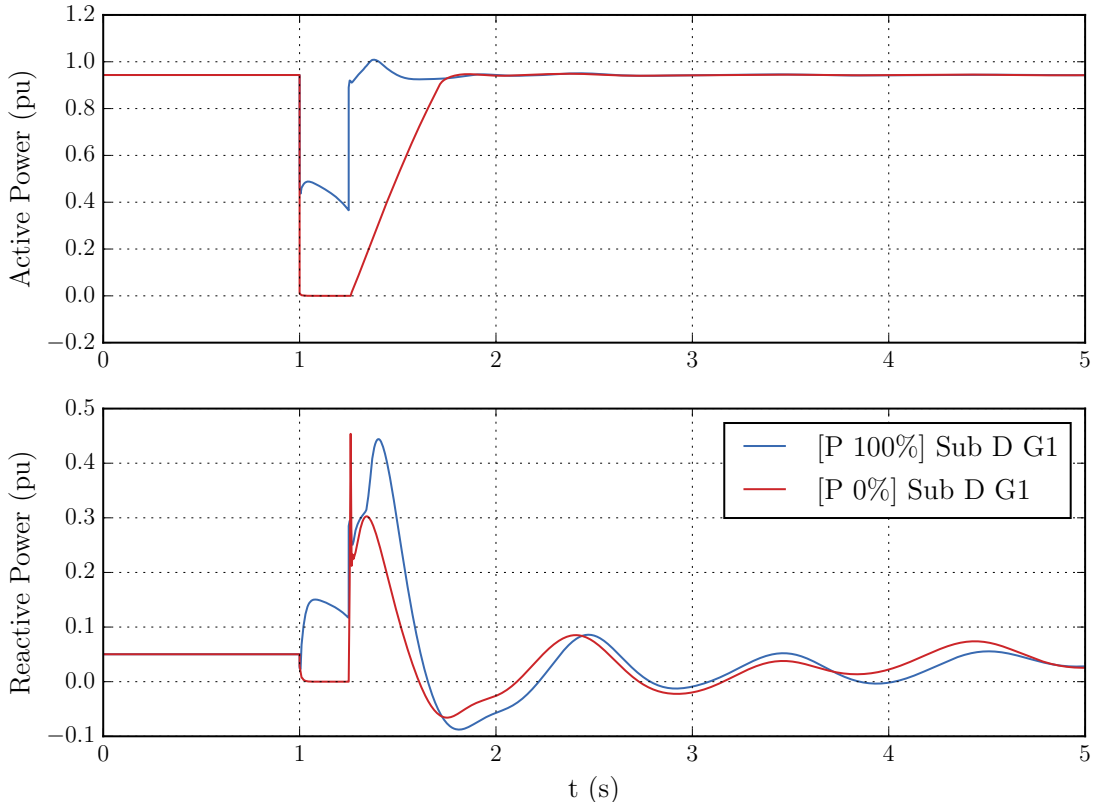

Figure 6.6: The injection of active and reactive power of wind power plant G1 connected to the substation D in case of 250 ms disturbance in a nearby substation C. The base-case of the simulation was the mid-winter day of import. The comparison is between active fault current contribution priority ([P 100%]) and without any fault current contribution ([P 0%]). Wind power plants operated at nominal active power production prior to the disturbance in both cases.

Similar voltage fluctuation as in the previous figures were observed in another case. Results from this case are illustrated in Appendix A in Figures A.1 and A.2. Next, the impact of fault current contribution on rotor angle stability is reviewed.

6.1.2 Impact of Fault Current Contribution on Rotor Angle Stability

The following section illustrates the impact of fault current contribution on rotor angle stability. Figure 6.7 presents the rotor angle oscillation of a large generator subsequent to a 100 ms substation disturbance at 1.0 second followed by the tripping of Fenno-Skan2. The base-case of the simulation was the winter night of export. As it can be seen from the figure, the rotor angle deviated in the first up-swing almost 30 degrees more in the case of active current injection compared with zero injection of the wind power plants. Also, the oscillation damping of the generator was poorer. This difference was due to the higher active power feeding of the wind power plants during and immediately after the fault. The large generator was able to feed less of its kinetic energy to the local loads after the fault clearing. This kinetic energy was

stored in the acceleration of the machine during the fault period.

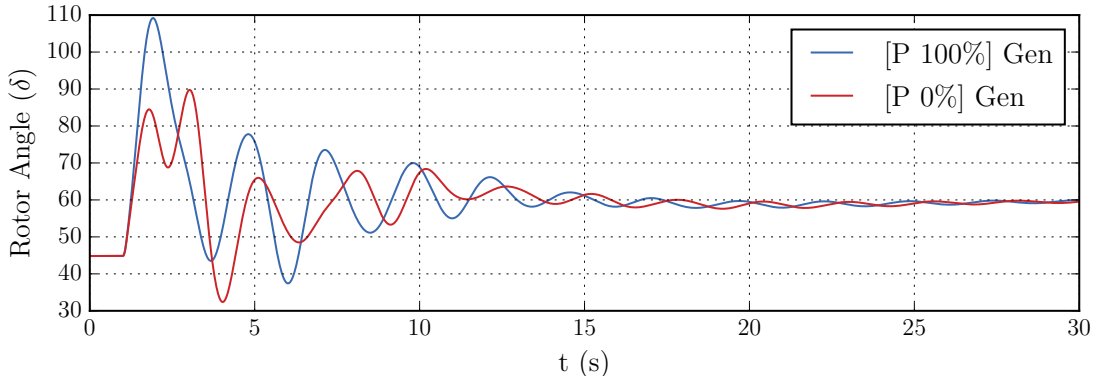

Figure 6.7: The rotor angle oscillation of a large generator in case of tripping Fenno-Skan2. The base-case of the simulation was the winter night of export. The comparison is between active fault current contribution priority ([P 100%]) and without any fault current contribution ([P 0%]). Wind power plants operated at nominal active power production prior to the disturbance in both cases.

Similar rotor angle oscillation were seen in Figure 6.8 as in the figure 6.7 above. The case was the same, but this time the wind power plants were modelled with reactive current priority. As the plot also illustrates in this case, the oscillation of the reviewed generator was increased with the reactive fault current injection. The magnitude of the oscillation was a bit smaller than in case of active fault current injection priority.

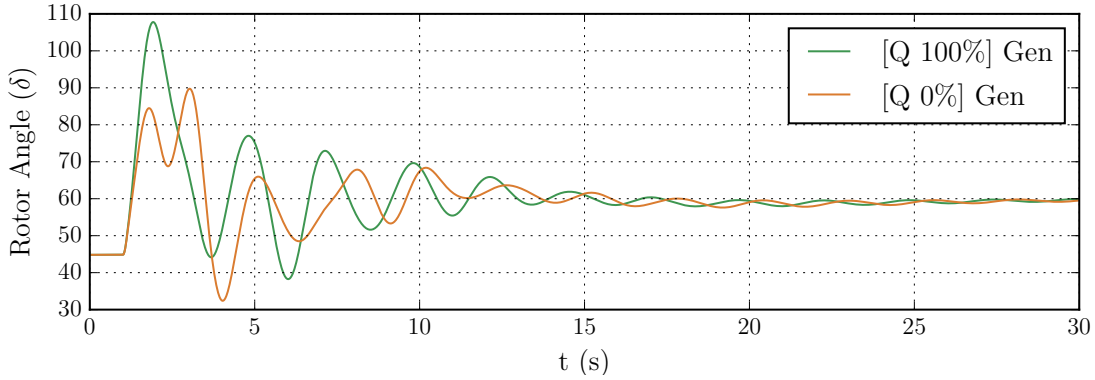

Figure 6.8: The rotor angle oscillation of a large generator in case of tripping Fenno-Skan2. The base-case of the simulation was the winter night of export. The comparison is between reactive fault current contribution priority ([Q 100%]) and without any fault current contribution ([Q 0%]). Wind power plants operated at nominal active power production prior to the disturbance in both cases.

Furthermore, when Olkiluoto 3 or Hanhikivi 1 generator was tripped, the oscillation was highly increased and the damping poorer with the zero fault current

injection. This was caused by the lack of active power support from the wind power plants not providing any fault current. The tripped generator created a production deficit which was compensated with other machines. Thus, these generators had to provide more active power to the network in the case of zero fault current injection. This increased their rotor angles. An example of this sort of oscillation is presented in Figure 6.9. The base-case was also the winter night of export in this result. The same phenomenon as in the below figure 6.9 was observed in another base-case. The results of this case are presented in Figures A.3 and A.4 of Appendix A.

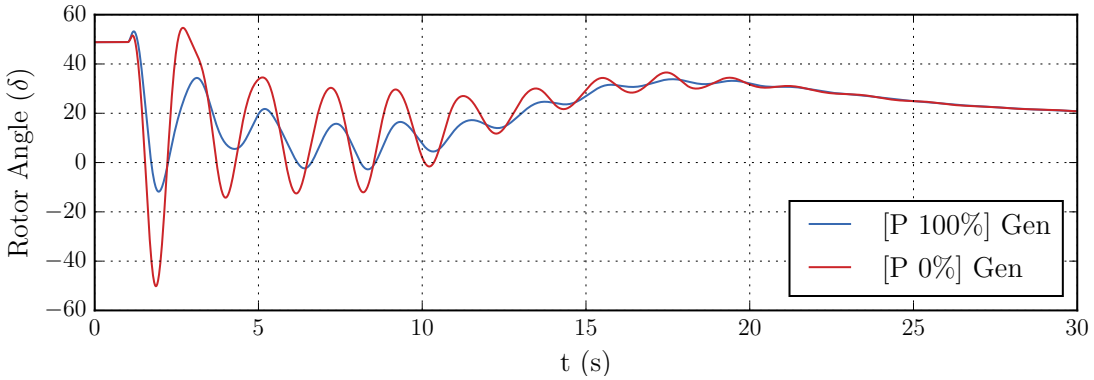

Figure 6.9: The rotor angle oscillation of a large generator in case of tripping Olkiluoto 3. The base-case of the simulation was the winter night of export. The comparison is between active fault current contribution priority ([P 100%]) and without any fault current contribution ([P 0%]). Wind power plants operated at nominal active power production prior to the disturbance in both cases.

6.1.3 Impact of Fault Current Contribution on Frequency Stability

This section examines the impact of the fault current contribution on frequency stability. Figure 6.10 illustrates the impact on the frequency stability with a 100 ms busbar disturbance at time 1.0 second followed by the tripping of Olkiluoto 3. The base-case of the simulation was the summer night of export. The power plants were modelled with active current priority. As it can be seen in the figure 6.10, the active current injection of the power plants keep the frequency higher during and instantly after the fault compared with the zero injection case. It must be considered that the wind power plants were not modelled with frequency control. Thus, they inject the fault current on the grounds of the seen voltage drop.

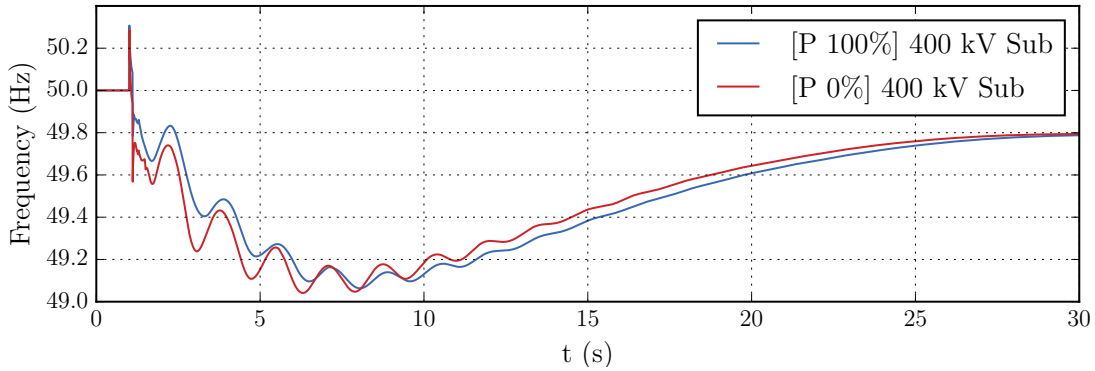

Figure 6.10: The frequency fluctuation at 400 kV substation in case of tripping Olkiluoto 3. The base-case of the simulation was the summer night of export. The comparison is between active fault current contribution priority ([P 100%]) and without any fault current contribution ([P 0%]). Wind power plants operated at nominal active power production prior to the disturbance in both cases.

The result of the same disturbance and base-case as in figure 6.10, but with reactive current priority, is shown in 6.11. The figure follows the same principles as in the active current priority case. Also, with another base-case the results were similar. These results are illustrated in Figures A.5 and A.6 of Appendix A.

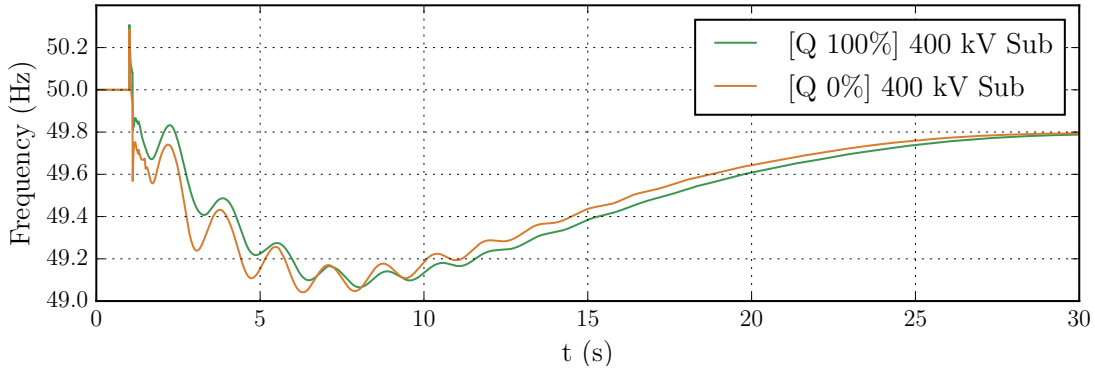

Figure 6.11: The frequency fluctuation at 400 kV substation in case of tripping Olkiluoto 3. The base-case of the simulation was the summer night of export. The comparison is between reactive fault current contribution priority ([Q 100%]) and without any fault current contribution ([Q 0%]). Wind power plants operated at nominal active power production prior to the disturbance in both cases.

The next section explores the impact of fault clearing time of a selected substation on power system stability. As in previous results, the comparison was between zero fault current and set fault current contribution. The set fault current contribution was also divided into both active and reactive current priority in this comparison.

6.1.4 Impact of Fault Current Contribution on Critical Fault Clearing Time

The following section illustrates the impact of the fault current contribution on critical fault clearing time of a substation disturbance. As in the above-reviewed sections, the comparison is reviewed between wind power plants without fault current contribution, indicated with 0% in the table, and plants with set fault current contribution, indicated with 100% in the table. As mentioned, set fault current contribution is further divided into active and reactive current priority, indicated with P-prio and Q-prio respectively in the table. The power plants without fault current contribution were not divided into different current priority. This is due to the fact that the current priority only influences the fault current contribution, which was modelled as zero in these cases. Thus, the results for both priorities were the same for zero injection cases.

The results in Table 3 were obtained with a disturbance at substation A. To illustrate the minimum difference in the critical clearing time of most of the cases, the fault time of the disturbance was from 250 to 360 ms in five ms intervals. The obtained critical clearing times indicate at which length the studied stability fell below the given limit after 30 seconds of simulating. The studied limits were 0.90 pu in voltage stability and either 49 or 51 Hz in frequency stability. In case of rotor angle stability, the time indicates the first loss of synchronism of a generator.

The results shown in the table and in the appendix are somewhat coherent with the results obtained in Section 6.1. As can be seen, the clearing time of the disturbance is longer with fault current contribution from wind power plants in some cases. Thus, with the contribution of the wind power plants, the power system can survive from longer faults. This follows the trend of the voltage stability studies shown earlier. When the voltage support is less without any fault current injection, the longer the fault is, the lower will the voltage drop. With long enough fault time, the power system is not able to recover steady voltages at the buses. This will lead to instability. In addition, the frequency instability in these cases is caused by the loss of generators and the collapse of the voltage.

On the other hand, the longer the fault, the more the synchronous machines accelerate and store kinetic energy. The stored kinetic energy is then fed back to the network after the fault clearing. If the feeding of the accumulated kinetic energy takes longer, the deceleration also takes longer. This leads to higher rotor angle which in turn can lead to rotor angle instability. However, as it can be seen in the results, the higher rotor angle with the reactive current injection does not lead to earlier loss of synchronism compared with the zero injection in any of the cases. The loss of synchronism is therefore due to the voltage collapse. On the other hand, with active current injection, the loss of synchronism is earlier in every case. These results are due to the rotor angle growing above the limit of a stable state with the slower deceleration.

What can be also be noticed from the results is that in most of the cases, the current contribution with active current priority leads to instability in less time compared with the zero injection cases. This is illustrated as a negative value in

the difference. This result is partly due to the behaviour of wind power plants immediately after the fault. In addition, other devices in the network provided additional support. The plants providing zero injection during the fault boost their reactive power feeding immediately after the fault. This boost is greater than the feeding given by the active current priority plants. This leads to higher voltages at the substations subsequent to the fault. The voltage support of the wind power plants also further supports the power output of all the other generators. This enhances the stability of the system.

Table 3: The impact of fault current contribution on the critical fault clearing time of a disturbance in substation A. The fault clearing time was simulated from 250 ms to 360 ms in five ms intervals. The comparison is between zero and set fault current contribution. Set fault current contribution is divided into active (P-prio) and reactive (Q-prio) current priority. 0% indicate that the modelled power plants did not inject any fault current. 100% indicate that the plants operated according to the set fault current contribution. Wind power plants operated at nominal active power production prior to the disturbance in all three cases.

Case	Stability	Crit. length with 0% (ms)	Crit. length with 100% P-prio (ms)	Crit. length with 100% Q-prio (ms)	0% difference with 100% P-prio (ms)	0% difference with 100% Q-prio (ms)
A	Voltage	350	325	>360[1)]	-25[2)]	>10
	Rotor angle	350	325	>360	-25	>10
	Frequency	350	325	>360	-25	>10
B	Voltage	335	340	>360	5	>25
	Rotor angle	335	325	>360	-10	>25
	Frequency	335	340	>360	5	>25
C[3)]	Voltage	-	-	-	-	-
	Rotor angle	-	-	-	-	-
	Frequency	-	-	-	-	-
D	Voltage	>360	340	>360	>-20	-
	Rotor angle	340	320	350	-20	10
	Frequency	>360	340	>360	>-20	-
E	Voltage	320	310	330	-10	10
	Rotor angle	320	310	330	-10	10
	Frequency	320	310	330	-10	10

[1)] If the length includes '>' symbol, the case passed the last interval of 360 ms.
[2)] If the value is negative, the zero injection case had a longer critical clearing time.
[3)] No instabilities occurred during the simulations with case C.

Additional results of this section with another two substation disturbance are found in Appendix A in Tables A.1 and A.2. In these results, the active current priority was seen to be better compared with zero injection in some cases. However, the reactive current injection cases had the longest clearing times in these cases.

An example of the active and reactive power feeding difference with the active current contribution priority and the zero contribution is shown in Figure 6.12. As can be seen in the figure, the reactive power output of the zero injection wind power plant is greater subsequent to the fault. This greater value is due to the current limit. In case of the active current contribution priority, the reactive injection immediately after the fault is limited by the maximum current. On the other hand, with the zero contribution, the slow recover of active power enables a greater injection of reactive power. The rapid fluctuation seen in the zero contribution case is likely a cause of the reaching the reactive current limit and non-optimized voltage control response. The overshoot of the response causes this short period fluctuation.

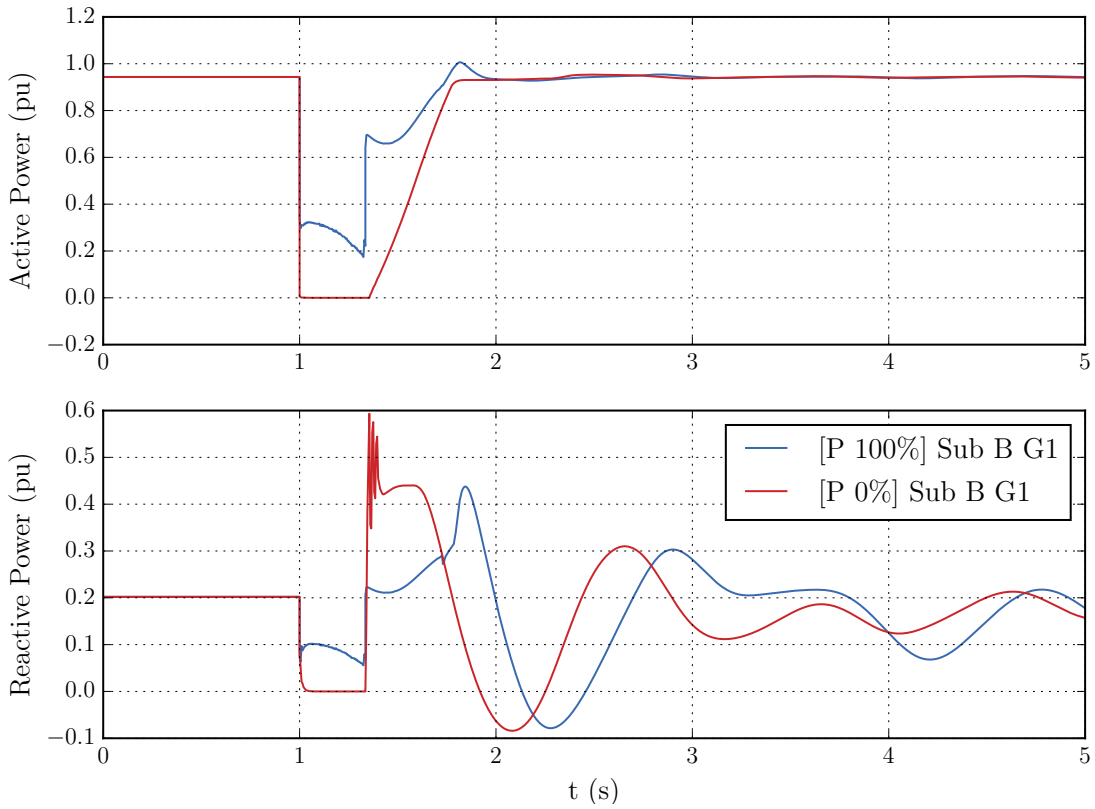

Figure 6.12: The active and reactive power feeding of a wind power plant G1 connected to substation B during 335 ms disturbance at substation D. The base-case of the simulation was the mid-winter day of import. The comparison is between active fault current contribution priority ([P 100%]) and without any fault current contribution ([P 0%]). Wind power plants operated at nominal active power production prior to the disturbance in both cases.

The results obtained in Section 6.1 indicate that the fault current contribution from the wind power plants affects the power system stability. The next section

illustrates the differences between the active and reactive current contribution priority of wind power plants in terms of power system stability.

6.2 Impact of Fault Current Contribution Priority on Power System Stability

The following section illustrates the impact of active and reactive current injection priority of the wind power plants on power system stability. The results were obtained with wind power plants with either half of nominal or nominal active power production prior to the disturbances.

6.2.1 Impact of Fault Current Contribution Priority on Voltage Stability

This section presents the impact of the fault current contribution priority on voltage stability. The following Figure 6.13 was obtained when the wind power plants were modelled with 50 % (indicated now and later as 50% in the legend of the figures) active power production of the nominal capacity prior to the disturbance. 250 ms busbar disturbance was applied to substation C at time 1.0 second in the early-winter day of import case. The figure presents the voltage fluctuation at substation F. As can be seen, the fluctuation difference between active current injection and reactive current injection priority is minor. During the fault, the difference was less than 0.006 pu, whereas subsequent to the fault the difference grew to 0.01 pu. With another case the results were similar as in the below figure. These results are illustrated in Figure B.1 of Appendix B.

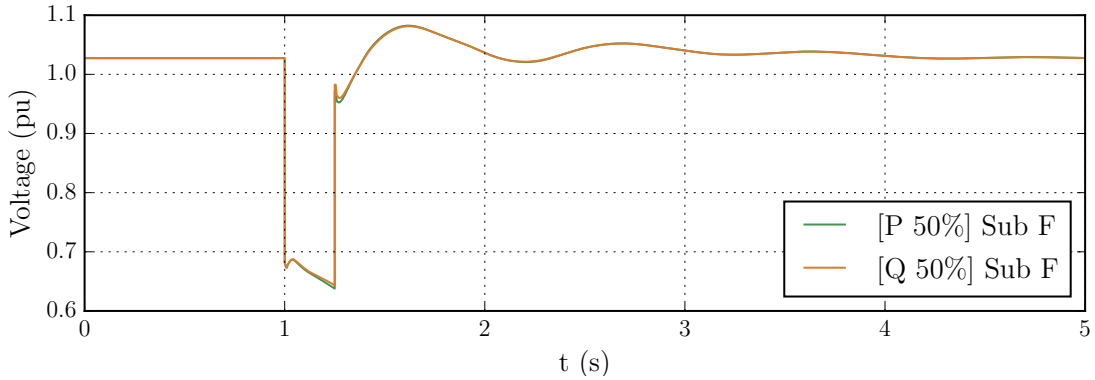

Figure 6.13: The voltage fluctuation at the substation F in case of 250 ms disturbance in substation C. The base-case of the simulation was the early-winter day of import. The comparison is between active ([P 50%]) and reactive ([Q 50%]) current contribution priority. Wind power plants operated at 50 % active power production from the nominal capacity prior to the disturbance in both cases.

The minor difference in the above result can be explained with the current injection of the wind power plants shown in Figure 6.14 below. The current injection is almost identical even with different priority given. This is due to the fact that the maximum

current limit shown in Equation (5) and (6) is never reached. Thus, in both priority cases, the injection of one current is not limited by the other. However, in some results, the maximum current limit was reached on certain wind power plants. This is dependent on the voltage drop seen by the individual power plant. Also, the initial feeding conditions prior to the disturbance affect the limit reaching. This is illustrated later.

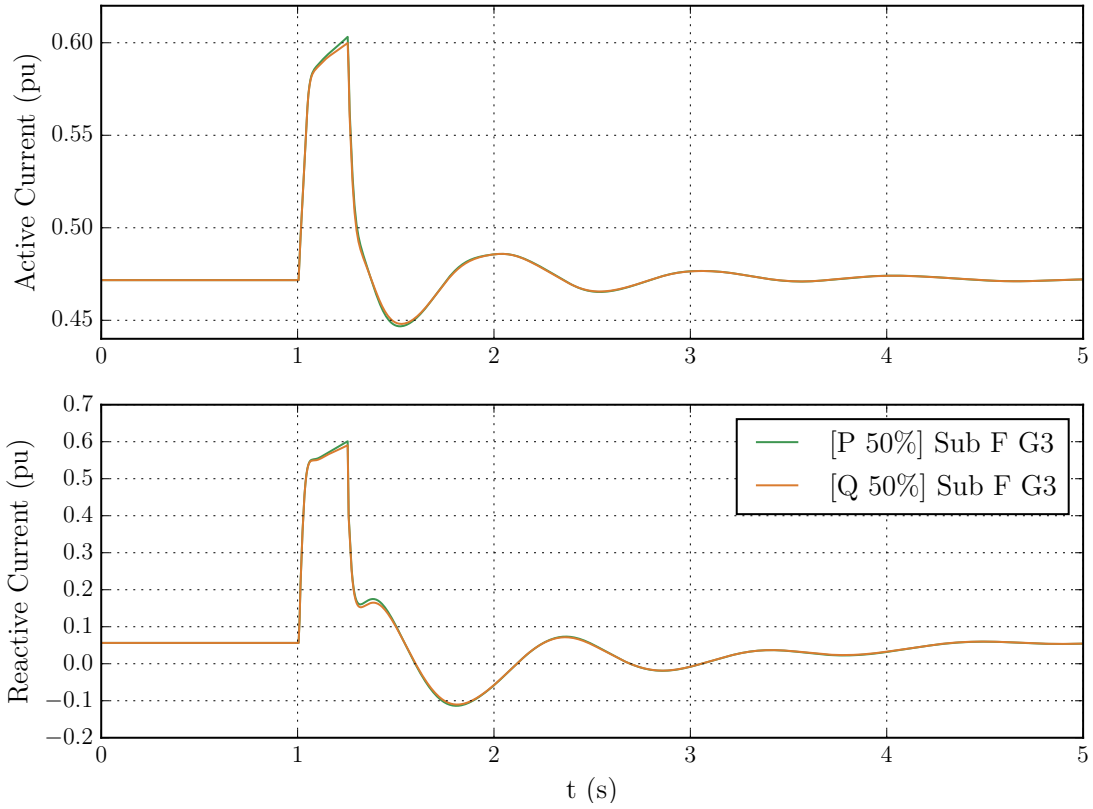

Figure 6.14: The injection of active and reactive current of wind power plant G3 connected to substation F in case of 250 ms disturbance in substation C. The base-case of the simulation was the early-winter day of import. The comparison is between active ([P 50%]) and reactive ([Q 50%]) current contribution priority. Wind power plants operated at 50 % active power production from the nominal capacity prior to the disturbance in both cases.

The actual active and reactive power feeding of the wind power plant is illustrated in Figure 6.15. Similar to the current injection, the power feeding of both cases is almost the same. The voltage fluctuation at the substation is coherent with the behaviour of the modelled wind power plants.

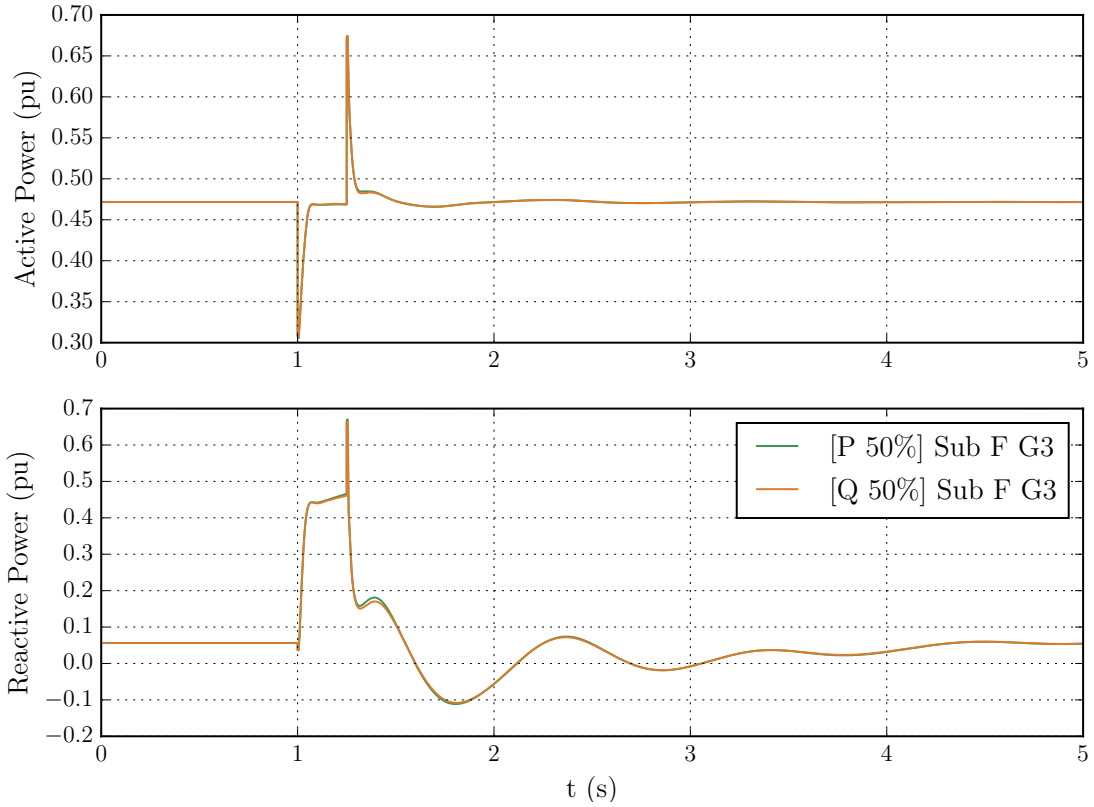

Figure 6.15: The active and reactive power feeding of wind power plant G3 connected to substation F in case of 250 ms disturbance in substation C. The base-case of the simulation was the early-winter day of import. The comparison is between active ([P 50%]) and reactive ([Q 50%]) current contribution priority. Wind power plants operated at 50 % active power production from the nominal capacity prior to the disturbance in both cases.

Simulations with nominal active power production prior to the disturbance illustrate that wind power plants reach their maximum current limit, and thus the priorities given affects the stability. The following Figure 6.16 presents the voltage fluctuation at the same substation F as was shown earlier. In addition, the disturbance and case were the same. The voltage difference is now clearly seen. During the fault, the difference is maximumly 0.08 pu, whereas immediately after the disturbance the difference grows to almost 0.1 pu. Clear differences were also obtained with the base-case summer night of export. These differences are presented in Figure B.2 of Appendix B.

Behaviour of one of the wind power plant during the disturbance is shown in Figure 6.17. As the figure illustrates, the priority given limits the other current. Thus, in case of active current priority, the reactive current is limited up to the maximum allowed capacity. With reactive current priority, the active current is decreased down to its limit given by the logic in Section 5.2.1.

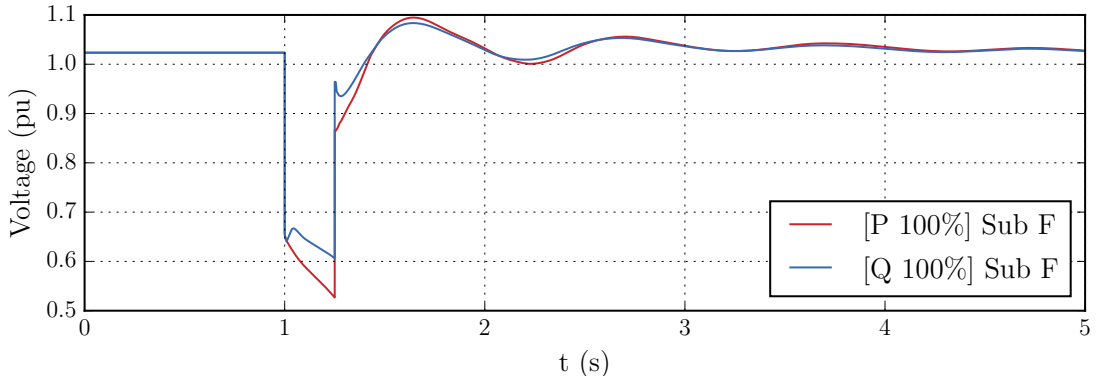

Figure 6.16: The voltage fluctuation at the substation F in case of 250 ms disturbance in substation C. The base-case of the simulation was the early-winter day of import. The comparison is between active ([P 100%]) and reactive ([Q 100%]) current contribution priority. Wind power plants operated at nominal active power production prior to the disturbance in both cases.

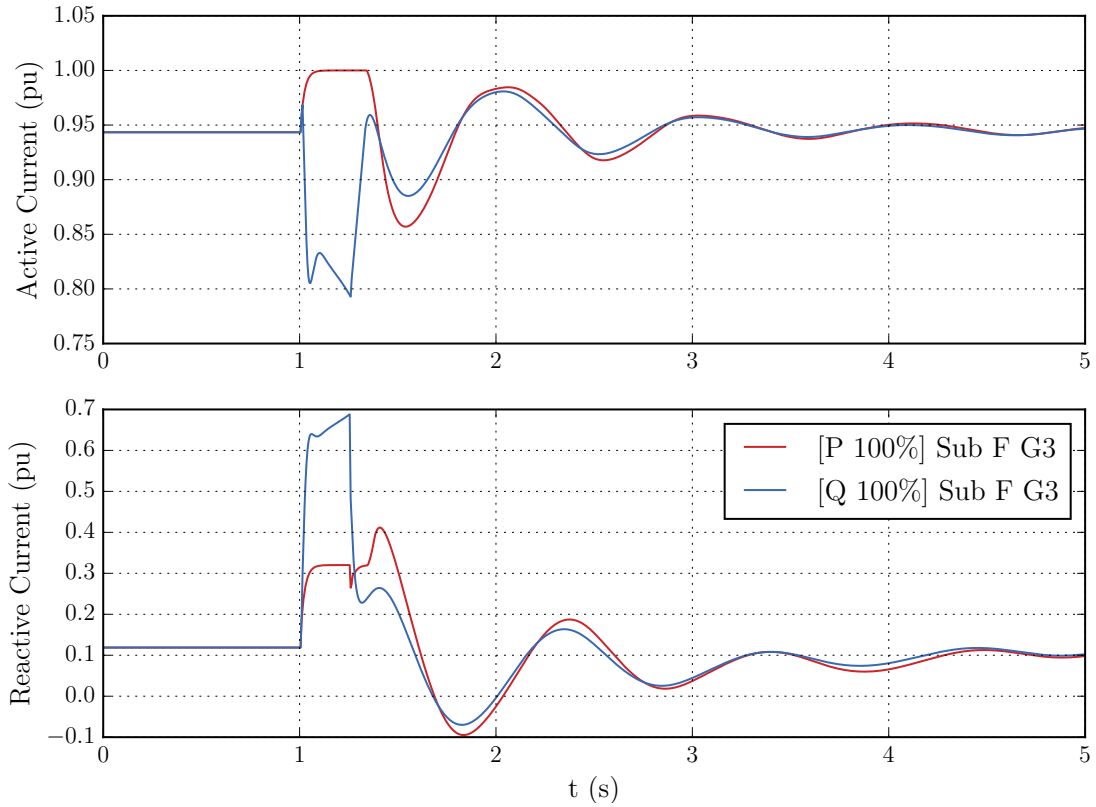

Figure 6.17: The injection of active and reactive current of wind power plant G3 connected to substation F in case of 250 ms disturbance in substation C. The base-case of the simulation was the early-winter day of import. The comparison is between active ([P 100%]) and reactive ([Q 100%]) current contribution priority. Wind power plants operated at nominal active power production prior to the disturbance in both cases.

Although the active current is higher in case of the prioritization of the active current, the actual active power feeding of this power plant is less during the fault. This is illustrated in Figure 6.18. A clear difference in the active power feeding can be seen in the figure. The difference can be explained with the higher reactive power and its impact on the voltage of the generator. The reactive current contribution priority boosts the voltage of the generator during the voltage drop. On the other hand, active current contribution priority limits the reactive current injection due to the priority. The smaller amount of reactive power feeding with the active current priority power plant leads to lower voltage at the generator. Therefore, the active power output can also be less. This phenomenon was also observed with some other wind power plants.

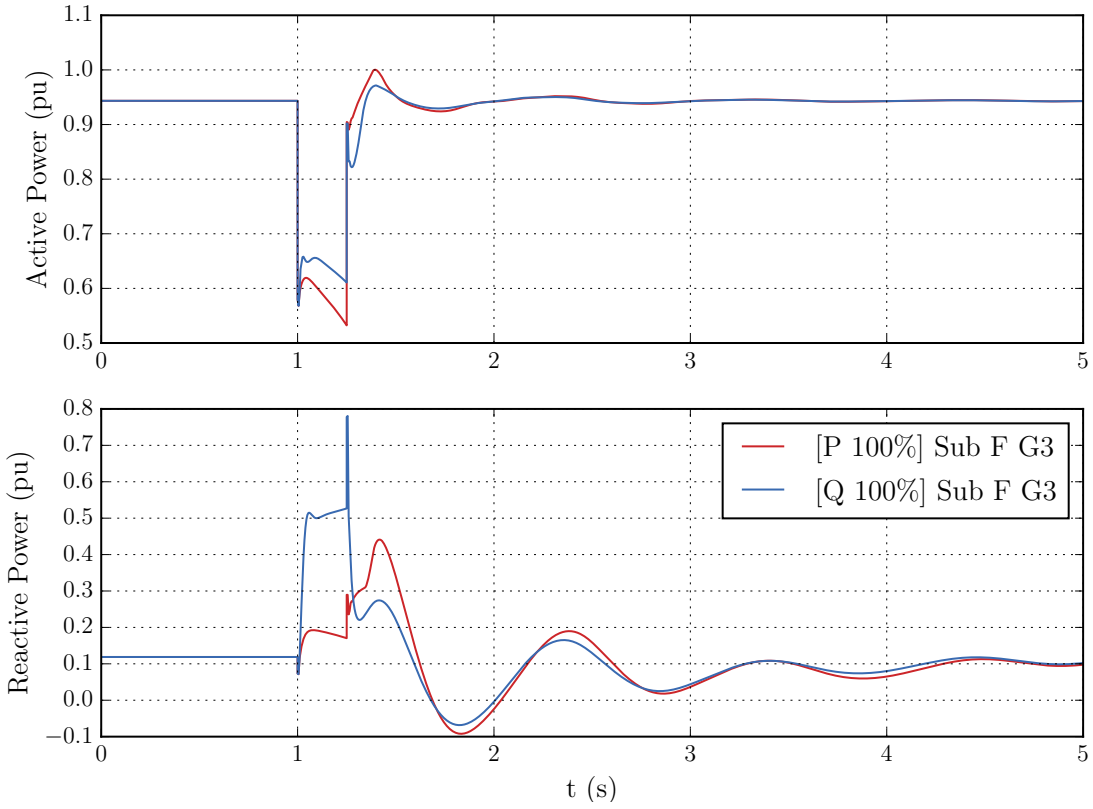

Figure 6.18: The active and reactive power feeding of wind power plant G3 connected to substation F in case of 250 ms disturbance in substation C. The base-case of the simulation was the early-winter day of import. The comparison is between active ([P 100%]) and reactive ([Q 100%]) current contribution priority. Wind power plants operated at nominal active power production prior to the disturbance in both cases.

6.2.2 Impact of Fault Current Contribution Priority on Rotor Angle Stability

The following section reviews the impact of fault current contribution priority on rotor angle stability. Figure 6.19 presents the rotor angle oscillation of a large generator subsequent to a 100 ms substation disturbance at 1.0 second followed by the tripping of Fenno-Skan2. The reviewed case was the summer night of export. The base-case was altered to include Hanhikivi 1 in the network. Wind power plants operated with 50 % active power production from the nominal capacity prior to the disturbance. As the figure shows, no remarkable difference is seen in the rotor angle. It was observed that the wind power plants did not reach their maximum current limit in the result. Similar observation was made with the tripping of Hanhikivi 1 in the same case and with the same active power production of the plants. This similarity is illustrated in Figure B.4 of Appendix B.

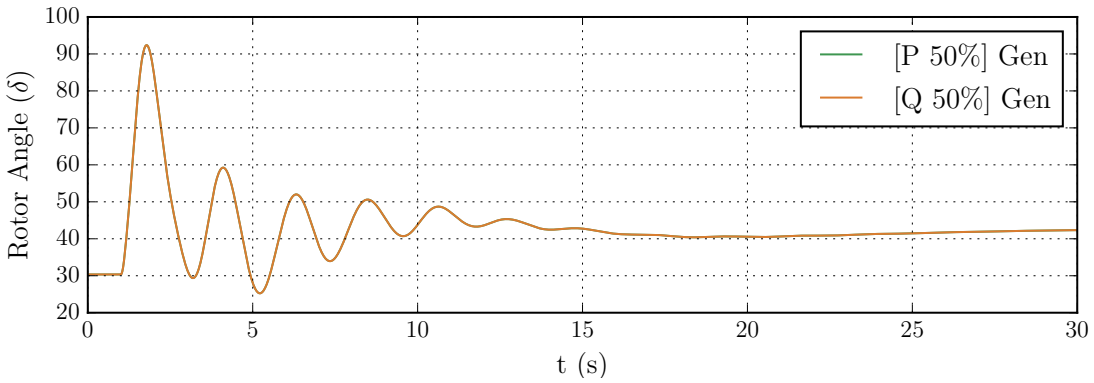

Figure 6.19: The rotor angle oscillation of a large generator in case of tripping Fenno-Skan2. The base-case of the simulation was the summer night of export. The base-case was altered to include Hanhikivi 1 in the network. The comparison is between active ([P 50%]) and reactive ([Q 50%]) current contribution priority. Wind power plants operated at 50 % active power production of nominal capacity prior to the disturbance in both cases.

When the wind power plants operated at nominal active power production prior to the disturbance, the result was similar although a small difference can be seen in the rotor angle oscillation. This result below in Figure 6.20 was simulated with the same disturbance and case as the above figure.

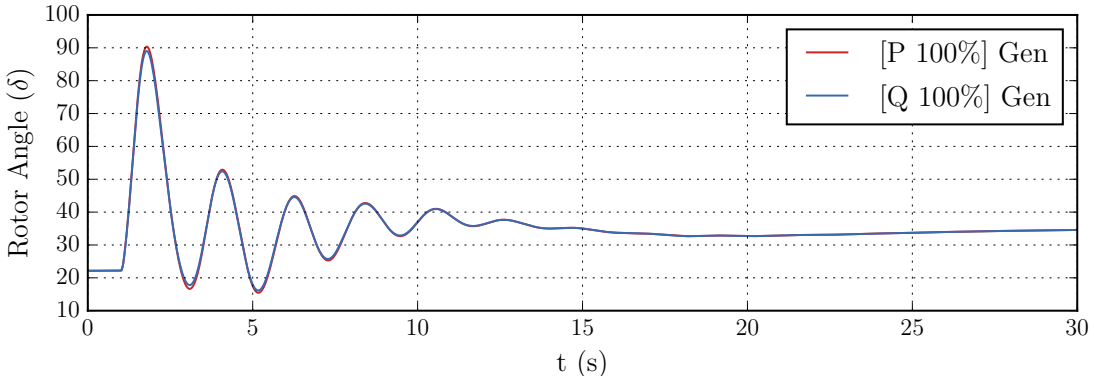

Figure 6.20: The rotor angle oscillation of a large generator in case of tripping Fenno-Skan2. The base-case of the simulation was the summer night of export. The base-case was altered to include Hanhikivi 1 in the network. The comparison is between active ([P 100%]) and reactive ([Q 100%]) current contribution priority. Wind power plants operated at nominal active power production prior to the disturbance in both cases.

Overall it was observed that the tripping of Fenno-Skan2 unit did not invoke large differences in the rotor angle oscillation of a large generator. On the other hand, with the tripping of Hanhikivi 1, differences were seen in the first up-swing of the generator. This is illustrated in Figure B.5 of Appendix B. In addition, when the oscillation was studied with a disturbance at a substation, the oscillation also differed. The observations were seen with the wind power plants operating at nominal active power feeding prior to the disturbance.

An example of the oscillation can be seen in Figure 6.21 where 250 ms disturbance was applied to substation D in the winter night of export case. The reviewed generator located near the faulty substation. As can be seen, this time the difference of the fluctuation of the rotor angle was nearly 20 degrees in the first up-swing. This higher angle was obtained with active current contribution priority. In addition, the oscillation damping is clearly less with active current priority.

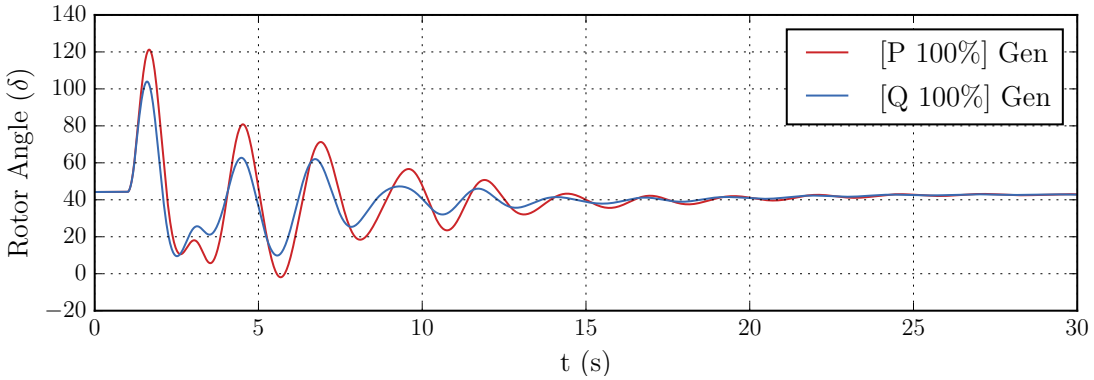

Figure 6.21: The fluctuation of the rotor angle of a large generator in case of 250 ms disturbance in substation D. The base-case of the simulation was the winter night of export. The base-case was altered to include Hanhikivi 1 in the network. The comparison is between active ([P 100%]) and reactive ([Q 100%]) current contribution priority. Wind power plants operated at nominal active power production prior to the disturbance in both cases.

6.2.3 Impact of Fault Current Contribution Priority on Frequency Stability

This section illustrates the impact of the fault current contribution priority on frequency stability. The frequency stability was studied with a 100 ms busbar disturbance at time 1.0 second followed by the tripping of Olkiluoto 3. In Figure 6.22, the stability was reviewed with the mid-winter day of import case. As the figure illustrates, even when the current contribution priority is dominant, the frequency deviation difference is minor. This was also observed with other cases. Results from another two cases are illustrated in Figure B.5 and B.6 of Appendix B. The next section illustrates the impact of fault clearing time of a substation disturbance on the power system stability.

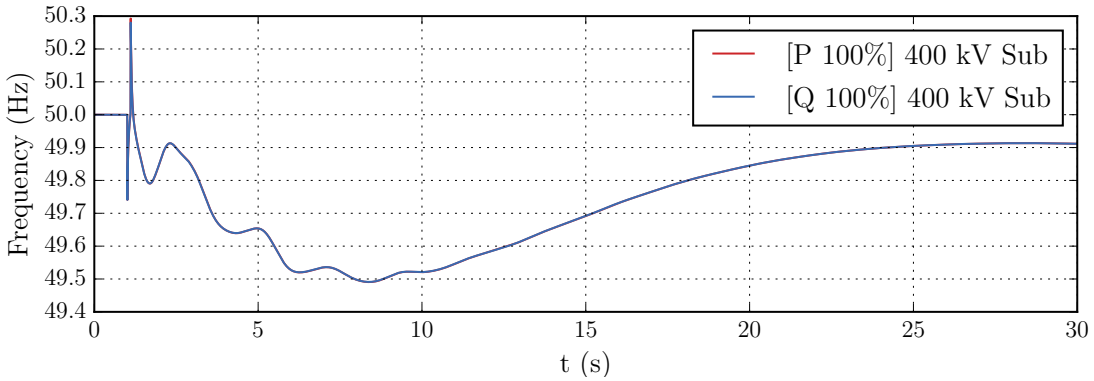

Figure 6.22: The frequency fluctuation at 400 kV substation in case of tripping Olkiluoto 3. The base-case of the simulation was the mid-winter day of import. The comparison is between active ([P 100%]) and reactive ([Q 100%]) current contribution priority. Wind power plants operated at nominal active power production prior to the disturbance in both cases.

6.2.4 Impact of Fault Current Contribution Priority on Critical Fault Clearing Time

The following section presents the impact of the fault current contribution priority on critical fault clearing time of a substation disturbance. As in the above sections, the comparison is between active and reactive fault current contribution. The disturbance was applied at substation A. To illustrate the minimum difference in the critical clearing time of most of the cases, the fault time of the disturbance was from 250 to 360 ms in five ms intervals.

Table 4 presents the results indicating at which clearing time the studied stability fell below the given limit after 30 seconds of simulation. The studied limits were 0.90 pu in voltage stability and either 49 or 51 Hz in frequency stability. In case of rotor angle stability, the critical length indicates the first loss of synchronism of a generator.

The results shown in the table and in the appendix support the results obtained in Section 6.2. As can be seen, the fault clearing time of the disturbance is longer with reactive current priority. The difference variates from unspecified, due to the limiting to 360 ms simulation, to up to at least 35 ms. This length depends on the reviewed case. Nevertheless, as can be seen in the table, if a difference exists, it is always in favour of reactive current contribution.

What can be also noticed from the results is that in most of the cases, different instabilities followed each other. Thus, the critical length was the same for each individual stability. However, with the early-winter day of import and winter night of export case, rotor angle stability was lost earlier than other stabilities. This was a result of a loss of synchronism of one generator. Even with the tripping of the generator, the system managed to stabilize the voltage and frequency for an additional 15 ms clearing time. This additional length was with active current priority in the early-winter day of import case (case B). With the winter night of export case (case D), the respective lengths were an additional 20 ms with active current priority and at least additional 10 ms with reactive current priority.

Additional results of this section with two other substation fault clearing times are found in Appendix B in Tables B.1 and B.2. They followed the same principles as in this substation fault clearing time.

Table 4: The impact of fault current contribution priority on critical fault clearing time of a disturbance in substation A. The fault clearing time was simulated from 250 ms to 360 ms in five ms intervals. The comparison is between active (P-priority) and reactive (Q-priority) current contribution priority. Wind power plants operated at nominal active power feeding prior to the disturbance in both cases.

Case	Stability	Critical length with P-priority (ms)	Critical length with Q-priority (ms)	Difference (ms)
A	Voltage	325	>360[1)]	>35
	Rotor angle	325	>360	>35
	Frequency	325	>360	>35
B	Voltage	340	>360	>20
	Rotor angle	325	>360	>35
	Frequency	340	>360	>20
C[2)]	Voltage	-	-	-
	Rotor angle	-	-	-
	Frequency	-	-	-
D	Voltage	340	>360	>20
	Rotor angle	320	350	30
	Frequency	340	>360	>20
E	Voltage	310	330	20
	Rotor angle	310	330	20
	Frequency	310	330	20

[1)] If the length includes '>' symbol, the case passed the last interval of 360 ms.
[2)] No instabilities occurred with neither priority during the simulations with case C.

Now that the power system stability has been studied with both active and reactive current contribution priority, Sections 6.3 and 6.4 present the impact of the reactive fault current gain and active power recovery time on power system stability.

6.3 Impact of Reactive Fault Current Gain on Power System Stability

The following section illustrates how the reactive fault current gain of the modelled wind power plants influences the power system stability. The logic of reactive fault current gain was explained in Section 5.2.2. The results are only shown for wind power plants with reactive current contribution priority. This is to illustrate the largest possible impact of the gain. The modelled wind power plants operated at nominal active power production prior to the disturbance.

6.3.1 Impact of Reactive Fault Current Gain on Voltage Stability

This section illustrates the impact of reactive fault current gain on voltage stability. Figure 6.23 presents the impact of the gain on voltage stability with a 250 ms substation disturbance at substation C. The base-case of the result is the summer night of export. The voltage fluctuation shown in the figure is from a nearby substation D. The difference in voltage between the extreme points was 0.1 pu during the fault, whereas immediately after the fault clearing the difference decreased to 0.09 pu.

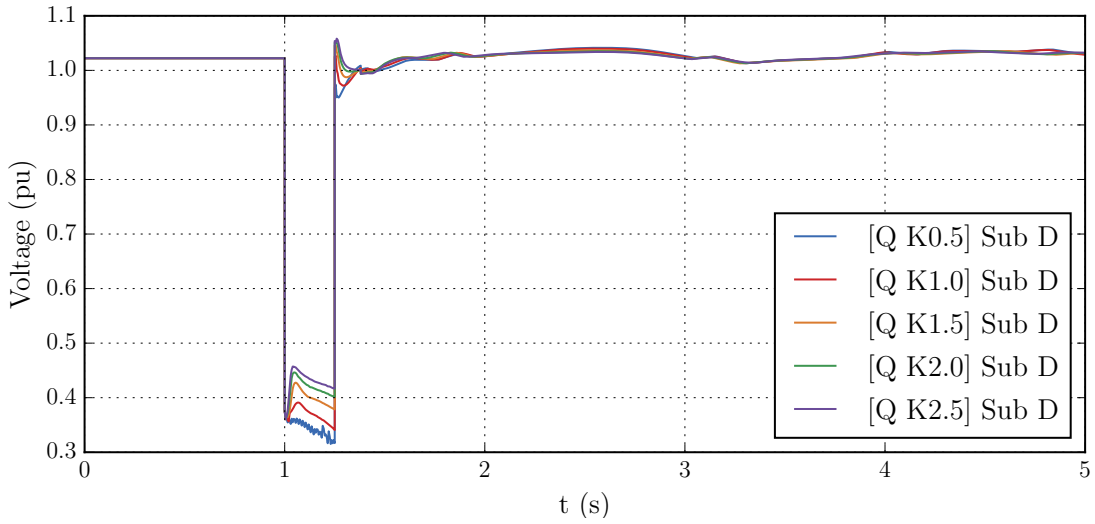

Figure 6.23: The voltage fluctuation at the substation D in case of 250 ms disturbance in a nearby substation C. The base-case of the simulation was the summer night of export. The comparison is between different reactive current gain value K (pu/pu) with reactive current contribution priority. Wind power plants operated at nominal active power production prior to the disturbance in all five cases.

The above-mentioned result is coherent with the logic explained in Section 5.2.2. With a higher reactive current gain, the modelled wind power plants are able to inject more reactive current with the same voltage drop seen. Thus, with the higher gain, the injected reactive current is also higher. This can be seen as a gradual voltage increase with each gain step in the substation reviewed. During and subsequent to the disturbance, the voltage is the lowest with the lowest gain, whereas the highest with the highest gain. Similar results were obtained with the mid-winter day of import case and with higher gain values. These results are illustrated in Figures C.1 and C.2 of Appendix C.

During the fault, some rapid fluctuation of voltage in the substation can be seen with low reactive current gain. This fluctuation is also noticed in the current injection of one of the wind power plants shown in Figure 6.24. This was presumably a numerical error in the model of the power plant. What can also be observed from the figure is that the set values for the reactive current response is not completely optimized for the current injection. Thus, the reactive current injection response

overshoots. In addition, it can be seen in the figure that the current injection of the power plant in the case of the lowest gain value 0.5 does not reach the current limit. This enables the increase in active current injection.

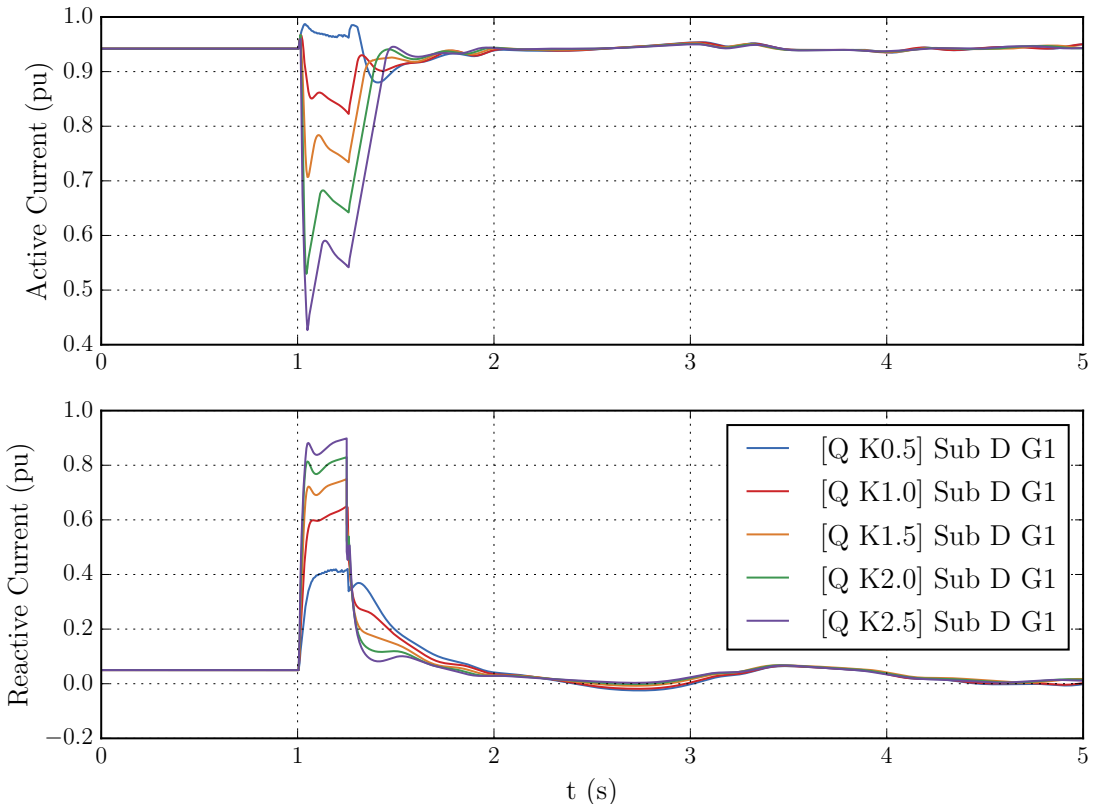

Figure 6.24: The injection of active and reactive current of wind power plant G1 connected to substation D in case of 250 ms disturbance in a nearby substation C. The base-case of the simulation was the summer night of export. The comparison is between different reactive current gain value K (pu/pu) with reactive current contribution priority. Wind power plants operated at nominal active power production prior to the disturbance in all five cases.

Ideally, the higher the voltage drop is, the better is a higher reactive current gain. However, due to their geographical location, individual wind power plants see a different magnitude voltage drop. Thus, with a high gain, the substantial reactive current injection with even a low voltage drop can increase the voltage above the normal operation limit. This kind of behaviour is illustrated in Figure 6.25. The figure was obtained with 250 ms substation disturbance at substation D with the base-case of summer night of export.

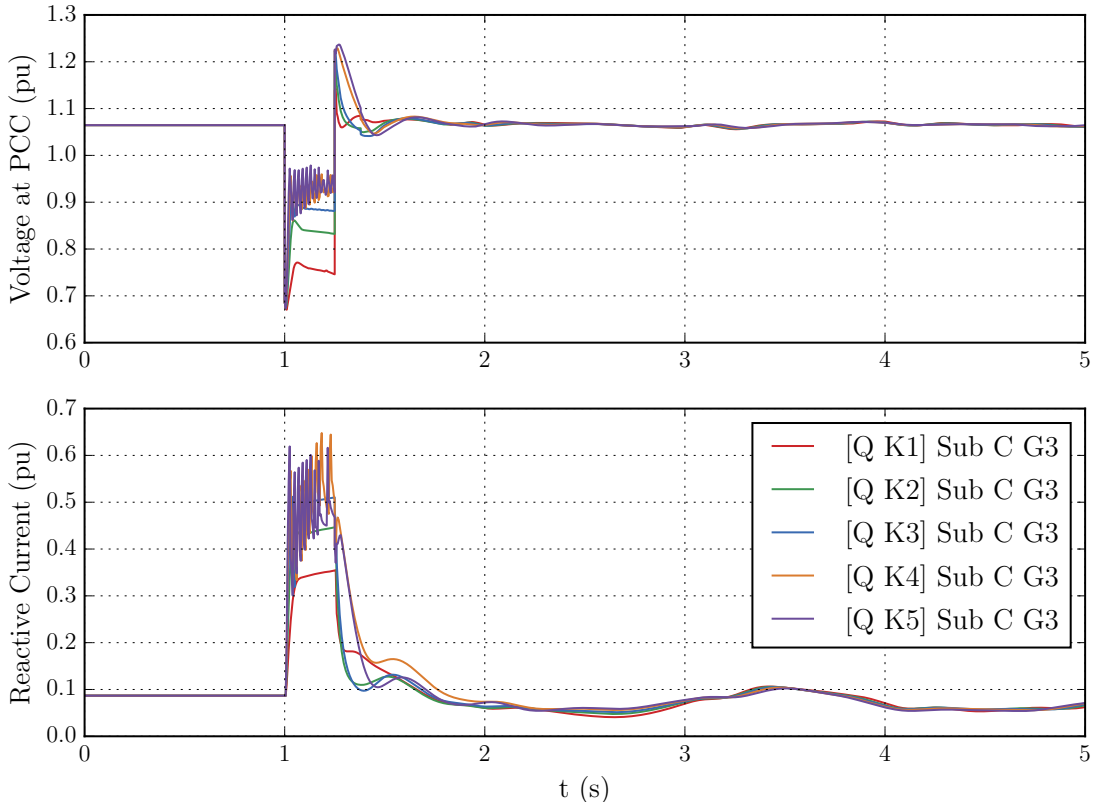

Figure 6.25: Voltage at the point of common coupling and the injection of reactive current of wind power plant G3 connected to substation C in case of 250 ms disturbance in substation D. The voltage at PCC is the voltage controlled by the wind power plant. The base-case of the simulation was the summer night of export. The comparison is between different reactive current gain value K (pu/pu) with reactive current contribution priority. Wind power plants operated at nominal active power production prior to the disturbance in all five cases.

The voltage in the figure is boosted up to 1.22 pu with high gain values at the connection point of the wind power plant. What can be also noticed in the result is that with a high gain, such as K4 and K5, the modelled wind power plant begins to fluctuate the injection of reactive current. This is due to the operation between the normal and fault condition mode set at 0.9 pu voltage. First, the high reactive current injection increases the voltage above the limit. Shortly after, the injection is restricted, but again the voltage falls below the limit. This begins a continuous rapid ramping of the injection between the normal and fault operation mode. In the next section 6.3.2, the impact of the gain on rotor angle stability is reviewed.

6.3.2 Impact of Reactive Fault Current Gain on Rotor Angle Stability

This section presents the impact of reactive current gain on rotor angle stability. The following Figure 6.26 illustrates the impact of reactive current gain on rotor angle stability. The result was obtained with a 100 ms substation disturbance followed by

the tripping of Fenno-Skan2 in the early-winter day of import case. The differences of the injection of active current with different gain levels are only slightly seen in the oscillation. Also, due to all the other power plants contributing to the system, the proportional influence of the wind power plants is less.

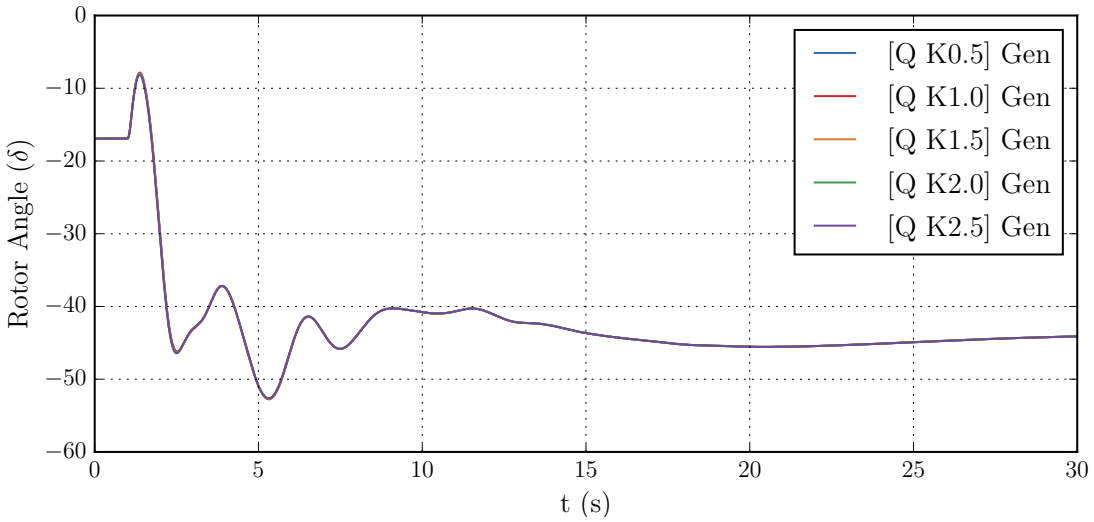

Figure 6.26: The rotor angle oscillation of a large generator in case of tripping Fenno-Skan2. The base-case of the simulation was the early-winter day of import. The comparison is between different reactive current gain value K (pu/pu) with reactive current contribution priority. Wind power plants operated at nominal active power production prior to the disturbance in all five cases.

On the other hand, when the tripping of Fenno-Skan2 was reviewed with the winter night of export case and with higher gain values, the differences began to be slightly more noticeable. The differences are illustrated in Figure 6.27. The trend is noticed to be towards the observations made in Section 6.1.2. When the modelled wind power plants have the possibility to inject more active current with lower reactive current gain, the amplitude of the rotor angle oscillation of a generator is higher. The active current injection given by the wind power plants during and after the disturbance decreases the possibility of the synchronous generator to inject its stored kinetic energy during the acceleration to the local loads subsequent to the clearing of the fault. Thus, the deceleration is slower. Therefore, the rotor angle also grows higher. With another export base-case, the above-mentioned observations were also seen. These are illustrated in Figures C.3 and C.4 of Appendix C.

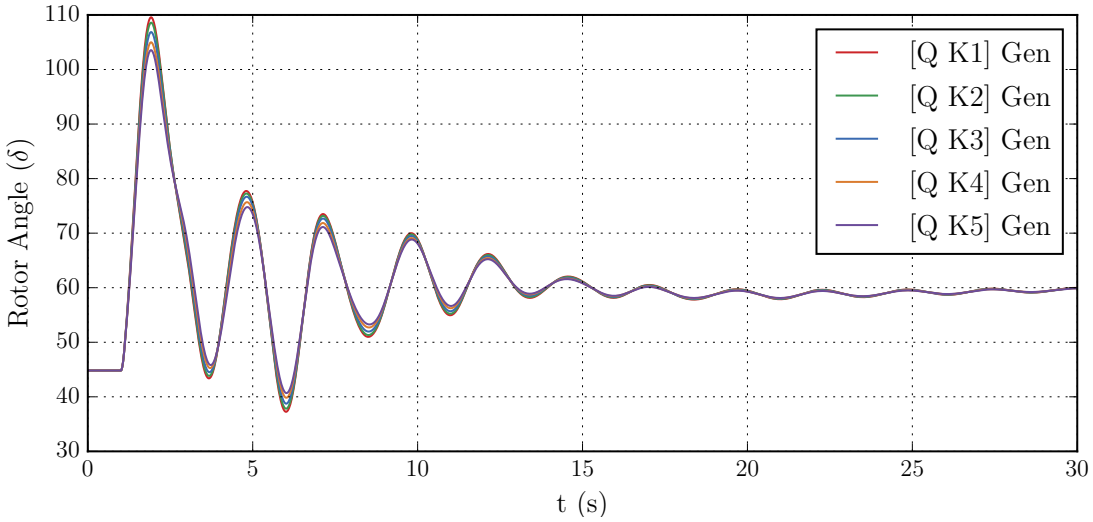

Figure 6.27: The rotor angle oscillation of a large generator in case of tripping Fenno-Skan2. The base-case of the simulation was the winter night of export. The comparison is between different reactive current gain value K (pu/pu) with reactive current contribution priority. Wind power plants operated at nominal active power production prior to the disturbance in all five cases.

As was mentioned in voltage stability discussion, ideally the higher the gain is, the better is also rotor angle stability. Nevertheless, the same voltage limit crossing with a high gain can occur in these cases. Next, the impact on frequency stability is illustrated in Section 6.3.3.

6.3.3 Impact of Reactive Fault Current Gain on Frequency Stability

This section reviews the impact of reactive current gain on frequency stability. Figure 6.28 presents the frequency fluctuation in the early-winter day of import case with a 100 ms busbar disturbance at time 1.0 second followed by the tripping of Olkiluoto 3. As the figure shows, the fluctuation differences are barely visible. The difference in the active current injection of the plants with different gain is not widely seen by the power system. Thus, the overall impact of the current injections of the wind power plants is not large enough to cause visible difference in the frequency of the system. Even with higher gain values and other cases, the results were similar. Figures C.5 and C.6 of Appendix C presents the result for another two case.

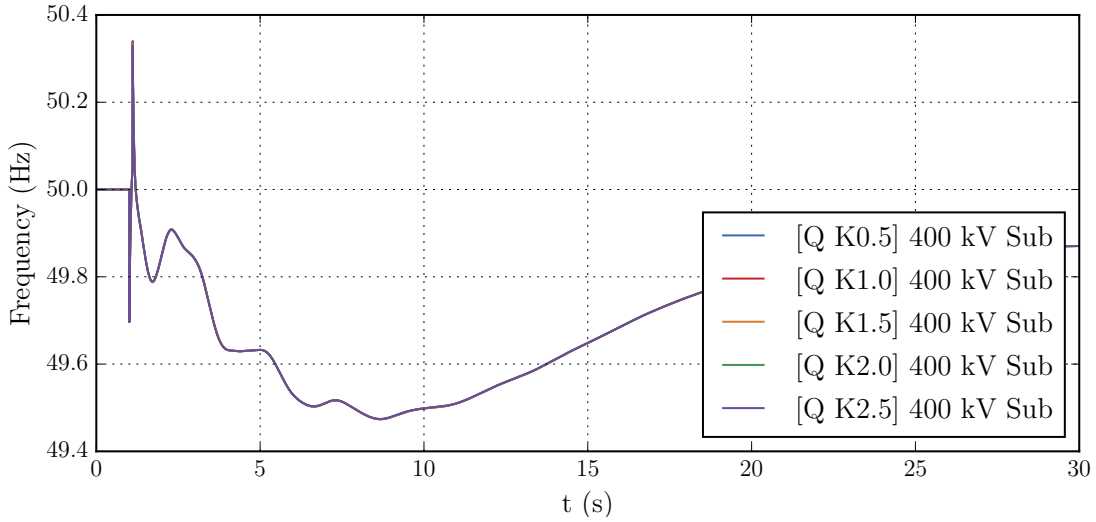

Figure 6.28: The fluctuation of the frequency of 400 kV substation in case of tripping Olkiluoto 3. The base-case of the simulation the early-winter day of import. The comparison is between different reactive current gain value K (pu/pu) with reactive current contribution priority. Wind power plants operated at nominal active power production prior to the disturbance in all five cases.

6.4 Impact of Active Power Recovery Time on Power System Stability

This section illustrates the impact of active power recovery time on power system stability. The modelled wind power plants operated at nominal active power capacity prior to the disturbance. As was mentioned in Section 5.2.3, the recovery time influences the time required for the wind power plant to recover its active power production.

6.4.1 Impact of Active Power Recovery Time on Voltage Stability

This section concentrates on the impact of the active power recovery time on voltage stability. The following Figure 6.29 presents the impact on voltage stability when the modelled wind power plants operated with active current priority. The disturbance was applied at substation C in the summer night of import case. The substation reviewed in the figure is located nearby. As suspected, the voltage fluctuation is similar with every recovery time. Similar fluctuation was also observed with base-case summer night of export illustrated in Figure D.1 of Appendix D. The similarity of the voltage fluctuation can be supported with the behaviour of the wind power plants discussed next.

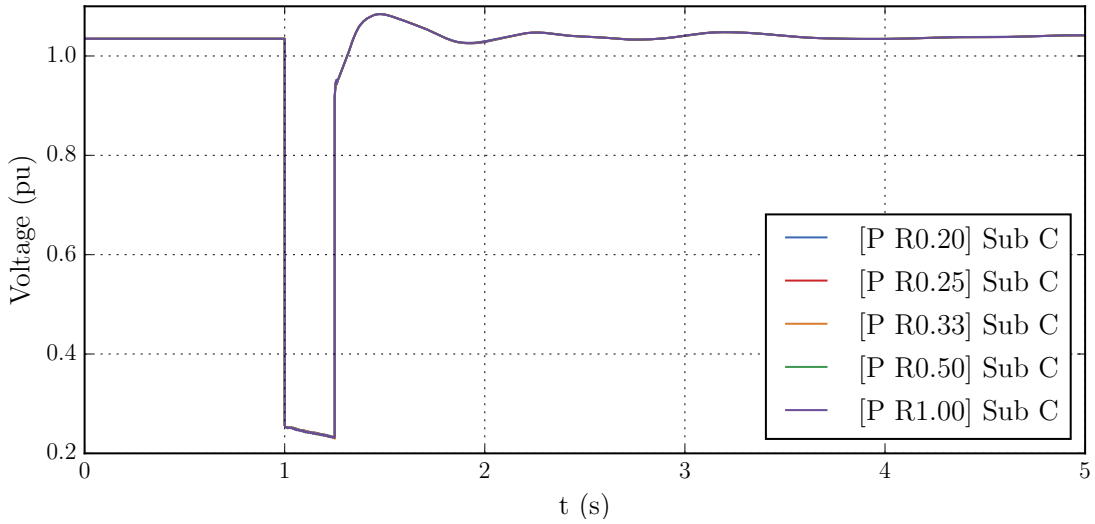

Figure 6.29: The voltage fluctuation at the substation C in case of 250 ms disturbance in a nearby substation D. The base-case of the simulation was the summer night of import. The comparison is between different active power recovery time value R (pu/s) with active current contribution priority. Wind power plants operated at nominal active power production prior to the disturbance in all five cases.

An example of the behaviour of one of the modelled plants is shown in Figure 6.30. As it can be seen in the current injection, the injection of reactive current during the fault is the same with every case. This is the maximum limit of the reactive current explained in Section 5.2.1 in Equation (6). Therefore, the voltage fluctuation was similar with every recovery time. On the other hand, the active current injection has a different slope. This is a result of a different recovery time. Rapid recovery time (e.g., higher P value) reduces the active current injection time. Nevertheless, the injection of active current in this case does not have an impact on the voltage of the substation.

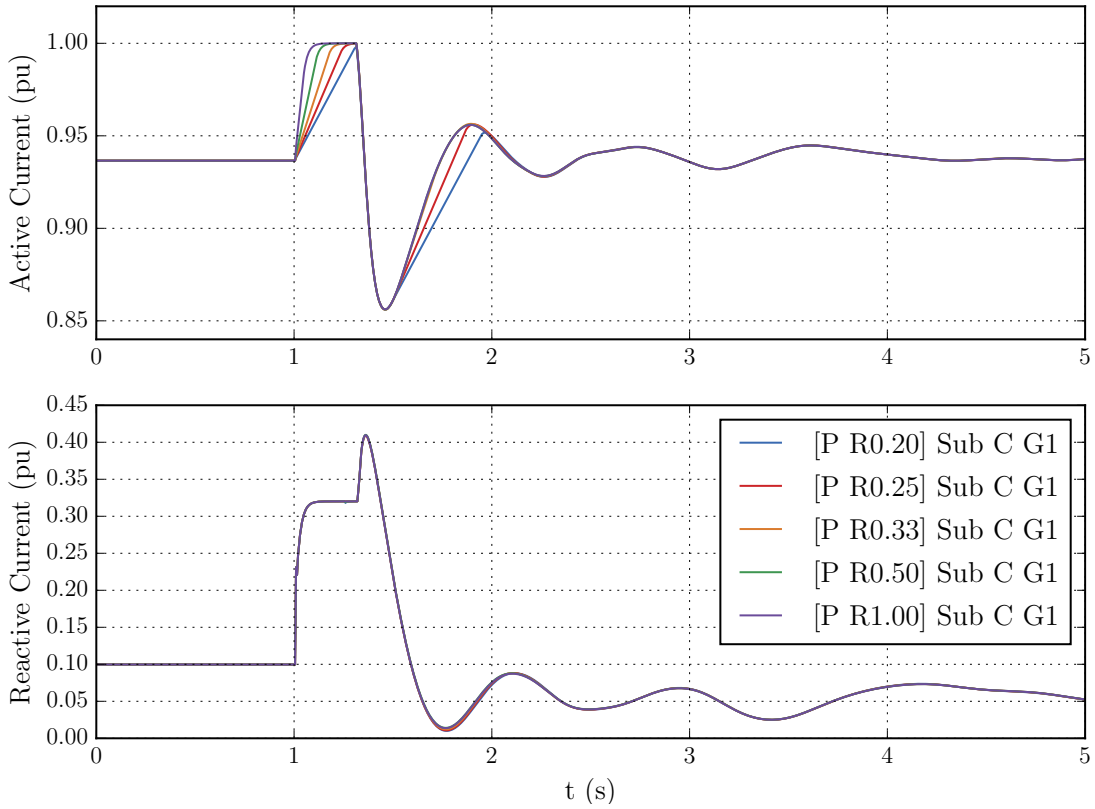

Figure 6.30: The injection of active and reactive current of wind power plant G1 connected to substation C in case of 250 ms disturbance in a nearby substation D. The base-case of the simulation was the summer night of import. The comparison is between different active power recovery time value R (pu/s) with active current contribution priority. Wind power plants operated at nominal active power production prior to the disturbance in all five cases.

With the same summer night of import case, but with reactive current priority, the results were similar. The voltage fluctuation at the same substation is shown in Figure 6.31. Similarly, the behaviour of one of the modelled wind power plant is shown in Figure 6.32. During the fault, the injection of active and reactive current is the same, but subsequent to the fault, the recovery time influences the active current injection. Nevertheless, since the reactive current injection is the same during the fault, and nearly the same subsequent to the fault, the voltage fluctuation is also nearly the same. Same results were also observed in the base-case summer night of export presented in Figure D.2 of Appendix D.

It was observed that the active power recovery time did not have a significant impact on the voltage stability in the reviewed cases. The next section illustrates the impact on the rotor angle stability.

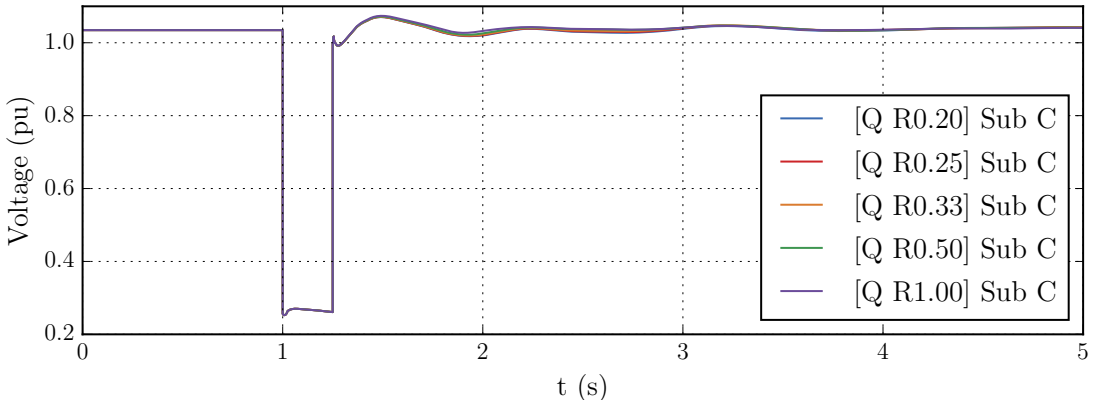

Figure 6.31: The voltage fluctuation at the substation C in case of 250 ms disturbance in a nearby substation D. The base-case of the simulation was the summer night of import. The comparison is between different active power recovery time value R (pu/s) with reactive current contribution priority. Wind power plants operated at nominal active power production prior to the disturbance in all five cases.

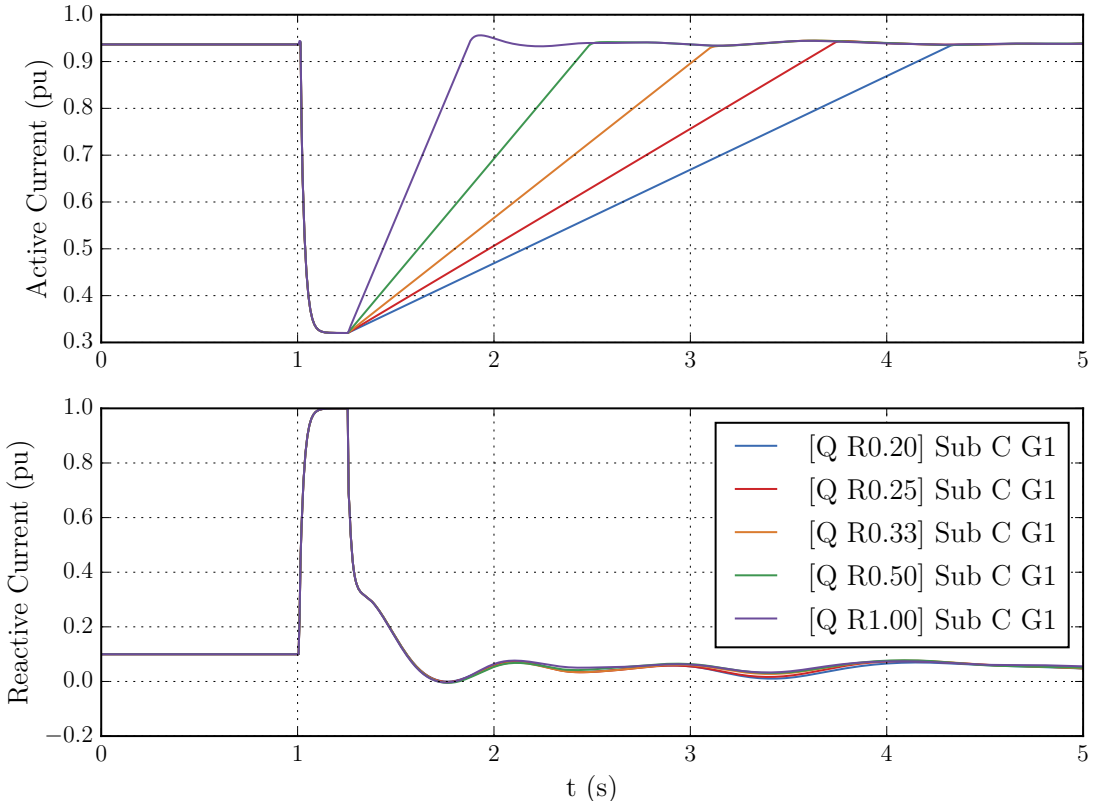

Figure 6.32: The injection of active and reactive current of wind power plant G1 connected to substation C in case of 250 ms disturbance in a nearby substation D. The base-case of the simulation was the summer night of import. The comparison is between different active power recovery time value R (pu/s) with reactive current contribution priority. Wind power plants operated at nominal active power production prior to the disturbance in all five cases.

6.4.2 Impact of Active Power Recovery Time on Rotor Angle Stability

This section presents the impact of the active power recovery time on rotor angle stability. Figure 6.33 presents the impact of the recovery time with reactive current priority on rotor angle stability. The figure was obtained with the tripping of Fenno-Skan2. The base-case of the simulation was the winter night of export. As it can be seen from the figure, noticeable differences can be seen in the oscillation of the rotor angle. This is due to the difference in the active current injection of the wind power plants subsequent to the disturbance. The fastest injection has the highest magnitude as presumed. The presumption is related to the kinetic energy of the synchronous machine. The deceleration is slower the lesser is the kinetic energy injection of the synchronous machine subsequent to the fault clearance. This conclusion was also discussed in Section 6.3.2.

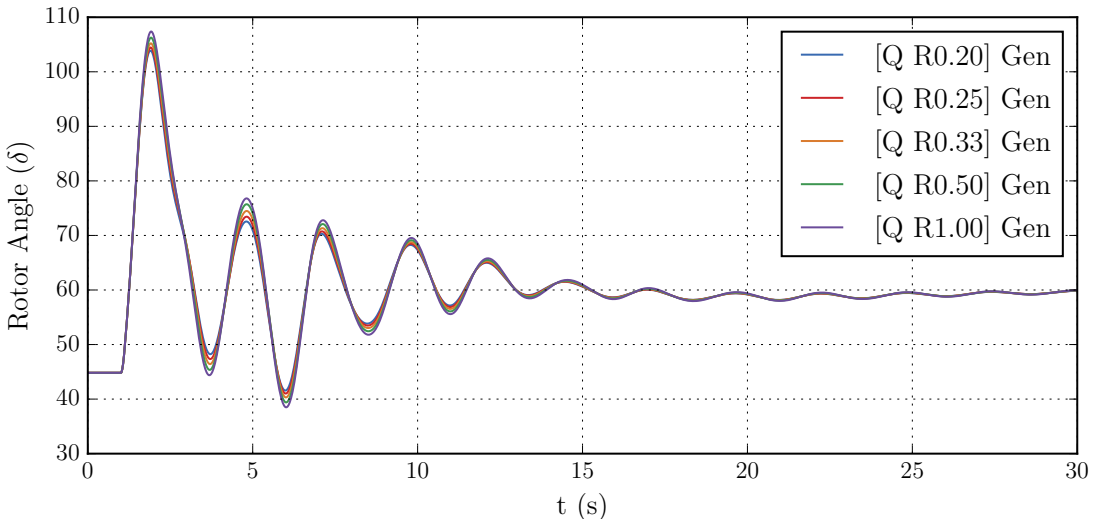

Figure 6.33: The rotor angle oscillation of a large generator in case of tripping Fenno-Skan2. The base-case of the simulation was the winter night of export. The comparison is between different active power recovery time value R (pu/s) with reactive current contribution priority. Wind power plants operated at nominal active power production prior to the disturbance in all five cases.

With faster active power recovery times, the rotor angle oscillation differences were minor. This is illustrated in Figure D.3 in Appendix D. Differences seen in the above figure 6.33 were also observed with reactive current priority in other cases. The rotor angle oscillation of a generator was higher, the faster was the active power recovery time. However, when the tripping of Fenno-Skan2 was reviewed with active current priority, the differences were not noticeable. One example of this is presented in Figure D.4 of Appendix D. These non-visible differences were due to the minimal differences in the active current injection of the power plants illustrated in Section 6.4.1.

Last section 6.4.3 finalizing the research of this thesis explores the impact of the active power recovery time on frequency stability.

6.4.3 Impact of Active Power Recovery Time on Frequency Stability

This section illustrates the impact of the active power recovery time on frequency stability. The impact on frequency stability was studied with a 100 ms busbar disturbance at time 1.0 second followed by the tripping of Olkiluoto 3. An example of the impact is shown in Figure 6.34. The result was obtained with active current priority in the mid-winter day of import case. As the figure illustrates, and as the previous results of frequency stability have shown, the impact of the active power recovery time is minor. Similar results were obtained with reactive current priority and with various cases. Results from another two cases are presented in Figures D.5 and D.6 of Appendix D.

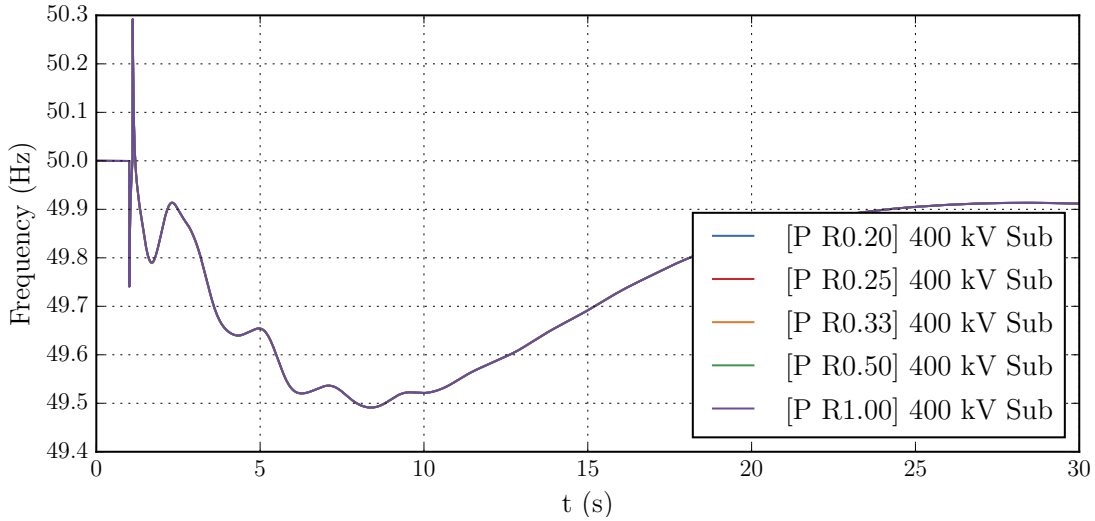

Figure 6.34: The fluctuation of the frequency of 400 kV substation in case of tripping Olkiluoto 3. The base-case of the simulation was the mid-winter day of import. The comparison is between different active power recovery time value R (pu/s) with active current contribution priority. Wind power plants operated at nominal active power production prior to the disturbance in all five cases.

7 Evaluation of the Results and Conclusions

The aim of this thesis was to determine the fault current contribution requirements for converter based power plants in Finland. The determination was implemented by studying the impact of the fault current contribution on power system stability. The subjects of this study were wind power plants. However, when using a full converter model, the results can be adjusted for other converter power plants to some extent. The fault current contribution study was divided into four different sections. This made it possible to cover the different parameters influencing this contribution.

This chapter consist of four different sections. The results are summarized and analysed in Section 7.1. In Section 7.2, the results of this thesis are evaluated. Section 7.3 addresses the importance of these results and proposes possible future studies. Last Section 7.4 finalises this thesis with conclusions.

7.1 Analysing the Results

The results illustrated in Chapter 6 indicate that different power system operation situation with different current contribution priorities of the modelled wind power plants have different impact on the power system stability. Also, the location and the type of the disturbance plays a significant role for the outcomes. With one case and one disturbance, the differences in the results were minor in comparison with another case and another disturbance results. Although in some cases the differences were small, and substantial in some others, the trend was always the same. This trend was towards a better power system stability enhancement with reactive fault current priority than with the active fault current priority.

The benefits from reactive fault current injection compared with no fault current injection were observed in the first comparison study in Section 6.1. A visible difference was seen in the voltages of substations during a 250 ms substation disturbance. Above-mentioned observations of the benefit were further supported in the study of substation fault clearing time in Section 6.1.4. Wind power plants with reactive current priority were able to stabilize the power system with the longest fault clearing times. The advance in the clearing time was from 10 to 100 ms compared with zero fault current injection. This means that the power system can survive from longer disturbances without losing the stability with reactive current priority plants. Although the reactive current contribution priority cases in Section 6.1.2 caused a higher rotor angle oscillation compared with the cases without fault current contribution, the critical substation fault clearing times were longer with reactive current priority. The longer lengths were a result of additional voltage support from the reactive current contribution power plants during and immediately after the fault.

On contrary to the reactive current priority, active current priority was in some cases even poorer in supporting the stability than the zero fault current injection. This was illustrated in Section 6.1.4. This shorter critical clearing time was a result of smaller reactive power feeding from the active current contribution priority plants immediately after the fault clearing. The system was not able to recover a steady state after the fault.

Further support for reactive current priority were obtained when the power system stability was studied by comparing active and reactive current contribution priority in Section 6.2. The voltage stability study in Section 6.2.1 presented visible differences in the voltage fluctuation at several substations. The voltages were higher with reactive current priority during and immediately after a substation fault. It was also observed in this section that in some cases the active power feeding of some of the wind power plants were even higher with reactive current contribution priority. This was a result of a higher voltage at the generator. Thus, in certain cases, with reactive current priority, the benefit of active power feeding during the fault is greater than the active power feeding achieved with active current priority. Up to some point, this result questions the active power feeding benefit from active current contribution priority. In addition to the above-mentioned results, in the critical fault clearing time study in Section 6.2.4, the reactive current priority was able to stabilize the system with up to 40 ms longer faults compared with active current priority. These obtained results were coherent with the theoretical background of the voltage stability and the operation principles of wind turbines explained in Sections 2.1 and 3.1.3 respectively. The reactive power support from machines increases the local voltage. This support was also obtained with wind power plants.

The oscillation of rotor angle illustrated in Section 6.2.2 was similar in both active and reactive current contribution priority with the tripping of Fenno-Skan2. On the other hand, with substation disturbances, the differences became visible. Similar notable differences were seen with the tripping of a generator near the modelled wind power plants. The rotor angle oscillation was shown to be higher and the damping poorer with active current priority. These observations follows the behaviour of synchronous machines during a disturbance presented in Section 2.3. The kinetic energy stored in the machine during the acceleration period is fed to the local loads of the system after the fault clearing. This power feeding decelerates the machine. If another machine (e.g., a wind power plant) also feeds active power to the system during this period, the deceleration is slower. Thus, the rotor angle grows higher. In addition, the better voltage support from the power plants with reactive current priority enables higher power output from other plants. This quickens the deceleration of the machines.

The results obtained in the frequency stability studies in Sections 6.2.3, 6.3.3, and 6.4.3 with the tripping of Olkiluoto 3 indicated that neither the fault current priority, the reactive current gain, nor the active power recovery time affects the frequency stability significantly. Whereas, without any fault current contribution the frequency fluctuated in lower level from the nominal 50 Hz frequency compared with the selected fault current contribution. These results were seen in Section 6.1.3. The insignificant differences are partly due to the operation of the plants. Each wind power plant controlled the voltage of the local busbar and the frequency control was neglected. Therefore, the operation during the fault was only dependent on this voltage.

In addition to the fault current contribution priority results, the results obtained from reactive current gain study in Section 6.3 illustrated that a higher gain led to a better voltage support. This was seen as a gradual increase in the voltage of a

substation the higher the gain was. Alternatively, it was observed with a high gain value in Section 6.3.1 that the voltage at the point of common coupling exceeded shortly the normal operation voltage after the fault clearance. On the other hand, a wind power plant began a rapid injection fluctuation of the reactive current when the plant operated between the normal and fault operation mode. On the other hand, with a higher gain, the rotor angle oscillation of a large generator was lower. Moreover, the gain did not have a remarkable effect on the frequency stability as it was seen in Section 6.3.3.

The last case about the active power recovery time in Section 6.4 indicated that the recovery time had only notable impact on the rotor angle stability. The rotor angle oscillation was higher, the faster was the active power recovery after the tripping of Fenno-Skan2. Higher rotor angle was caused by a faster active power feeding from the plants after the fault clearance. These visible impacts on the rotor angle oscillation were illustrated in Section 6.4.2.

7.2 Evaluating the Results

The clear differences explained in the previous section were obtained with wind power plants operating at nominal active power production prior to the disturbance. The nominal power was utilized to invoke the reaching of the maximum current of the converter, and therefore, the current priority limiting the injection of the other current as was explained in Section 6.2.1. The maximum current was less frequently reached when the power plants operated at half of the nominal capacity. This was illustrated in Section 6.2.1. Thus, in these cases no remarkable differences were seen in the comparison of active and reactive current contribution. This difference questions the remarkable benefit from reactive current priority. If the power plants operate far below the nominal power, and the maximum current of the converter is never reached, the priority does not remarkably affect the stability. Whereas, if the plants operate near or at nominal power, it does clearly affect the stability of the system. Nevertheless, the stability enhancement in the results was always at least even or greater with the reactive current priority than with the active current priority.

As a result of the decision about letting the maximum current and the current commands select the current injection, the results did not take into account the possibility to inject the currents with fixed curves dependent on the voltage drop. The injection could have been set more precisely to include the reduction of active or reactive current with certain piecewise voltage–current curve. On the contrary, no universal setting for the piecewise curve exists. Thus, the simplification was as justified as any made-up piecewise curve.

The constant value of the voltage control response raises questions about the precise operation of the modelled plants in some cases. Although the response was within the limits of the network connection requirements, the reactive power response of a wind power plant overshoot after the fault clearance. This was illustrated in Section 6.1.4. The overshoot also began a short fluctuation of the reactive power injection. It was not clear whether this was caused by the actual constant values or

due to the fast voltage recovery after the fault.

The values of selected parameters related to the fault current contribution were easily varied. The variation was possible with the generic wind power plant model used in the simulations. However, because the model was generic, it lacks certain control systems of the actual wind power plants. These control systems are commonly modelled in the manufacturer specific models. The control systems include, but are not limited to, specific fault ride through behaviour of the plant. This includes the use of crowbar or DC-link chopper for example. On the other hand, since the research of this thesis was analysed from the long-term planning perspective of the system, the details are commonly not necessary for the overall system behaviour. In addition, some of the parameters of the manufacturer specific models can be hard-coded. Thus, the variation of the selected parameters would not have been possible.

The results from fault current contribution priority study in Section 6.2 of this thesis contradict the result obtained in study [37] which was shortly presented in Section 4.3. The study illustrated that active current contribution priority was the most stable, whereas reactive current contribution priority was said to be leading to rotor angle instabilities. This observation was the opposite in comparison with the results obtained in this thesis. The difference indicates that the initial conditions and the characteristics of the power system have an impact on the results. As it was stated in study [36] reviewed in Section 4.3, the voltage support priority scheme becomes more relevant when the network is weak.

On the other hand, other studies [38–40] presented in Section 4.3 are coherent with the results in Sections 6.2, 6.3 and 6.4. These studies also indicate that the power system can benefit more from reactive current contribution priority. In addition, as was observed in the reactive current gain study in Section 6.3, voltage stability benefits more from a higher gain. This was also noted in [38]. Although, as it was seen in Section 6.3.1 that with a high gain, the voltage can increase above the normal operation voltage at the point of common coupling of the wind power plant. Also, some of the modelled wind power plants began a rapid reactive current injection fluctuation if the controlled voltage was near the fault current injection voltage limit. This fluctuation was due to the operation between normal and fault current contribution mode. In addition to the above-mentioned results, as the study [39] declared, slower active power recovery time improves the transient stability in exporting areas. This was also noted in the rotor angle stability study in Section 6.4.2. The consistent results and the support from other studies reasserts that a beneficial requirement for fault current contribution of the plants is to prioritize reactive fault current injection.

7.3 Importance of the Results and Future Prospects

Although the fault current contribution has been widely studied from different perspectives, the initial circumstances of those simulations does not provide sufficient information for this research frame. The specific circumstances affect the results as was observed while analysing them in this thesis. Thus, to acquire comprehensive and precise overall picture, the entire power system with different operation situations

must be taken into account. With the results obtained from this study and with the support from earlier research related to the fault current contribution, this thesis presents a fairly comprehensive ensemble. Hence, a requirement for fault current contribution was able to be determined. The potential knowledge users of this study are the transmission system operators.

These results can be utilized as initial information when planning and determining on new network connection requirements for converter based power plants. In addition, with the modelled cases and with the knowledge about the behaviour of the wind power plants in various operation modes, the groundwork for the future studies has already been carried out. These future studies are suggested next.

First, as was mentioned in the evaluation of the results in Section 7.2, the generic models used in these simulations lack certain control systems often modelled in manufacturer specific models. Although it is not known which manufacturers power plants will be installed in the future, these models can have different responses to the system. These manufacturer specific models could be further studied with the modelled cases of this study.

Second, the wind power plants were not modelled with frequency control. This decision partly affected the results obtained from the frequency stability study. In addition, as a result of the frequency decoupling from the system, the plants do not contribute to the inertia of the power system. However, the provision of synthetic inertia by extracting the stored kinetic energy through the converter is possible. Both the frequency control and especially the synthetic inertia are important subjects to be further studied.

Last, the variation of the reactive current gain and the active power recovery time was studied one at a time. Thus, their interact with each other was not taken into account. As the results indicated, both of the parameters had a different impact on the power system stability. Therefore, their joint effect can also invoke different stability advantages or disadvantages. This prevented the determination of optimum values for them. With the interaction study, optimum values for these parameters could be researched in terms of power system stability enhancement. With the obtained knowledge of the individual behaviour of these parameters on the power system stability, their common effect could be reviewed in detail in a future study.

7.4 Conclusions

The aim of this thesis was to determine requirements for fault current contribution of converter based power plants in Finland. The determination was conducted by studying the impact of the fault current contribution on power system stability.

A power system is a diverse ensemble where different components interact with each other. As the results in this thesis indicated, different power system operation situations with certain fault current contribution responses of wind power plants had different impact on the power system stability. In addition, the location and type of the disturbance played a major role for the outcomes. These observations must be taken into account when studying the impact of the responses of power plants on power system stability. To find beneficial parameters, the examination must be

conducted from multiple perspective.

Even though different initial conditions and responses from the plants had different impact on the stability, a beneficial requirement was able to be determined in this thesis. This requirement was the prioritization of reactive fault current injection. This selection led to better outcomes in the enhancement of power system stability during outages. It was further supported in multiple cases and different studies. In addition, several other studies related to fault current contribution were coherent with this selection.

The results from the additional parameters influencing the fault current contribution illustrated that they had different impact on the stability. Studying their interact with each other was not in the scope of this thesis and therefore limited the determination of requirements for these. A further study is recommended if additional requirements for the fault current contribution are also to be determined. The comprehensive outcomes presented in this thesis can be utilized as initial information when planning and determining the specific responses on new network connection requirements for converter based power plants.

References

[1] Hydro-Québec TransÉnergie. *Transmission Provider Technical Requirements for the Connection of Power Plants to the Hydro-Québec Transmission System*, 2009. Available at: `http://www.hydroquebec.com/transenergie/fr/commerce/pdf/exigence_raccordement_fev_09_en.pdf`. Accessed at 03.05.2016.

[2] Energinet.dk. *Technical Regulation 3.2.5 for Wind Power Plants with a Power Output Above 11 kW*, 2015. Available at: `http://www.energinet.dk/EN/El/Forskrifter/Technical-regulations/Sider/Forskrifter-for-nettilslutning.aspx`. Accessed at 03.05.2016.

[3] The Union of German Network Operators (Verband der Netzbetreiber [VDN]). *TransmissionCode 2007 - Network and System Rules of the German Transmission System Operators*, 2007. Available at: `www.bdew.de`. Accessed at 03.05.2016.

[4] National Grid Electricity Transmission Plc. *The Grid Code - Issue 5 - Revision 15*, 2016. Available at: `http://www2.nationalgrid.com/UK/Industry-information/Electricity-codes/Grid-code/The-Grid-code/`. Accessed at 03.05.2016.

[5] EirGrid Plc. *EirGrid Grid Code - Version 6.0*, 2016. Available at: `http://www.eirgridgroup.com/library/`. Accessed at 03.05.2016.

[6] Statnett. *Functional Requirements for the Norwegian Power System, unofficial version*, 2012. Official version available at: `http://www.statnett.no/Global/Dokumenter/Kraftsystemet/Systemansvar/FIKS2012.pdf`. Accessed at 22.06.2016.

[7] Svenska Kraftnät. *Affärsverket Svenska Kraftnäts Föreskrifter och Allmänna Råd om Driftsäkerhetsteknisk Utformning av Produktionsanläggningar*, 2005. Available at: `http://www.svk.se/om-oss/foreskrifter/`. Accessed at 30.05.2016.

[8] Fingrid Oyj. *Voimalaitosten Järjestelmätekniset Vaatimukset VJV2013*, 2013. Available at: `http://www.fingrid.fi/fi/asiakkaat/asiakasliitteet/Liittyminen/2013/VoimalaitostenjärjestelmäteknisetvaatimuksetVJV2013.pdf`. Accessed at 25.05.2016.

[9] Prabha Kundur. *Power System Stability and Control*. McGraw-Hill, Inc., 1994.

[10] Prabha Kundur, John Paserba, Venkat Ajjarapu, Göran Andersson, Anjan Bose, Claudio Canizares, Nikos Hatziargyriou, David Hill, Alex Stankovic, Carson Taylor, et al. *Definition and Classification of Power System Stability IEEE/Cigre Joint Task Force on Stability Terms and Definitions*. Power Systems, IEEE Transactions on, 19(3):1387–1401, 2004.

[11] Gonzalo Abad, Jesus Lopez, Miguel Rodríguez, Luis Marroyo, and Grzegorz Iwanski. *Doubly Fed Induction Machine: Modeling and Control for Wind Energy Generation*, volume 85. John Wiley & Sons, 2011.

[12] Frede Blaabjerg, Zhe Chen, and Soeren Baekhoej Kjaer. *Power Electronics as Efficient Interface in Dispersed Power Generation Systems.* IEEE transactions on power electronics, 19(5):1184–1194, 2004.

[13] Pouyan Pourbeik et al. *Modeling and Dynamic Behavior of Wind Generation as it Relates to Power System Control and Dynamic Performance.* CIGRE Technical Brochure, (328), 2007.

[14] Thomas Ackermann et al. *Wind Power in Power Systems*, volume 140. Wiley Online Library, 2005.

[15] Abram Perdana. *Dynamic Models of Wind Turbines.* PhD thesis, Chalmers University of Technology, 2008.

[16] Dao Zhou, Frede Blaabjerg, Toke Franke, Michael Tonnes, and Mogens Lau. *Reduced Cost of Reactive Power in Doubly Fed Induction Generator Wind Turbine System with Optimized Grid Filter.* Power Electronics, IEEE Transactions on, 30(10):5581–5590, 2015.

[17] Marco Liserre, Frede Blaabjerg, and Antonio Dell'Aquila. *Step-by-step Design Procedure for a Grid-connected Three-phase PWM Voltage Source Converter.* International Journal of Electronics, 91(8):445–460, 2004.

[18] Gillian Lalor, Alan Mullane, and Mark O'Malley. *Frequency Control and Wind Turbine Technologies.* Power Systems, IEEE Transactions on, 20(4):1905–1913, 2005.

[19] Iñigo Martinez de Alegría, Jon Andreu, José Luis Martín, Pedro Ibanez, José Luis Villate, and Haritza Camblong. *Connection Requirements for Wind Farms: A Survey on Technical Requierements and Regulation.* Renewable and Sustainable Energy Reviews, 11(8):1858–1872, 2007.

[20] Arantxa Tapia, Gerardo Tapia, J Xabier Ostolaza, and Jose Ramon Saenz. *Modeling and Control of a Wind Turbine Driven Doubly Fed Induction Generator.* Energy Conversion, IEEE Transactions on, 18(2):194–204, 2003.

[21] Marina Tsili and S Papathanassiou. *A Review of Grid Code Technical Requirements for Wind Farms.* Renewable power generation, IET, 3(3):308–332, 2009.

[22] Chong Han, Alex Q Huang, Mesut E Baran, Subhashish Bhattacharya, Wayne Litzenberger, Loren Anderson, Anders L Johnson, and Abdel-Aty Edris. *STATCOM Impact Study on the Integration of a Large Wind Farm into a Weak Loop Power System.* Energy conversion, IEEE Transactions on, 23(1):226–233, 2008.

[23] Pranesh Rao, ML Crow, and Zhiping Yang. *STATCOM Control for Power System Voltage Control Applications.* Power Delivery, IEEE Transactions on, 15(4):1311–1317, 2000.

[24] Christian Wessels, Malte Laubrock, Uwe Bellgardt, and Adreas Genius. *Flexible Fault Ride Through of DFIG Wind Turbines with DC-Chopper Solution.* In Proceedings of the 11th Wind Integration Workshop on Large-Scale Integration of Wind Power into Power Systems as well as on Transmission Networks for Offshore Wind Power Plants, 2012.

[25] G Ramtharan, Atputharajah Arulampalam, Janaka Bandara Ekanayake, FM Hughes, and Nick Jenkins. *Fault Ride Through of Fully Rated Converter Wind Turbines with AC and DC Transmission.* Renewable Power Generation, IET, 3(4):426–438, 2009.

[26] Héctor A Pulgar-Painemal and Peter W Sauer. *Dynamic Modeling of Wind Power Generation.* In North American Power Symposium (NAPS), pages 1–6. IEEE, 2009.

[27] Paul C Krause, Oleg Wasynczuk, Scott D Sudhoff, and Steven Pekarek. *Analysis of Electric Machinery and Drive systems*, volume 75. John Wiley & Sons, 2013.

[28] R Pena, JC Clare, and GM Asher. *Doubly Fed Induction Generator Using Back-to-back PWM Converters and its Application to Variable-Speed Wind-Energy Generation.* In Electric Power Applications, IEE Proceedings-, volume 143, pages 231–241. IET, 1996.

[29] Nicholas W Miller, William W Price, and Juan J Sanchez-Gasca. *Dynamic Modeling of GE 1.5 and 3.6 Wind Turbine-generators.* GE-Power systems energy consulting, 2003.

[30] Kara Clark, Nicholas W Miller, and Juan J Sanchez-Gasca. *Modeling of GE Wind Turbine-generators for Grid Studies.* GE Energy, 4, 2010.

[31] Rogério G De Almeida and JA Peças Lopes. *Participation of Doubly Fed Induction Wind Generators in System Frequency Regulation.* IEEE transactions on power systems, 22(3):944–950, 2007.

[32] JF Conroy and R Watson. *Low-voltage Ride-through of a Full Converter Wind Turbine with Permanent Magnet Generator.* IET Renewable Power Generation, 1(3):182–189, 2007.

[33] J Conroy and R Watson. *Aggregate Modelling of Wind Farms Containing Full-converter Wind Turbine Generators with Permanent Magnet Synchronous Machines: Transient Stability Studies.* IET Renewable Power Generation, 3(1):39–52, 2009.

[34] Luis M Fernández, Francisco Jurado, and José Ramón Saenz. *Aggregated Dynamic Model for Wind Farms with Doubly Fed Induction Generator Wind Turbines*. Renewable energy, 33(1):129–140, 2008.

[35] International Electrotechnical Commission (IEC). *IEC TR 61000-2-8:2002*, 2002. Available at: `https://webstore.iec.ch/publication/4140`. Accessed at 17.10.2016.

[36] Francesco Sulla. *Fault Behavior of Wind Turbines*. PhD thesis, Lund University, 2012.

[37] Eirgrid. *All Island TSO Facilitation of Renewables Studies*, 2010. Available at: `http://www.eirgridgroup.com/site-files/library/EirGrid/Facilitation-of-Renewables-Report.pdf`. Accessed at 22.8.2016.

[38] Nayeem Rahmat Ullah, Torböjrn Thiringer, and Daniel Karlsson. *Voltage and Transient Stability Support by Wind Farms Complying With the E. ON Netz Grid Code*. IEEE Transactions on Power Systems, 22(4):1647–1656, 2007.

[39] Dan Tong, Xiaoming Yuan, and Jiabing Hu. *Transient Control of Grid-Connected Converters for Wind Turbines to Fulfill Emerging Grid Codes*. In Proceedings of the 14th Wind Integration Workshop on Large-Scale Integration of Wind Power into Power Systems as well as on Transmission Networks for Offshore Wind Power Plants, 2015.

[40] Nayeem Rahmat Ullah and Torbjrn Thiringer. *Variable Speed Wind Turbines for Power System Stability Enhancement*. IEEE Transactions on energy conversion, 22(1):52–60, 2007.

[41] European Network of Transmission System Operators for Electricity (ENTSO-E). *Network Code on Requirements for Generators (NC RfG)*, 2013. Available at: `https://www.entsoe.eu/major-projects/network-code-development/requirements-for-generators/Pages/default.aspx`. Accessed at 08.06.2016.

[42] EUR-Lex. *Commission Regulation (EU) 2016/631 of 14 April 2016 Establishing a Network Code on Requirements for Grid Connection of Generators*, 2016. Available at: `http://eur-lex.europa.eu/legal-content/EN/TXT/PDF/?uri=CELEX:32016R0631&from=EN`. Accessed at 08.06.2016.

[43] European Network of Transmission System Operators for Electricity (ENTSO-E). *Implementation Guideline for Network Code "Requirements for Grid Connection Applicable to all Generators"*, 2013. Available at: `https://www.entsoe.eu/major-projects/network-code-development/requirements-for-generators/Pages/default.aspx`. Accessed at 3.10.2016.

[44] Electric Power Research Institute (EPRI). *WECC Type 3 Wind Turbine Generator Model – Phase II*, 2013. Available at: `https://www.wecc.biz/Pages/home.aspx`. Accessed at 06.06.2016.

[45] Electric Power Research Institute (EPRI). *WECC Wind Plant Dynamic Modeling Guidelines*, 2014. Available at: `https://www.wecc.biz/Pages/home.aspx`. Accessed at 06.06.2016.

[46] Electric Power Research Institute (EPRI). *WECC Type 4 Wind Turbine Generator Model – Phase II*, 2013. Available at: `https://www.wecc.biz/Pages/home.aspx`. Accessed at 06.06.2016.

[47] Fingrid Oyj. *Voimajärjestelmän tila*, 2016. Available at: `http://www.fingrid.fi/fi/sahkomarkkinat/voimajarjestelman-tila/Sivut/default.aspx`. Accessed at 03.10.2016.

[48] Siemens PTI. *PSS®E 33.9 Model Library*, 2016.

Appendix A: Additional Results from Fault Current Contribution Study

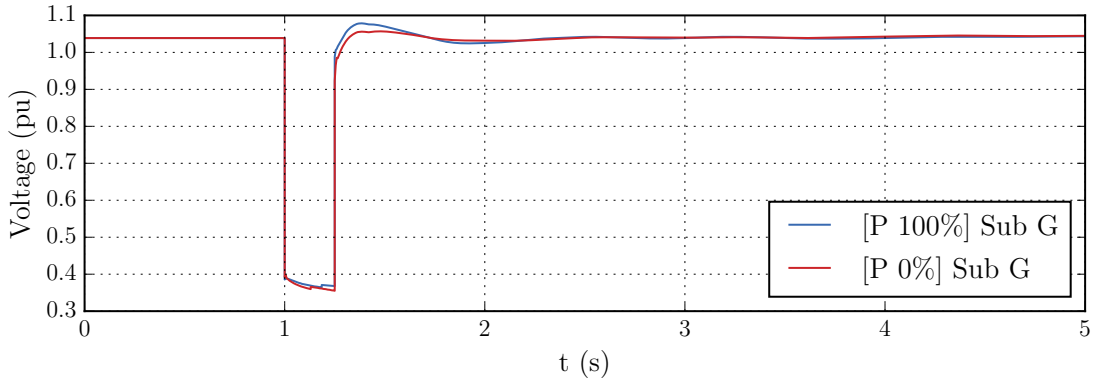

Figure A.1: The voltage fluctuation at the substation G in case of 250 ms disturbance in a nearby substation H. The base-case of the simulation was the summer night of import with active current contribution priority on both plots. [P 100%] presents the result for wind power plants with set current contribution. [P 0%] presents the result for wind power plants without any current contribution during the fault. Wind power plants operated at nominal active power production prior to the disturbance in both cases.

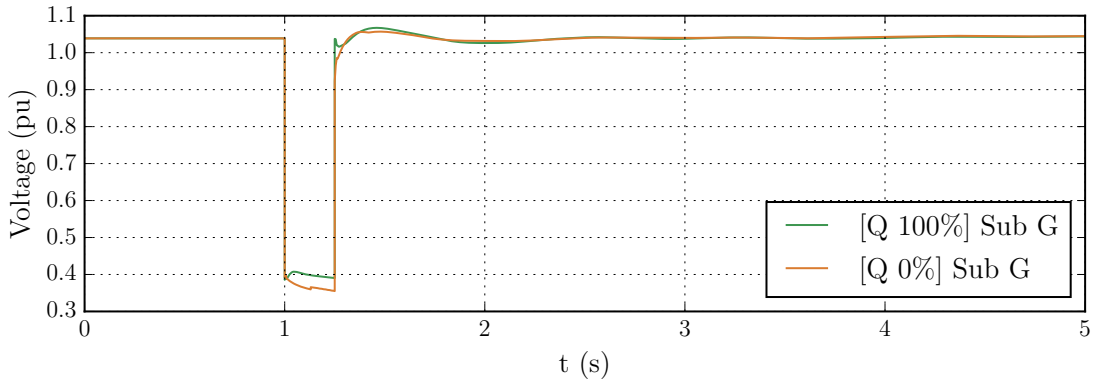

Figure A.2: The voltage fluctuation at the substation G in case of 250 ms disturbance in a nearby substation H. The base-case of the simulation was the summer night of import with reactive current contribution priority on both plots. [Q 100%] presents the result for wind power plants with set current contribution. [Q 0%] presents the result for wind power plants without any current contribution during the fault. Wind power plants operated at nominal active power production prior to the disturbance in both cases.

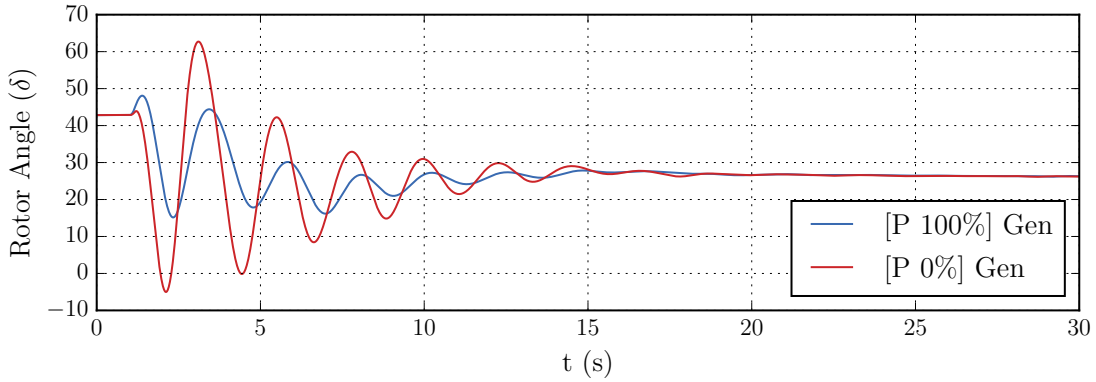

Figure A.3: The rotor angle oscillation of a large generator in case of tripping Hanhikivi 1. The base-case of the simulation was the winter night of export with active current contribution priority on both plots. The base-case was altered to include Hanhikivi 1 in the network. [P 100%] presents the result for wind power plants with set current contribution. [P 0%] presents the result for wind power plants without any current contribution during the fault. Wind power plants operated at nominal active power production prior to the disturbance in both cases.

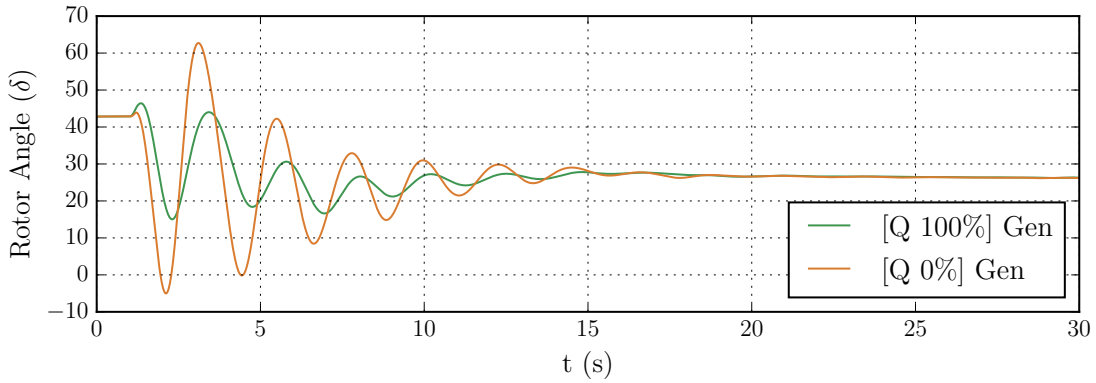

Figure A.4: The rotor angle oscillation of a large generator in case of tripping Hanhikivi 1. The base-case of the simulation was the winter night of export with reactive current contribution priority on both plots. The base-case was altered to include Hanhikivi 1 in the network. [Q 100%] presents the result for wind power plants with set current contribution. [Q 0%] presents the result for wind power plants without any current contribution during the fault. Wind power plants operated at nominal active power production prior to the disturbance in both cases.

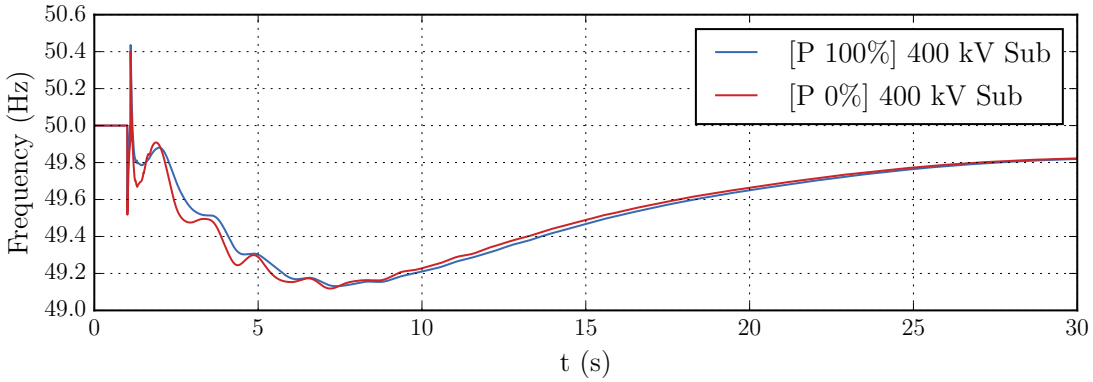

Figure A.5: The frequency fluctuation at 400 kV substation in case of tripping Olkiluoto 3. The base-case of the simulation was the summer night of import with active current contribution priority on both plots. [P 100%] presents the result for wind power plants with set current contribution. [P 0%] presents the result for wind power plants without any current contribution during the fault. Wind power plants operated at nominal active power production prior to the disturbance in both cases.

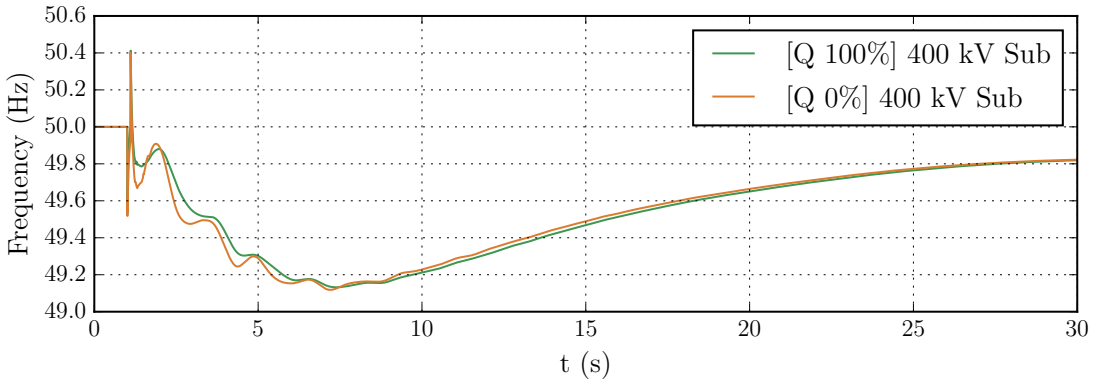

Figure A.6: The frequency fluctuation at 400 kV substation in case of tripping Olkiluoto 3. The base-case of the simulation was the summer night of import with reactive current contribution priority on both plots. [Q 100%] presents the result for wind power plants with set current contribution. [Q 0%] presents the result for wind power plants without any current contribution during the fault. Wind power plants operated at nominal active power production prior to the disturbance in both cases.

Table A.1: The impact of fault current contribution on the critical fault clearing time of a disturbance in substation D. The fault clearing time was simulated from 250 ms to 360 ms in five ms intervals. The comparison is between zero and set fault current contribution. Set fault current contribution is divided into active (P-prio) and reactive (Q-prio) current priority. 0% indicate that the modelled power plants did not inject any fault current. 100% indicate that the plants operated according to the set priority and fault current contribution. Wind power plants operated at nominal active power production prior to the disturbance in all three cases.

Case	Stability	Crit. length with 0% (ms)	Crit. length with 100% P-prio (ms)	Crit. length with 100% Q-prio (ms)	0% difference with 100% P-prio (ms)	0% difference with 100% Q-prio (ms)
A	Voltage	>360[1)]	340	>360	>-20[2)]	-
	Rotor angle	>360	340	>360	>-20	-
	Frequency	>360	340	>360	>-20	-
B	Voltage	350	340	>360	-10	>10
	Rotor angle	350	340	>360	-10	>10
	Frequency	350	340	>360	-10	>10
C–D[3)]	Voltage	-	-	-	-	-
	Rotor angle	-	-	-	-	-
	Frequency	-	-	-	-	-
E	Voltage	270	285	325	15	55
	Rotor angle	270	285	325	15	55
	Frequency	270	285	325	15	55

[1)] If the length includes '>' symbol, the case passed the last interval of 360 ms.
[2)] If the value is negative, the zero injection case had a longer critical disturbance length.
[3)] No instabilities occurred during the simulations with cases C and D.

Table A.2: The impact of fault current contribution on the critical fault clearing time of a disturbance in substation F. The fault clearing time was simulated from 250 ms to 360 ms in five ms intervals. The comparison is between zero and set fault current contribution. Set fault current contribution is divided into active (P-prio) and reactive (Q-prio) current priority. 0% indicate that the modelled power plants did not inject any fault current. 100% indicate that the plants operated according to the set priority and fault current contribution. Wind power plants operated at nominal active power feeding prior to the disturbance in all three cases.

Case	Stability	Crit. length with 0% (ms)	Crit. length with 100% P-prio (ms)	Crit. length with 100% Q-prio (ms)	0% difference with 100% P-prio (ms)	0% difference with 100% Q-prio (ms)
A–C[1)]	Voltage	-	-	-	-	-
	Rotor angle	-	-	-	-	-
	Frequency	-	-	-	-	-
D	Voltage	-	-	-	-	-
	Rotor angle	335	>360[2)]	>360	>25	>25
	Frequency	-	-	-	-	-
E	Voltage	255	325	355	70	100
	Rotor angle	255	325	355	70	100
	Frequency	255	325	355	70	100

[1)] No instabilities occurred during the simulations with cases A–C.
[2)] If the length includes '>' symbol, the case passed the last interval of 360 ms.

Appendix B: Additional Results from Fault Current Contribution Priority Study

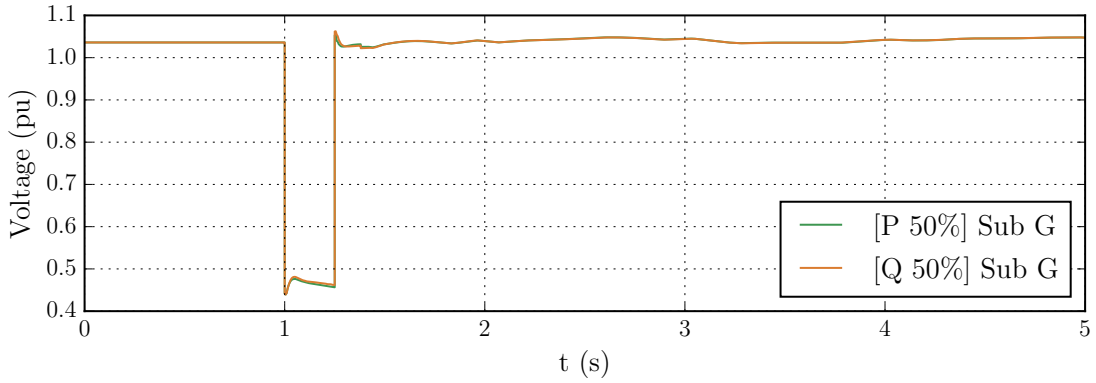

Figure B.1: The voltage fluctuation at the substation G in case of 250 ms disturbance in a nearby substation H. The base-case of the simulation was the summer night of export. [P 50%] presents the result for wind power plants with active current contribution priority. [Q 50%] presents the result for wind power plants with reactive current contribution priority. Wind power plants operated at 50 % active power production from the nominal capacity prior to the disturbance in both cases.

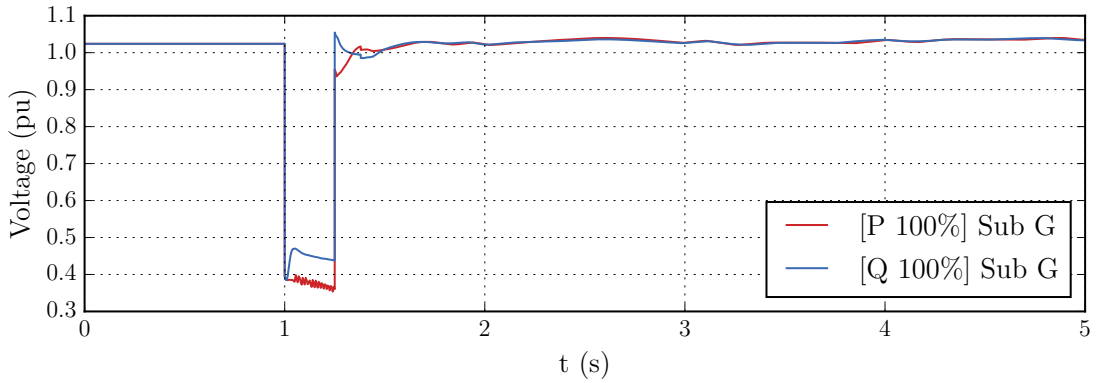

Figure B.2: The voltage fluctuation at the substation G in case of 250 ms disturbance in a nearby substation H. The base-case of the simulation was the summer night of export. [P 100%] presents the result for wind power plants with active current contribution priority. [Q 100%] presents the result for wind power plants with reactive current contribution priority. Wind power plants operated at nominal active power production prior to the disturbance in both cases.

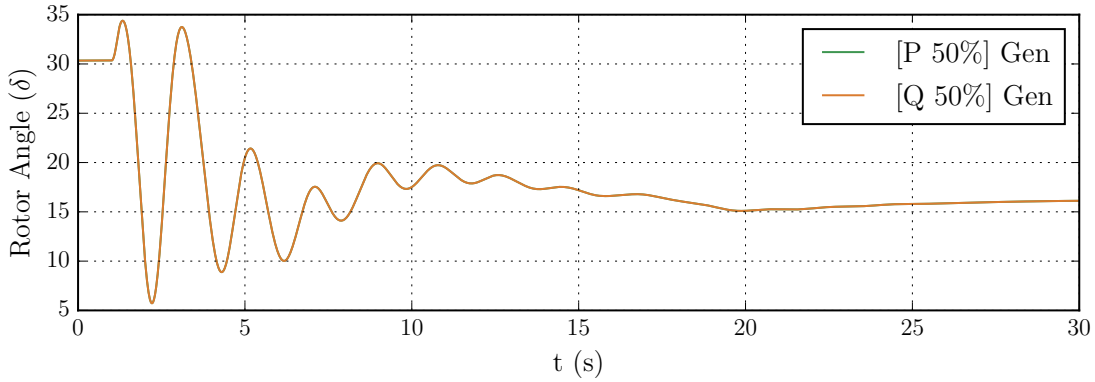

Figure B.3: The rotor angle oscillation of a large generator in case of tripping Hanhikivi 1. The base-case of the simulation was the summer night of export. The base-case was altered to include Hanhikivi 1 in the network. [P 50%] presents the result for wind power plants with active current contribution priority. [Q 50%] presents the result for wind power plants with reactive current contribution priority. Wind power plants operated at 50 % active power production from the nominal capacity prior to the disturbance in both cases.

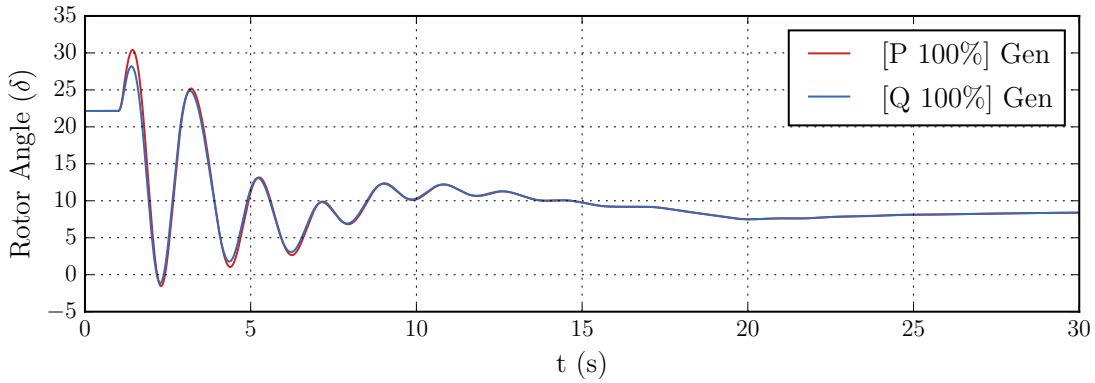

Figure B.4: The rotor angle oscillation of a large generator in case of tripping Hanhikivi 1. The base-case of the simulation was the summer night of export. The base-case was altered to include Hanhikivi 1 in the network. [P 100%] presents the result for wind power plants with active current contribution priority. [Q 100%] presents the result for wind power plants with reactive current contribution priority. Wind power plants operated at nominal active power production prior to the disturbance in both cases.

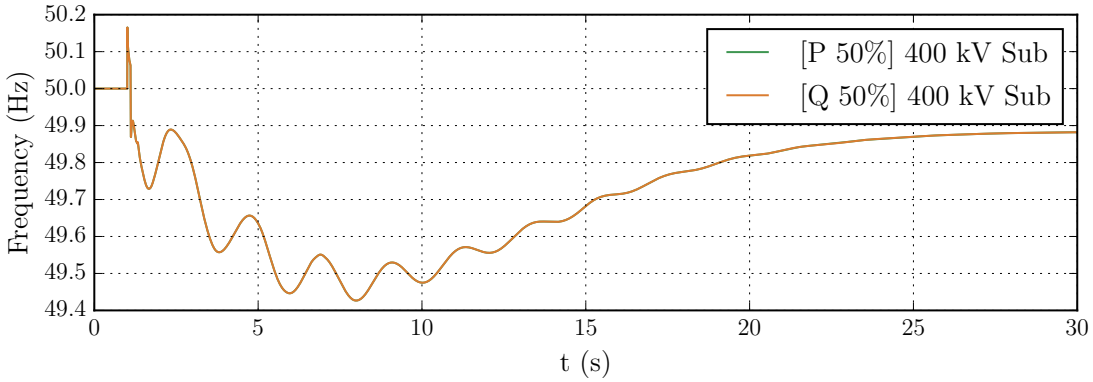

Figure B.5: The frequency fluctuation at 400 kV substation in case of tripping Olkiluoto 3. The base-case of the simulation was the winter night of export. [P 50%] presents the result for wind power plants with active current contribution priority. [Q 50%] presents the result for wind power plants with reactive current contribution priority. Wind power plants operated at 50 % active power production from the nominal capacity prior to the disturbance in both cases.

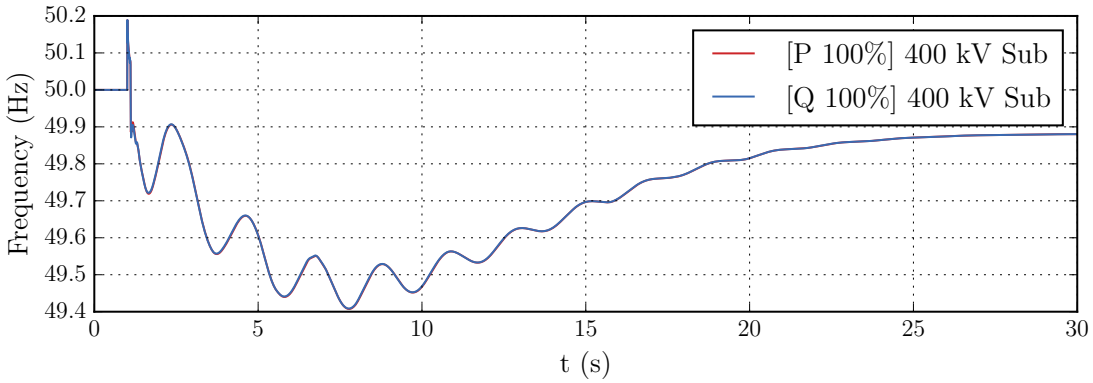

Figure B.6: The frequency fluctuation at 400 kV substation in case of tripping Olkiluoto 3. The base-case of the simulation was the winter night of export. [P 100%] presents the result for wind power plants with active current contribution priority. [Q 100%] presents the result for wind power plants with reactive current contribution priority. Wind power plants operated at nominal active power production prior to the disturbance in both cases.

Table B.1: The impact of fault current contribution priority on critical fault clearing time of a disturbance in substation D. The fault clearing time was simulated from 250 ms to 360 ms in five ms intervals. The comparison is between active (P-priority) and reactive (Q-priority) current contribution priority. Wind power plants operated at nominal active power feeding prior to the disturbance in both cases.

Case	Stability	Critical length with P-priority (ms)	Critical length with Q-priority (ms)	Difference (ms)
A	Voltage	340	>360[1)]	>20
	Rotor angle	340	>360	>20
	Frequency	340	>360	>20
B	Voltage	340	>360	>20
	Rotor angle	340	>360	>20
	Frequency	340	>360	>20
C-D[2)]	Voltage	-	-	-
	Rotor angle	-	-	-
	Frequency	-	-	-
E	Voltage	285	325	40
	Rotor angle	285	325	40
	Frequency	285	325	40

[1)] If the length includes '>' symbol, the case passed the last interval of 360 ms.
[2)] No instabilities occurred with neither priority during the simulations with cases C and D.

Table B.2: The impact of fault current contribution priority on critical fault clearing time of a disturbance in substation F. The fault clearing time was simulated from 250 ms to 360 ms in five ms intervals. The comparison is between active (P-priority) and reactive (Q-priority) current contribution priority. Wind power plants operated at nominal active power feeding prior to the disturbance in both cases.

Case	Stability	Critical length with P-priority (ms)	Critical length with Q-priority (ms)	Difference (ms)
A–D[1)]	Voltage	-	-	-
	Rotor angle	-	-	-
	Frequency	-	-	-
E	Voltage	325	355	30
	Rotor angle	325	355	30
	Frequency	325	355	30

[1)] No instabilities occurred with neither priority during the simulations with cases A–D.

Appendix C: Additional Results from Reactive Fault Current Gain Study

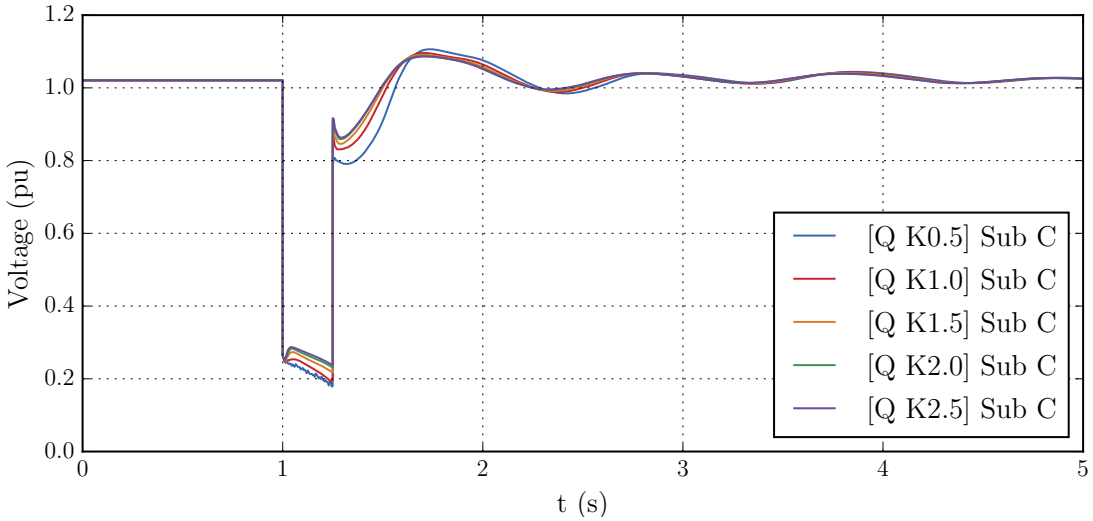

Figure C.1: The voltage fluctuation at the substation C in 250 ms disturbance in a nearby substation A. The base-case of the simulation was the mid-winter day of import. The value of reactive current gain (pu/pu) is presented subsequent to K in the legend. The wind power plants operated with reactive current contribution priority. These plants produced nominal active power prior to the disturbance in all cases.

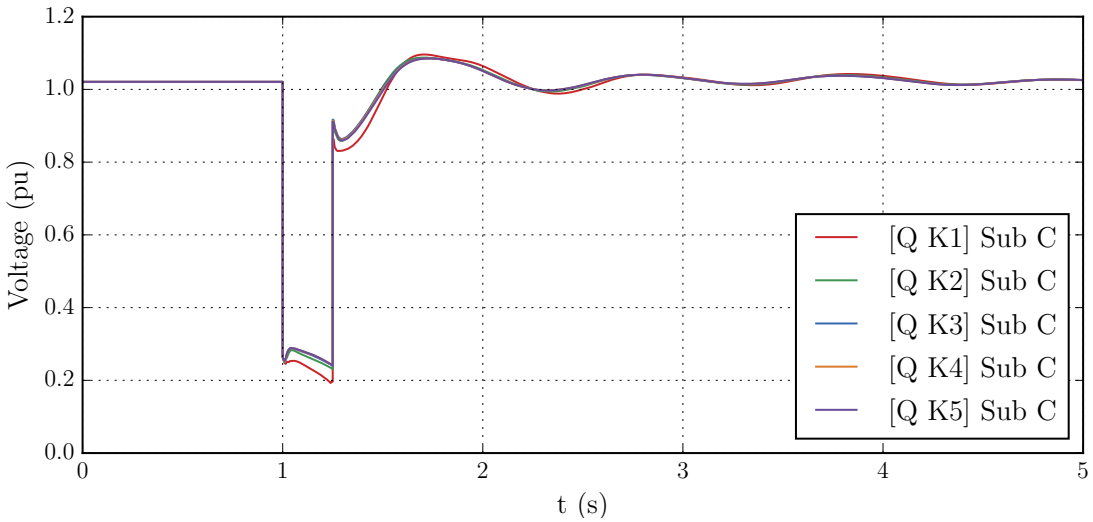

Figure C.2: The voltage fluctuation at the substation C in 250 ms disturbance in a nearby substation A. The base-case of the simulation was the mid-winter day of import. The value of reactive current gain (pu/pu) is presented subsequent to K in the legend. The wind power plants operated with reactive current contribution priority. These plants produced nominal active power prior to the disturbance in all cases.

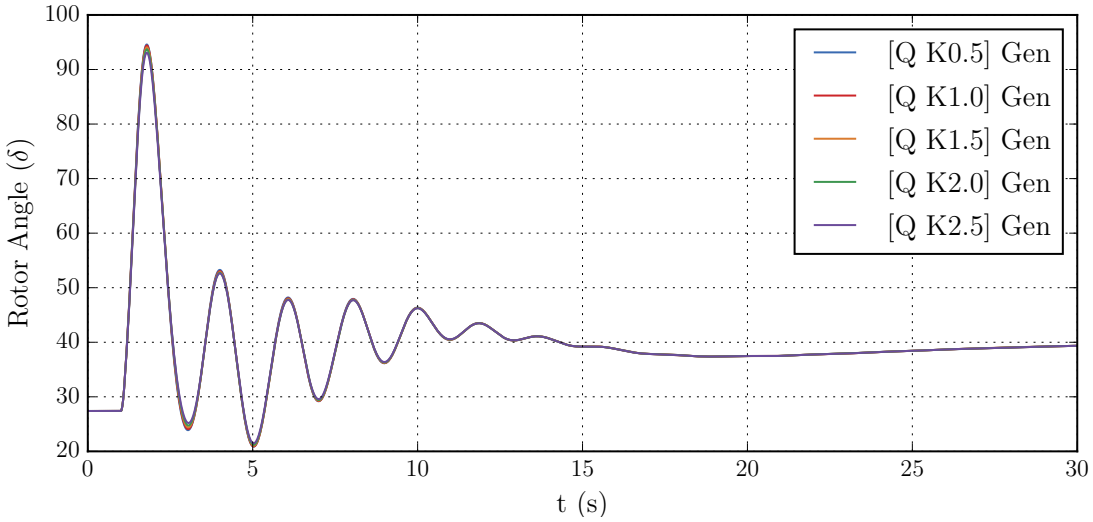

Figure C.3: The rotor angle oscillation of a large generator in case of tripping Fenno-Skan2. The base-case of the simulation was the summer night of export. The value of reactive current gain (pu/pu) is presented subsequent to K in the legend. The wind power plants operated with reactive current contribution priority. These plants produced nominal active power prior to the disturbance in all cases.

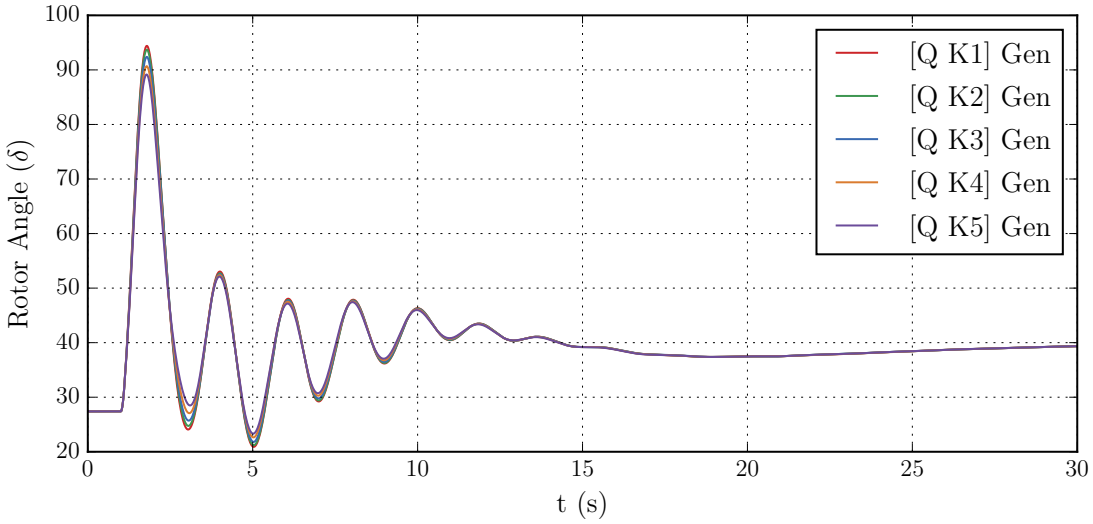

Figure C.4: The rotor angle oscillation of a large generator in case of tripping Fenno-Skan2. The base-case of the simulation was the summer night of export. The value of reactive current gain (pu/pu) is presented subsequent to K in the legend. The wind power plants operated with reactive current contribution priority. These plants produced nominal active power prior to the disturbance in all cases.

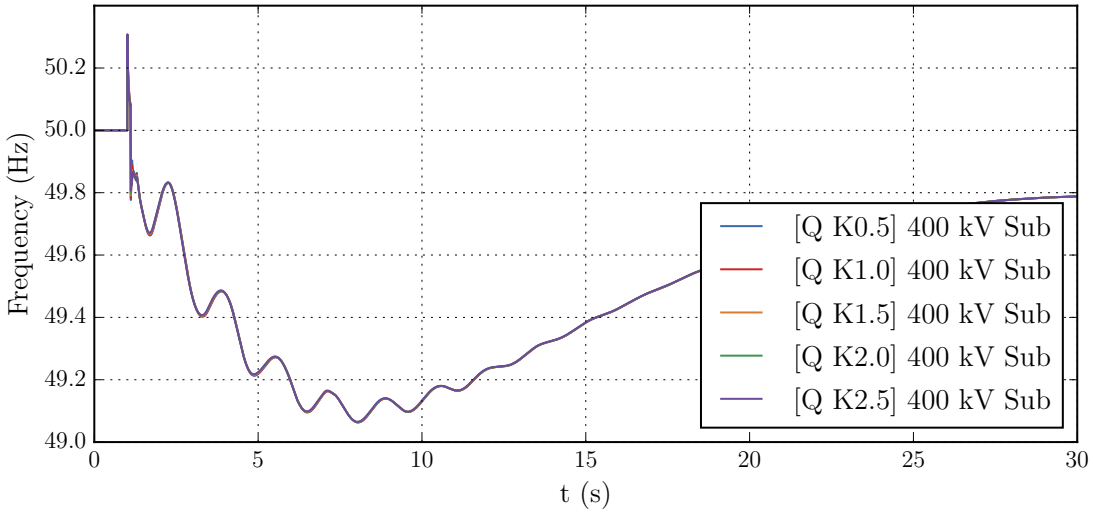

Figure C.5: The frequency fluctuation at 400 kV substation in case of tripping Olkiluoto 3. The base-case of the simulation was the summer night of export. The value of reactive current gain (pu/pu) is presented subsequent to K in the legend. The wind power plants operated with reactive current contribution priority. These plants produced nominal active power prior to the disturbance in all cases.

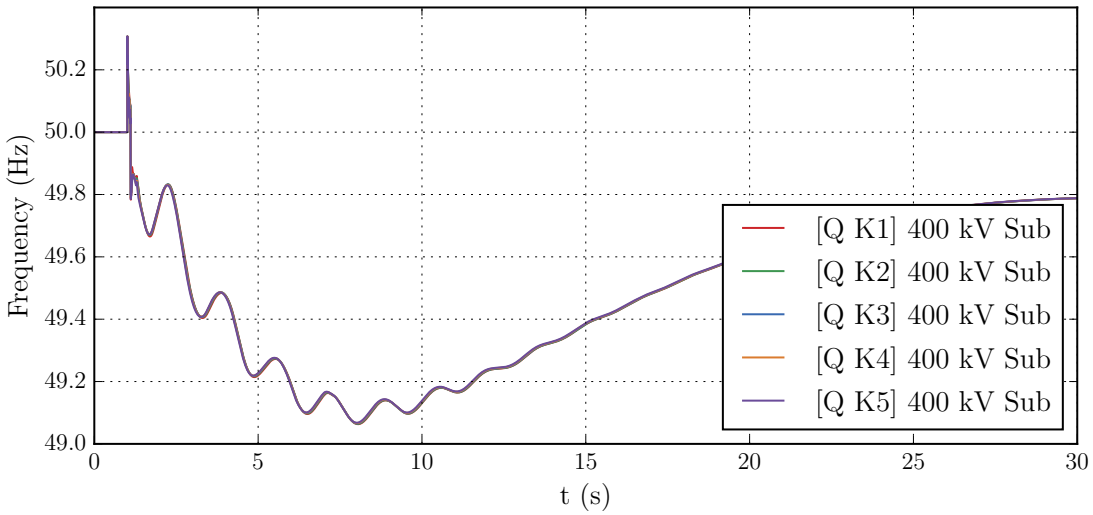

Figure C.6: The frequency fluctuation at 400 kV substation in case of tripping Olkiluoto 3. The base-case of the simulation was the summer night of export. The value of reactive current gain (pu/pu) is presented subsequent to K in the legend. The wind power plants operated with reactive current contribution priority. These plants produced nominal active power prior to the disturbance in all cases.

Appendix D: Additional Results from Active Power Recovery Time Study

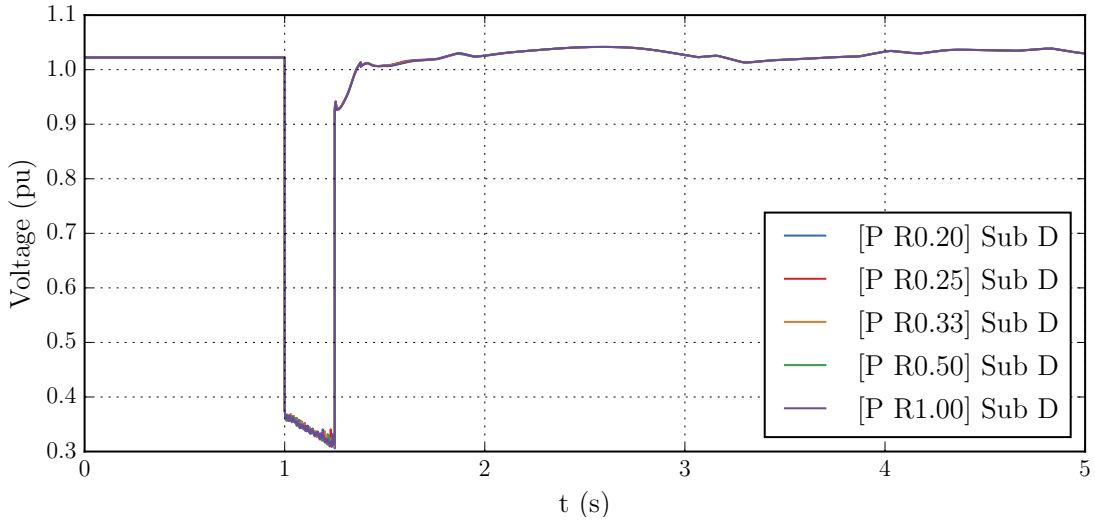

Figure D.1: The voltage fluctuation at the substation D in 250 ms disturbance in a nearby substation C. The base-case of the simulation was the summer night of export. The value of active power recovery time (pu/s) is presented subsequent to R in the legend. The wind power plants operated with active current contribution priority. These plants produced nominal active power prior to the disturbance in all cases.

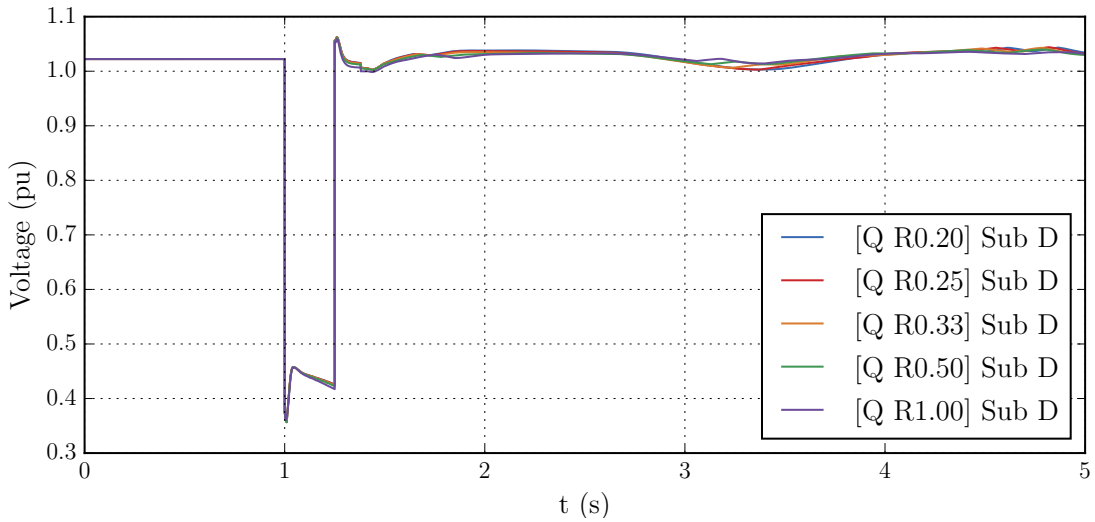

Figure D.2: The voltage fluctuation at substation D in 250 ms disturbance in a nearby substation C. The base-case of the simulation was the summer night of export. The value of active power recovery time (pu/s) is presented subsequent to R in the legend. The wind power plants operated with reactive current contribution priority. These plants produced nominal active power prior to the disturbance in all cases.

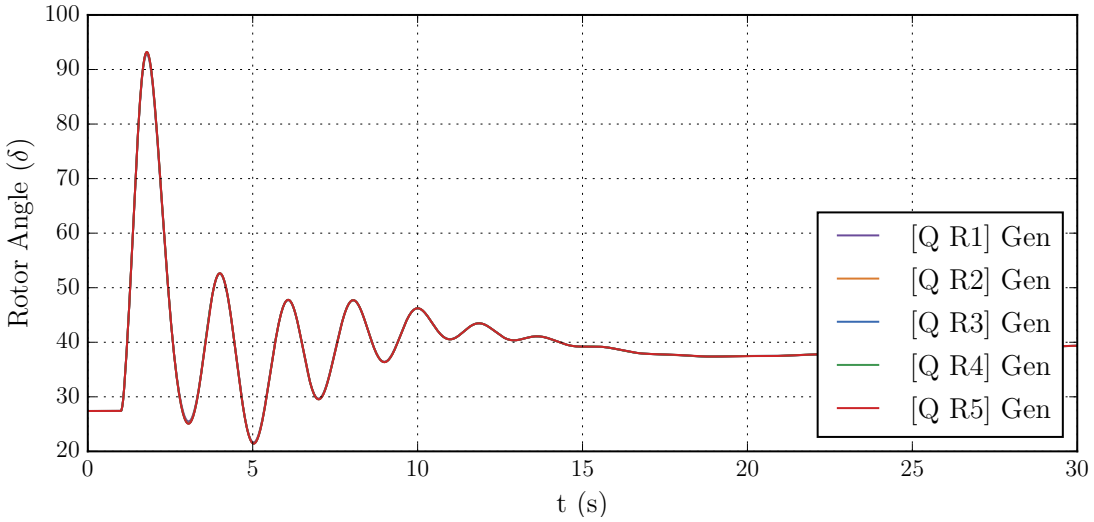

Figure D.3: The rotor angle oscillation of a large generator in case of tripping Fenno-Skan2. The base-case of the simulation was the summer night of export. The value of active power recovery time (pu/s) is presented subsequent to R in the legend. The wind power plants operated with reactive current contribution priority. These plants produced nominal active power prior to the disturbance in all cases.

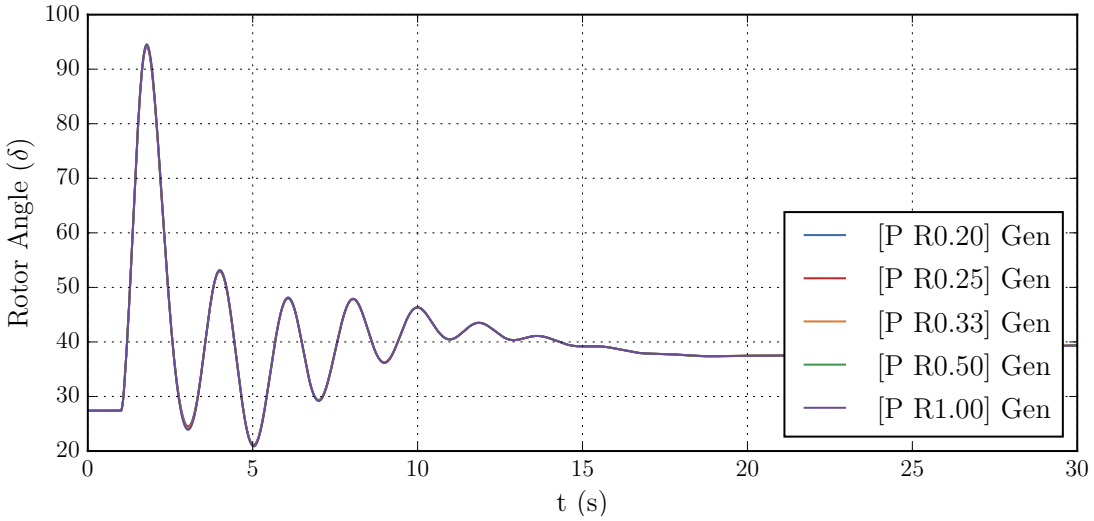

Figure D.4: The rotor angle oscillation of a large generator in case of tripping Fenno-Skan2. The base-case of the simulation was the summer night of export. The value of active power recovery time (pu/s) is presented subsequent to R in the legend. The wind power plants operated with active current contribution priority. These plants produced nominal active power prior to the disturbance in all cases.

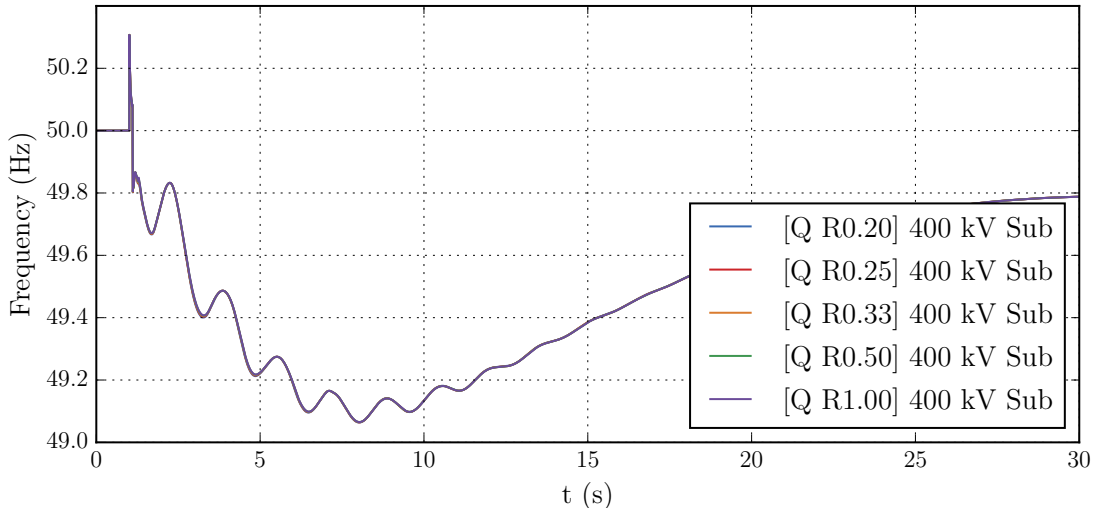

Figure D.5: The frequency fluctuation at 400 kV substation in case of tripping Olkiluoto 3. The base-case of the simulation was the summer night of export. The value of active power recovery time (pu/s) is presented subsequent to R in the legend. The wind power plants operated with reactive current contribution priority. These plants produced nominal active power prior to the disturbance in all cases.

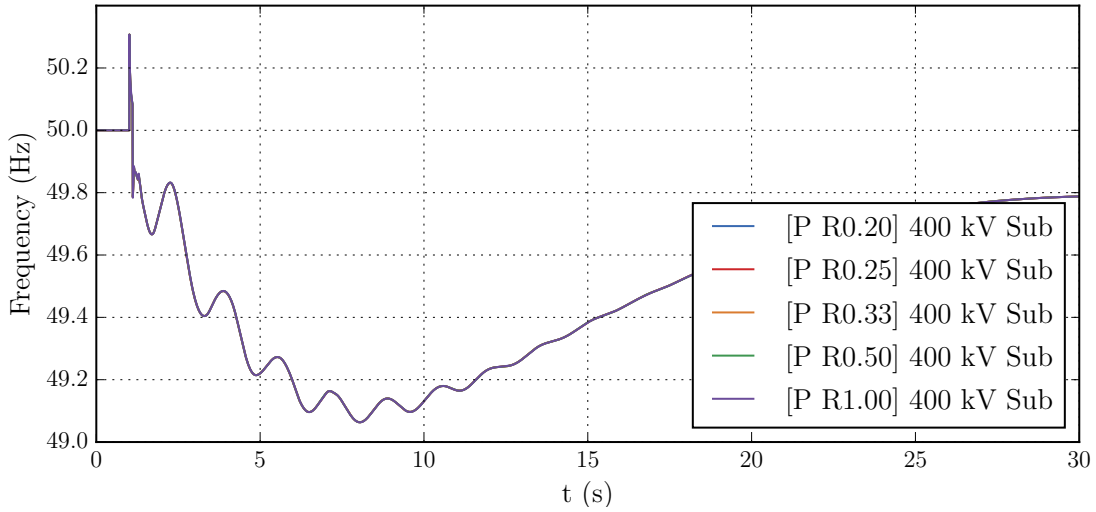

Figure D.6: The frequency fluctuation at 400 kV substation in case of tripping Olkiluoto 3. The base-case of the simulation was the summer night of export. The value of active power recovery time (pu/s) is presented subsequent to R in the legend. The wind power plants operated with active current contribution priority. These plants produced nominal active power prior to the disturbance in all cases.

Appendix E: Parameters and Values of the Modelled Wind Power Plants

Table E.1: The dynamic simulation parameters and values of the wind power plant controller model (repc_a) of the modelled wind power plants. The description of the parameter is according to PSS/E [48].

Parameter	Value	Name and Description
J	0.02	T_{fltr}, Voltage or reactive power measurement filter time constant (s))
J+1	0.2	K_{p}, Reactive power PI control proportional gain (pu)
J+2	20	K_{i}, Reactive power PI control integral gain (pu)
J+3	0	T_{ft}, Lead time constant (s)
J+4	0	T_{fv}, Lag time constant (s)
J+5	0.9	V_{frz}, Voltage below which State s2 is frozen (pu)
J+6	-[1)]	R_{c}, Line drop compensation resistance (pu)
J+7	-	X_{c}, Line drop compensation reactance (pu)
J+8	0.05	K_{c}, Reactive current compensation gain (pu)
J+9	100	e_{max}, upper limit on deadband output (pu)
J+10	-100	e_{min}, lower limit on deadband output (pu)
J+11	0	dbd1, lower threshold for reactive power control deadband (<=0)
J+12	0	dbd2, upper threshold for reactive power control deadband (>=0)
J+13	*[2)]	Q_{max}, Upper limit on output of V/Q control (pu)
J+14	*	Q_{min}, Lower limit on output of V/Q control (pu)
J+15...J+26	-	

[1)] The values marked with - were not used in the simulations.
[2)] The values marked with * were varied according to the simulation case.

Table E.2: The dynamic simulation parameters and values of the electrical control model (reec_a) of the modelled wind power plants. The description of the parameter is according to PSS/E [48].

Parameter	Value	Name and Description
J	0.9	Vdip (pu), low voltage threshold to activate reactive current injection logic
J+1	2.0	Vup (pu), Voltage above which reactive current injection logic is activated
J+2	0.02	T_{rv} (s), Voltage filter time constant
J+3	0	dbd1 (pu), Voltage error dead band lower threshold (<=0)
J+4	0	dbd2 (pu), Voltage error dead band upper threshold (>=0)
J+5	*[1)]	K_{qv} (pu), Reactive current injection gain during over and undervoltage conditions
J+6	1	I_{qh1} (pu), Upper limit on reactive current injection Iqinj
J+7	-1	I_{ql1} (pu), Lower limit on reactive current injection Iqinj
J+8	0	V_{ref0} (pu), User defined reference
J+9	0	Iqfrz (pu), Value at which Iqinj is held for Thld seconds following a voltage dip if Thld > 0
J+10	0	Thld (s), Time for which Iqinj is held at Iqfrz after voltage dip returns to zero
J+11	0	Thld2 (s) (>=0), Time for which the active current limit (I_{pmax}) is held at the faulted value after voltage dip returns to zero
J+12	0.05	T_{p} (s), Filter time constant for electrical power
J+13...J+21	-[2)]	
J+22	0.02	T_{iq} (s), Time constant on delay s4
J+23	0.5	dP_{max} (pu/s) (>0) Power reference max. ramp rate
J+24	-0.5	dP_{min} (pu/s) (<0) Power reference min. ramp rate
J+25	1	P_{max} (pu), Max. power limit
J+26	0	P_{min} (pu), Min. power limit
J+27	1.05	Imax (pu), Maximum limit on total converter current
J+28	0.05	T_{pord} (s), Power filter time constant
J+29	0.1	V_{q1} (pu), Reactive Power V-I pair, voltage
J+30	1	I_{q1} (pu), Reactive Power V-I pair, current
J+31	1	V_{q2} (pu) (Vq2>Vq1), Reactive Power V-I pair, voltage
J+32	1	I_{q2} (pu) (Iq2>Iq1), Reactive Power V-I pair, current
J+33...J+36	-	
J+37	0.1	V_{p1} (pu), Real Power V-I pair, voltage
J+38	1	I_{p1} (pu), Real Power V-I pair, current
J+39	1	V_{p2} (pu) (Vp2>Vp1), Real Power V-I pair, voltage
J+40	1	I_{p2} (pu) (Ip2>Ip1), Real Power V-I pair, current
J+41...J+44	-	

[1)] The values marked with * were varied according to the simulation case.
[2)] The values marked with - were not used in the simulations.

Table E.3: The dynamic simulation parameters and values of the generator and converter model (regc_a) of the modelled wind power plants. The description of the parameter is according to PSS/E [48].

Parameter	Value	Name and Description
J	0.02	T_g, Converter time constant (s)
J+1	*[1)]	Rrpwr, Low Voltage Power Logic (LVPL) ramp rate limit (pu)
J+2	-[2)]	Brkpt, LVPL characteristic voltage 2 (pu)
J+3	-	Zerox, LVPL characteristic voltage 1 (pu)
J+4	-	Lvpl1, LVPL gain (pu)
J+5	1.20	Volim, Voltage limit (pu) for high voltage reactive current management
J+6	0.10	Lvpnt1, High voltage point for low voltage active current management (pu)
J+7	0.00	Lvpnt0, Low voltage point for low voltage active current management (pu)
J+8	-2.00	Iolim, Current limit (pu) for high voltage reactive current management (specified as a negative value)
J+9	0.02	T_{fltr}, Voltage filter time constant for low voltage active current management (s)
J+10	0.80	K_{hv}, Overvoltage compensation gain used in the high voltage reactive current management
J+11	1000	I_{qrmax}, Upper limit on rate of change for reactive current (pu)
J+12	-1000	I_{qrmin}, Lower limit on rate of change for reactive current (pu)
J+13	1.0	Accel, acceleration factor ($0 < \text{Accel} \leq 1$)

[1)] The values marked with * were varied according to the simulation case.
[2)] The values marked with - were not used in the simulations.